



UNIVERSITA' DEGLI STUDI DI NAPOLI
FEDERICO II

GEOSTATISTICAL ANALYSIS OF FLOWS IN THE VADOSE ZONE

Maddalena Scarfato

Tesi di Dottorato in Scienze Agrarie ed Agroalimentari
XXXI Ciclo



Dipartimento di Agraria

Tutor Ch.mo Prof. Gerardo Severino

Coordinatore Ch.mo Prof. Guido D'Urso

INTRODUCTION

The hydrology is the science that studies the water cycle and the physical processes involved, such as: evaporation, condensation, precipitation, flow, underground flow and infiltration (see figure 0.0.1). The hydrological cycle represents one of the most important Earth's life cycle, i.e. the succession of water flow and circulation phenomena and the endless exchanges of water mass between the atmosphere and the Earth's crust through surface waters, groundwater and organisms. Groundwater recharge, irrigation efficiency, runoff, evapotranspiration, transport of contaminants, vapors and solutes in the vadose zone are examples of the different and important issues associated with a good understanding of soil water dynamics.

Among the many hydrodynamic processes, infiltration and vertical flow problems have received more attention, both for empirical formulations and for applications. Infiltration through unsaturated soils is defined as “the entry of water into the soil surface and its subsequent vertical motion through the soil” [Brutsaert, 2005][22]. This phenomenon occurs on the soil surface when water flows through the spaces between the particles that form the surface. Once the water infiltrates into the soil, its journey continues under the effect of gravity and capillary forces that promotes the percolation between soil particles. The mathematical instrument modelling this process is the Richards equation, cardinal equation in hydrology and starting point for many other process, such as pollutant transport. When the infiltration phase stops, i.e.

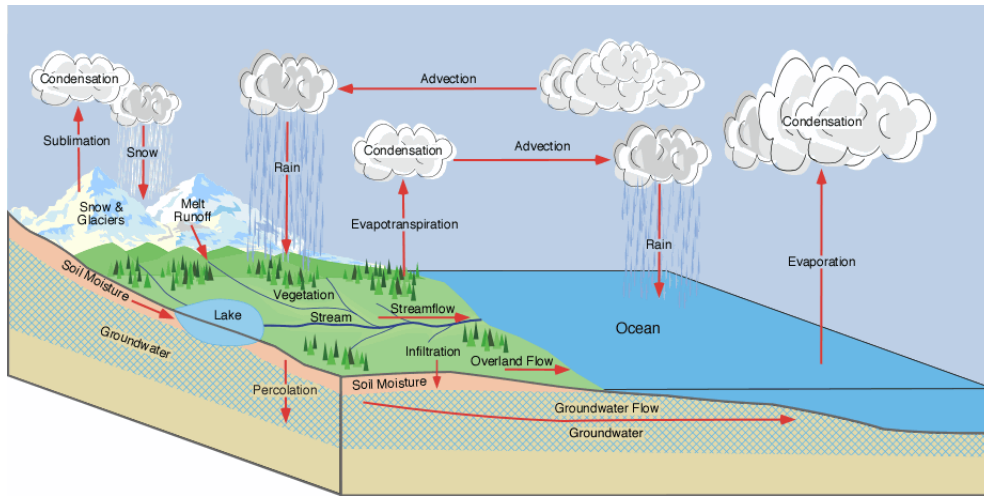


FIGURE 0.0.1. Hydrological cycle

Water moves from one reservoir to another by way of processes and can be stored in any one of the following reservoirs: atmosphere, oceans, lakes, rivers, soils, glaciers, snowfields, and groundwater.

no more water is applied to the surface and only the water previously infiltrated continues its journey in the ground, the redistribution phase begins. The interchange of these two phenomena names infiltration-redistribution cycle. Mathematically speaking we only have a change of boundary conditions in the model, see the section 2.1.

The study involves the knowledge of a lot of properties which are difficult to calculate or modelling, since the strong soil heterogeneity. For this reason, the determination of the space and time variability of certain infiltration variables, hydraulic parameters, initial and boundary conditions, is necessary in several applications in soil physics. The main applications are in the field of protection and management of environmental resources and on the hydrodynamic dispersion of contaminants in surface waters and soils, since the rapid changes suffered by the territory especially due to anthropogenic forcing and a growing danger for both the quality and the availability of water resources. The practices related, for example, to the storage of waste and/or agro-zootechnical activities play a role of great importance such as diffuse sources of pollution of groundwater and surface water. The only way

to control and remove at the origin the risk related to the huge injections of synthetic or natural chemical compounds is an hard territorial management.

Nowadays, the theoretical and applied research in the field of hydrology is oriented towards the development of techniques for the monitoring of water and organic, inorganic and microbiological pollutant transport and, at the same time, the development of specific calculation, mathematical and statistical tools for the prediction of phenomena. From the theoretical (and also experimental) point of view, we must face insurmountable difficulties to give an accurate and detailed definition of the transport properties in natural porous media.

With these premises, the thesis aims to evaluate the theoretical-applicative aspects related to the monitoring (i.e. the description of some aspects of resources at the current state or during a space-time evolution) and forecasting of soil water dynamics at practical interest scale. The work is focused on the development of models for the description of water flow in homogeneous and heterogeneous soils and the resolution of them. The spatial variations of the hydraulic properties of the soil and of the solute concentration are a consequence of soil heterogeneity. Therefore, considering these variations as a consequence of a limited knowledge of the porous medium, methods will be developed that allow to estimate the main statistical indices (mean, variance and covariance) of the transport process variables, namely: water content, pressure head, hydraulic conductivity and solute concentration. The validity of the predictions of mathematical models is linked not only to the correct schematisation adopted to describe the physical phenomena involved in the processes during the study, but also by their validation with reference to a typical case of study.

The main elements of innovation is the development of modern methods for monitoring the processes of soils, related to agro-zootechnical practices and to the use of soils as a waste disposal area, to be used at different scales for prediction aims. Further specific elements of innovation are tools (friendly-user softwares) to progress quickly in decontamination strategies for polluted sites and management or protection of groundwater.

Specifically, the thesis is composed of four chapters.

In the chapter 1, the general problem is introduced and all the variables involved are shortly described .

In the chapter 2, the main mathematical instruments, studied in depth and used during the work, are exposed, in order to give mathematical theoretical basis that allows the readers to better understand the chapter 3. In particular: PDEs equations, numerical and stochastic methods.

In the chapter 3, the main results are shown. The chapter is a sort of a dissertation of the papers published or submitted during the Ph.D course.

In the chapter 4, the conclusions are presented with some suggestions for future works.

CONTENTS

INTRODUCTION	i
List of Figures	vi
List of Tables	viii
Chapter 1. GENERAL PROBLEM AND STATE OF THE ART	1
Chapter 2. MATERIALS AND METHODS	18
2.1. Partial differential equations	18
2.2. Numerical methods	23
2.3. Stochastic methods	30
Chapter 3. RESULTS AND DISCUSSION	36
3.1. Data mining for geostatistics	36
3.2. Nonstationary unsaturated steady flows	46
3.3. Geostatistics for IoT in hydrology	90
Chapter 4. CONCLUSIONS	105
From theory to the applications	107
ACKNOWLEDGMENTS/RINGRAZIAMENTI	110
BIBLIOGRAPHY	126

LIST OF FIGURES

0.0.1 Hydrological cycle	ii
1.0.1 Soil formation	2
1.0.2 The subsurface water regimes	3
1.0.3 Particle-size classification	4
1.0.4 Hydraulic head	8
2.1.1 Fundamental solution of diffusive equation	22
3.1.1 Distribution of the iso-values of λ_c (cm) along a vertical cross-section at the Ponticelli site (Naples, Italy); vertical exaggeration: 250/6	40
3.1.2 Cumulative distribution function of α (m^{-1}) (red), and its log-transform $\zeta \equiv \ln \alpha$ (black)	42
3.1.3 Scaled variogram $\gamma_\zeta/\sigma_\zeta^2$ at the three measuring depths along the horizontal distance \boldsymbol{x}	43
3.2.1 Sketch of a flow taking place into a vadose zone delimited at the bottom ($z = 0$) by the water-table and at the top ($z = L$) by the soil surface	51
3.2.2 The normalized leading order pressure head $\Psi_0(z)/\Psi_0(\infty)$ as function of the scaled depth $z\alpha_G$, and different values of the non dimensional flux q_0/K_G	58

3.2.3 Cumulative distribution functions of measured (symbols) $Y \equiv \ln K_s$ (blue) and $\zeta \equiv \ln \alpha$ (red)	67
3.2.4 Residuals of Y versus residuals of ζ	69
3.2.5 Horizontal autocorrelation function for the log-conductivity Y	71
3.2.6 Dependence of the weight-functions (horizontal axe) $\omega_{\Psi Y} - \omega_{\Psi}$ upon the depth z (normalized by $\alpha_G^{-1} = 27.4\text{cm}$)	74
3.2.7 Distribution of the cross-variance $\sigma_{\Psi Y}$ (black), and the head-pressure variance σ_{Ψ}^2 (red) along the depth z (from the water-table)	76
3.2.8 Dependence of the weight function $\omega_{q_h} \equiv \omega_{q_h}(z)$ (horizontal axe) upon the dimensional depth z (vertical axe)	80
3.2.9 Normalized variance $\sigma_{q_z}^2(z)/\sigma_{q_z}^2(\infty)$ of the vertical specific flux as a function of the (dimensional) depth from the water-table under a few values of the dimensionless infiltration rate q_0	82
3.2.10 Distribution of the scaled head-factor $\psi(z)/\sigma_Y^2$ as computed from equation 3.2.43, and accounting for the data of the Ponticelli site along the dimensional depth z from the water-table ($z = 0$), and a few values of the dimensionless infiltration rate q_0	83
3.3.1 Distribution of the iso-values of $Y \equiv \ln K_s$ along a vertical cross-section at the Ponticelli site (Naples, Italy); vertical exaggeration: 250/6	95
3.3.2 Cumulative distribution functions of measured (symbols) $Y \equiv \ln K_s$ and theoretical CDF with the D - test of normal (null) hypothesis	98
3.3.3 Normalized variograms	99

LIST OF TABLES

1.0.1 Hydraulic functional relationships most used	12
1.0.2 Some Richards equation formulations	15
3.1.1 Estimates of the: i) mean, and ii) variance, together with the test (D) of normal/log-normal (null) hypothesis	42
3.2.1 Estimates of the: i) mean, ii) standard deviation, and iii) coefficient of variation together with the D - test of normal (null) hypothesis	66
3.2.2 Intervals of (5%)-confidence of $(\sigma_u/\mu_u)^2$ as determined by the u -data, and by the expression $\exp(\sigma_{\ln u}^2) - 1$	67
3.2.3 Intervals of 5%-confidence for the estimates of the mean and variance of Y at laboratory and field scale	68
3.2.4 Steady-state values of the experimental spatial variables	75
3.2.5 Lower and upper limit of the interval of confidence of the mean pressure head	75

CHAPTER 1

GENERAL PROBLEM AND STATE OF THE ART

Soil constitutes the interface between atmosphere and lithosphere. As a consequence of the fluxes of matter and energy between these two spheres and a large number of interacting physical, chemical and biological processes, the soil evolves into an exceedingly complex structure whose properties vary in space and time. Even if we abstract the system to a few important aspects it cannot still be described quantitatively, and consequently, all knowledge deduced from abstract models eventually must be verified by experiments.

From a geological point of view we can assume a profile similar to that shown in figure 1.0.1-D. The first zone encountered is the soil zone. This soil has developed from parent material through biological, figure 1.0.1-B, and other factors of weathering. At greater depths the soil merges with additional unconsolidated material and then, eventually, bedrock is encountered. The dimensions of these various zones are highly variable. Soil is a precious asset for human being that need a very long time to form as a very short time to be destroyed. It is a limited and hardly renewable resource and preserve, protect and defend it is one of the main human task of this century.

The subsurface can also be described in terms of water regimes that exist. In the most simple model, we reduce soil to a system that consist of three phases: solid soil matrix, liquid soil water, and gaseous soil air [*Sposito, 1989*][203]. We assume that the solid soil matrix is a rigid porous structure (porous medium or porous material), presumed to be invariant in time. Soil

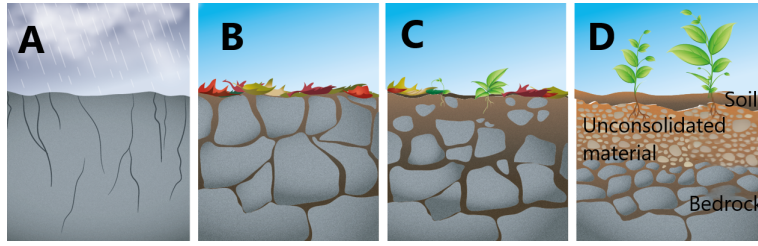


FIGURE 1.0.1. Soil formation

Soil starts to form when, due to atmospheric agents, the mother rocks disintegrate (A) and life forms can grow on the mineral thus formed (B). Then, organic residues of plants and animals, under the action of bacteria (C), create a surface layer called humus (D).

water consists of water with some dissolved chemicals and soil air is mostly composed of molecules with a negligible electrical field, so soil air fills all the available space. From an hydrological point of view the profile consists of the vadose zone and the phreatic zone, see figure 1.0.2. The system is unsaturated above the capillary fringe, meaning that some of the pore space is filled with both air and water. The capillary fringe is the subsurface layer in which groundwater seeps up from a water table by capillary action to fill pores and its extent is dependent on the porous material. Generally, it can extend a few centimeters for coarse material, or perhaps a meter for fine materials. Often in our study it can be neglected as its thickness is significant only when the water table largely fluctuates in the time [Li and Yeh, 1998][115], or the water table is shallow [Gillham, 1984][76]. The water table is the upper surface of the zone of saturation. The zone of saturation is where the pores and fractures of the ground are saturated with water. The water at the water table is at the atmospheric pressure; above the water table the pressure is less than atmospheric pressure and below it is greater.

In this thesis, for expediency, “soil” will mean the porous medium composed of solids with air and water (and/or other liquids) filling the inner spaces situated between the surface and bedrock. Soils are classified by the particles size of the media, see figure 1.0.3, and they can be distinguished in homogenous soils and heterogeneous soils, depending on whether the hydraulic properties are the same at every point in space. As soils are seldom

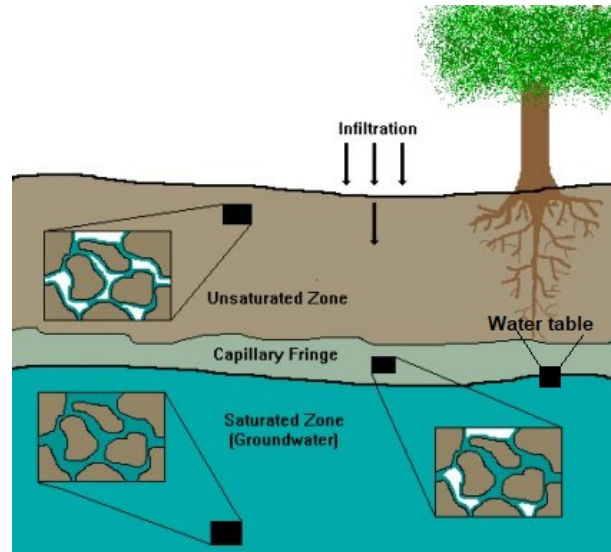


FIGURE 1.0.2. The subsurface water regimes

The vertical profile of the Earth's subsurface is divided into vadose zone (root zone, unsaturated zone and capillary fringe) and phreatic zone (water table and saturated zone).

homogenous over the past three decades a great deal of effort has been expended on the study of heterogeneity of soil properties, in particular the hydraulic conductivity (see the definition 1.0.10). Citing Freeze "heterogeneity is in the geology, whereas uncertainty is in the mind of the analyst" [*Freeze et al., 1990*][143]. The soils, as a result of their genesis, can exhibit layers that are mainly parallel to the surface and, generally, treated as deterministic variations [*Smith, 2002*][199]; but in a more general case variations are random and this leads to two important implications: different velocities in different parts of the medium and uncertainty in predictions. First is a feature of the physico-chemical system, second is a consequence of our limited knowledge of the system [*Selroos, 1996*][171]. Commonly, simulations of the effect of a randomly varying parameter in a system are done using Monte Carlo sampling, in which a random number generator produces a large number of samples of a parameter of interest with a desired statistical distribution. This set of parameter values may be used in a system to generate an output for each sample parameter value, so that an ensemble average behavior can be obtained [*Sharma et al., 1980; Smith and Hebbert, 1979*][126, 200]. Very

Millimeters (mm)	Micrometers (μm)	Phi (ϕ)	Wentworth size class
4096		-12.0	Boulder
256		-8.0	Cobble
64		-6.0	Pebble
4		-2.0	Granule
2.00		-1.0	Very coarse sand
1.00		0.0	Coarse sand
1/2	0.50	1.0	Medium sand
1/4	0.25	2.0	Fine sand
1/8	0.125	3.0	Very fine sand
1/16	0.0625	4.0	Coarse silt
1/32	0.031	5.0	Medium silt
1/64	0.0156	6.0	Fine silt
1/128	0.0078	7.0	Very fine silt
1/256	0.0039	8.0	Clay
0.00006	0.06	14.0	

FIGURE 1.0.3. Particle-size classification

The canonical definition of sediment grain sizes as defined by geologist Chester K. Wentworth [*Wentworth, 1922*].[230]

often some assumptions, as ergodicity and stationarity, are needed but the reader is referred to the section 2.3.

Two densities are of concern regarding the physical properties of soil solids. The *particle density*, ρ_p , given by

$$(1.0.1) \quad \rho_p = \frac{\text{Mass of solids}}{\text{Volume of solids}},$$

and the *bulk density* ρ_b :

$$(1.0.2) \quad \rho_b = \frac{\text{Mass of solids}}{\text{Volume of solids} + \text{Pore space}},$$

measured in [kgm^{-3}].

In any fixed volume, the fraction of space, i.e. the pore space, available to the water/air is assumed to be ω , which is called the *total porosity* of the medium and defined as

$$(1.0.3) \quad \omega = 1 - \frac{\rho_b}{\rho_p} .$$

Clearly, $0 < \omega < 1$ (the porosity would be either zero or one if we looked on a small scale), as $\rho_b < \rho_p$. The highest values tend to occur for materials in which the particle density is high or in which have a small percentage of pore space (e.g. coarse sand); conversely, smaller values tend to occur for materials with low particle density, as in organic soils and some volcanic soils, or an high percentage of pore space (e.g. clay). In general, the porosity can vary with position, or even pressure, but we will assume ω to be constant throughout the medium. When we say the porosity is constant, that means we are observing from a distance where there is uniformity in the porosity and the representative volume element is on an order where averages of percentage pore space are constant over the entire medium [*Juri et al, 1991*][**222**].

Maybe, the most important variable involved in the soil water physics is the *water content* or *soil moisture*, the dimensionless quantity of water contained in the soil. The most elementary measurement technique, for it, is by weighing the sample, followed by oven drying and weighing once again. But there are also several geophysical methods available that can approximate in situ soil water content [*Juri et al, 1991*][**222**]. Water content can be given on mass (gravimetric) or a volumetric basis, respectively:

$$(1.0.4) \quad \vartheta_m = \frac{\text{Mass of water}}{\text{Mass of solids}} ,$$

$$(1.0.5) \quad \vartheta = \frac{\text{Volume of water}}{\text{Total volume}} ;$$

two definitions can be related through the expression:

$$(1.0.6) \quad \vartheta = \frac{\rho_b}{\rho_{H_2O}} \vartheta_m ,$$

where ρ_{H_2O} is the water density. In this thesis we will often prefer the 1.0.5 despite the 1.0.4, but the majority of our applications will probably be better served by S , the *effective saturation* or *reduced water content* or normalized water content, defined by:

$$(1.0.7) \quad S = \frac{\vartheta - \vartheta_r}{\vartheta_s - \vartheta_r},$$

where ϑ_s is the *volumetric water content at saturation* and ϑ_r is the *residual water content*. The residual water content is somewhat arbitrarily defined as the water content at which the corresponding hydraulic conductivity (which we will discuss later, see the equation 1.0.10) is appreciably zero, but very often the equation 1.0.7 is used with $\vartheta_r = 0$. The effective saturation was defined, first, by Van Genuchten [*Van Genuchten, 1980*][**218**] and it is also called normalized water content as it varies between zero and one.

The flow of both surface water and groundwater is driven by differences in potential energy. In the case of surface water, flow occurs in response to differences in gravitational potential energy, due to elevation differences, in other words, and unsurprisingly, water flows downhill, from high potential energy to low potential energy. In groundwater systems, things are a bit more interesting. Unlike surface water, which is in contact with the atmosphere and therefore rarely under pressure, water in groundwater systems is isolated from the land surface, with the consequence that the water can also have potential energy associated with pressure. In extreme cases, water in confined aquifers may be under sufficient pressure to drive flow upward, against gravity. Note that we restrict ourselves to the simple case where the kinetic energy may be neglected with respect to the potential energy. Kinetic energy depends both on water flow (in a macroscopic scale) and on thermal motion of molecules (microscopic scale). We will thus be restricted to consider sufficiently slow flow with sufficiently small temperature gradients. To define the flow direction, we need to account for the two types of potential energy: the potential energy contained by the water by virtue of its elevation above a reference datum (gravitational potential energy) and the additional energy contributed by pressure (tensiometer pressure potential energy). This last potential encompasses the effects of surface adsorption, surface tension, air

pressure, hydrostatic pressure and many others. An important special case is a rigid, unsaturated soil where the air pressure is constant everywhere and equal to the atmospheric pressure. this energy is associated with a change in the curvature of the water-air interface and it is negative for unsaturated soil. In this case the potential is named matric potential. Generally, the potential energy of the soil water may be defined by the work that is required for moving an infinitesimal volume of water from a reference state into the desired state within the soil. Note that there is no need to specify which is the reference state as the gradient of energy, which is the physically relevant quantity, is independent of it. Actually, in accordance with the recommendations of the International Soil Science Society [*Bolt, 1976*][18], we distinguish three partial potentials. In addition to those already exposed, the osmotic potential exists, i.e. a measure of the potential of water to move between regions of differing concentrations. The sum of these three potential is called soil water potential, a concept having a long and well documented history in soil physics [*Corey and Klute, 1985; Hillel, 1998; Jury et al., 1991*].[39, 89, 222]

In fluid dynamics, head is a concept that relates the energy in an incompressible fluid to the height of an equivalent static column of that fluid. From Bernoulli's Principle [*Hydrodynamica, Britannica Encyclopedia*][1], the total energy at a given point in a fluid is the energy associated with the movement of the fluid, plus energy from static pressure in the fluid, plus energy from the height of the fluid relative to an arbitrary datum (often the sea level). Head is expressed in units of height and it is obtained dividing the potential energy by the specific weight. Heads of our interest are: the *elevation head* (z), *pressure head or capillary suction* (ψ), and the *hydraulic head* (h). The first two are the heads, respectively, derived from the potential energies described above and have the dimension of a length [m]. Now, we can give another definition of the water table in terms of pressure head. The water table is defined as the "surface on which $\psi = 0$ "; below $\psi > 0$ (phreatic zone) and above $\psi < 0$ (vadose zone). The hydraulic head can be expressed as:

$$(1.0.8) \quad h = \psi + z ,$$

if the z -axis is positive upward oriented, otherwise:

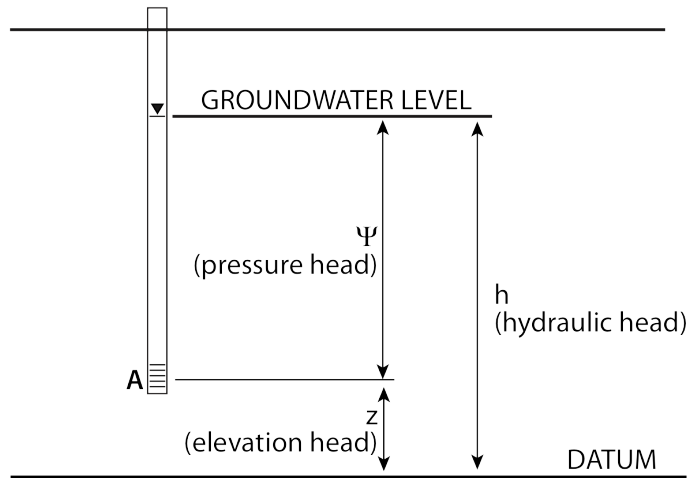


FIGURE 1.0.4. Hydraulic head

Hydraulic head measurements are essential pieces of information that are required for characterizing groundwater flow systems.

$$(1.0.9) \quad h = \psi - z ;$$

and the measurement instrument is the piezometer (see figure 1.0.4). A piezometer is a hollow tube, or pipe, drilled or forced into a profile to a specific depth. Water rises inside the tube to a level corresponding to the pressure head at the terminus. The level to which water rises in the piezometer, with reference to a datum is the hydraulic head [Yolcubal *et al.*, 2004][94]. The dimension is a length too.

The distribution of hydraulic head through an aquifer determines where groundwater will flow. In a hydrostatic example, where the hydraulic head is constant, there is no flow. However, if there is a difference in hydraulic head from the top to bottom due to draining from the bottom, the water will flow downward, due to the difference in head, also called the hydraulic gradient (dh/dz). Observe that the head of groundwater at the water table is equal to the elevation of the water table relative to an arbitrarily chosen reference elevation as the water pressure at such locations is equal to atmospheric pressure (and for the restriction about the kinetic energy).

Hydraulic conductivity, symbolically represented as K , is another fundamental property of soils that describes the ease with a fluid (usually water) can move through pore spaces or fractures. In unsaturated soils K depends on S (or that is the same on the water content ϑ):

$$(1.0.10) \quad K(S) = K_S K_r(S) ,$$

where $K_r(S)$ names relative hydraulic conductivity; while in saturated soils K can be regarded as a constant, $K = K_S$ [Bear, 1972].[13] This yields for homogenous soils, while for heterogeneous soils, generally, K_S depends on depth, i.e. $K_S = K_S(z)$. The hydraulic conductivity is measured in [ms^{-1}].

Measuring K for saturated soils is not an hard task like in unsaturated soils. The hydraulic conductivity can be computed both with an empirical approach by which it is correlated to soil properties like pore and particle size, soil texture and with experimental approach by which the hydraulic conductivity is determined from hydraulic experiments using Darcy's law (that it will be discussed later) [van Bavel and Kirkham, 1948][216]. As a consequence, various methods for estimating $K(S)$ have been explored. The methods may be grouped into three categories: (i) using purely statistical regression analysis where K is related to soil properties like bulk density, fraction of silt and clay, and organic matter [Wosten and van Genuchten, 1988][236]; (ii) assuming a simplified geometrical structure for the pore space, the parameters of the soil are measured and used to calculate K [Mualem, 1976; van Genuchten, 1980][218]; (iii) K is deduced from monitoring the water content and the water potential as a function of time and space. This method has been used to estimate the spatial variations of the saturated hydraulic conductivity in aquifers [Yeh, 1986][239] and it is the current state of the art method for measuring the hydraulic functions in the laboratory [Kool et al., 1985; Parker et al., 1985; Toorman et al., 1992][3, 102, 101] and in the field [Green et al., 1986][146]. Some of the methods used attempt to resolve the functional form of the hydraulic conductivity, they are called the "inverse methods" [Mahbod et al., 2010; van Dam et al., 1992][122, 99]; other, called "parameter estimations", require a parametric model for the hydraulic functions yielding the

values of the parameters which lead to an optimal agreement with the data [Mualem, 1976; van Genuchten, 1980][127, 217].

The relationship between the water content ϑ (or S) and the pressure head ψ , $\vartheta(\psi)$, has a crucial role for modeling the movement of water in soils, and it is called “soil water characteristic” or “water retention curve”. The trend of the curve offers an instant overview of the hydrological properties of a soil. In general, soils with a high reservoir capacity, capable of receiving large quantities of water (e.g. soils with a rich in colloids, such as clay soils, or in organic matter), have water retention curves expanded in width, while coarse soils or poor in colloids (e.g. sandy or stony soils) have tight water characteristics. The width of the curve is related with the total porosity of the soil [Tassinari, 1976; Belsito, 1988][210, 16]. All possible curves are limited by the desorption curve, $\vartheta_d(\psi)$, and the adsorption curve, $\vartheta_a(\psi)$, i.e. the two limit cases. Desorption occurs when water is slowly and monotonically removed from an initially water saturated soil until the soil is air saturated. After that ψ get a certain value, called air-entry value, the air can enter the porous medium, the water content decreases monotonically and the negative pressure head increases, with continuous stretches and discontinuous jumps due to cavities [Feder, 1988][63]. The adsorption curve describes the reverse process. Several methods exist to build the water retention curve for a given soil on a logarithmic scale or on a linear scale. Experimentally, a hanging water column, also called “Haines” apparatus is used [Dane and Hopmans, 2002][53]; empirically, the suction method [Haines, 1930; Klute, 1986b][108, 83] and the pressure method [Richards and Fireman, 1943][148] are the most used, combined too. Recently, a pore space representation, called angular pore space model, was proposed [Tuller et al., 1999; Or and Tuller, 1999,2000; Tuller and Or, 2001][121, 133, 134, 214], which offers a more realistic representation of natural pore space and leads to natural relationships for the interfacial areas between phases and to natural expressions for unsaturated hydraulic conductivity.

Note that, through the water retention curve, the hydraulic conductivity can be done in terms of ψ just like S . Several algebraic forms have been used to describe soil water characteristics. In the table 1.0.1, we present some examples of water retention curves and expressions of K/K_S . Unless explicitly

specified, the relations which will be taken in consideration in this thesis is the number 6 of the table 1.0.1.

There are many other forms and variations as many scientists have focused on the topic [*Campbell and Shiozawa, 1992; Rossi and Nimmo, 1994; Fayer and Simmons, 1995; Kosugi, 1996*][**26, 156, 62, 109**].

Important to mention a second application of the soil water characteristics in the rough ecological assessment of a site where typical variables of interest are the storage capacity of the soil and the availability of the stored water for plants.

To study the flow of soil water, another important clarification is needed. We are going to talk about stationary systems or nonstationary systems. In a stationary system all temporal changes are negligible, so, if the system is described by the function $\phi(t, \dots)$, the steady-state condition implies $\partial_t \phi(t, \dots) = 0$. As a consequence, the state variables of the soil are also constant in time. The soil thus appears to be unchanging with the exception of the water flowing through it. This is denoted as a state of dynamic equilibrium. Conversely, the non-stationary systems are those where the soil water flux varies in space and time, and therefore the variables involved too. We will find that the exact description is rather difficult and that the arising equations can only be solved analytically for highly simplified cases. For this reasons, even if the first is a rarer case, it is also important to study to better understand the conditions and get solutions when it is not possible in the other case. In fact, the steady case is the large-time asymptotic condition for most infiltration boundary conditions found at the soil surface. More realistic systems are studied using numerical simulations.

The primary flow equation to be presented, which is a starting point to examine the fluid dynamics, both in saturated and unsaturated porous media, is the Darcy's law, formulated as an empirical equation in the 19th century. Darcy's law combined with conservation mass gives as a result a continuity equation that can has several different forms and, generally, for unsaturated soils, it is called Richards equation. Darcy's law states that *flux*, or flow per unit area, q , is proportional to the gradient of the hydraulic head and the hydraulic conductivity:

	K/K_S (hydraulic relative conductivity)	S or ψ (water retention curve)
1. GR; [Gardner, 1958; Russo, 1988][73, 159]	$\exp(\alpha\psi)$	$S = [\exp(\alpha\psi/2)(1 - \alpha\psi/2)]^{2/(m+2)}, m > 0$
2. VG [Van Genuchten, 1980][218]	$S^p [1 - (1 - S^{1/m})^m]^2, p = 0.5$	$S = (1 + \alpha\psi ^n)^{-m}, n = 17(1 - m), 0 < m < 1$
3. BC [Brooks and Corey, 1964][21]	$\begin{cases} S^{2m+3} & \text{if } \alpha\psi < -1 \\ 1 & \text{if } -1 < \alpha\psi < 0 \end{cases}$	$\begin{cases} \alpha\psi ^{-1/m} & \text{if } \alpha\psi < -1 \\ 1 & \text{if } -1 < \alpha\psi < 0 \end{cases}, m > 0$
4. FBW [Fujita, 1952; Broadbridge and White, 1987][71, 19]	$\frac{(m-1)S^2}{(m-S)}$	$\psi = \alpha^{-1} \left(1 - \frac{1}{S}\right) + \frac{1}{m} \ln \left[\frac{(m-1)S}{m-S} \right]^{\alpha^{-1}}, m > 1$
5. Linear	S	$\psi = \alpha^{-1} \ln S$
6. LI [Lessoff and Indelman, 2003][114]	$S^{1/\beta}, \beta < 1$	$\psi = (\alpha\beta)^{-1} \ln S$

TABLE 1.0.1. Hydraulic functional relationships most used

α is the inverse capillary length scale, and, typically $1/\alpha$ varies from a few centimeters in sandy soils to a few meters in clay soils;

$$(1.0.11) \quad q = -Kgradh ;$$

q is also called *Darcian velocity* and, obviously, has dimension $[ms^{-1}]$. Actually, the equation 1.0.12, today, is called Buckingham-Darcy law [Sposito, 1986][202], since Buckingham was the first to postulate the Darcy's law in the more general form in which the unsaturated hydraulic conductivity depends on water content [Buckingham, 1907][23]. In the contest of infiltration calculations, i.e. in a one-dimensional vertical flow, if we adopt the convention of measuring z (a convention holding also forward, with the water table at $z = 0$), the measure of distance in the direction of flow, positive downwards and remembering the definition 1.0.9 we can redefine the flux as:

$$(1.0.12) \quad q_z = K \left(1 - \frac{d\psi}{dz} \right) .$$

Note that Darcy's law is valid only for laminar flow (or streamline flow), i.e. when a fluid flows in parallel layers, with no disruption between the layers. Laminar flow generally occurs when the fluid is moving slowly or the fluid is very viscous [Rogers, 1992][151]. The dimensionless Reynolds number, Re , is an important parameter that describe whether fully developed flow conditions lead to laminar ($Re < 1$) or turbulent flow ($Re > 1$) and it depends on the flux q_z [Bear, 1972][13].

Actually, the Darcian velocity is a fictitious velocity since it assumes that the flow occurs in the entire cross-section of the soil sample. In fact, within the column, the water only flows through the pore space and thus has the higher *average vertical velocity*:

$$(1.0.13) \quad v = \frac{q_z}{\vartheta} ,$$

also called convective velocity, advective velocity and pore water velocity. For fully saturated conditions ϑ can be replaced by the porosity ω [Warrick, 2003][228].

The mathematical descriptions of soil water dynamics will present a set of simplifying assumptions. Perhaps the most important assumption is that the

movement of water into relatively dry soil can be described without explicit treatment of the flow of air. Infiltration or absorption involves the replacement by water of air in the soil pores. This is not necessarily the case when rainfall moves into the surface of a soil. Air can compress and cause a reduction in the pressure gradient across a wetting "front" of water entering a soil, and it also has a viscous resistance to movement through the soil ahead of entering water. However, the hydraulic potential gradient required to move air against the resistance of the soil pore structure is often quite small compared to the capillary pressure gradient. Nevertheless, air compression, in some cases, will modify to some extent the results shown here. The vapor-based movement due to thermal gradients, the effects of soil swelling and the soil water hysteresis, mentioned above, are also ignored. The general flow equation for water in unsaturated soil, the Richards equation, is obtained from the Darcy-Buckingham equation, 1.0.12, and the continuity equation:

$$(1.0.14) \quad \frac{\partial \vartheta}{\partial t} + \frac{\partial q}{\partial z} = j ,$$

where j is an external gain/loss rate such as root water use, which will be left at zero for the present purposes. The equation 1.0.14 combined with 1.0.12 leads to:

$$(1.0.15) \quad \frac{\partial \vartheta}{\partial t} + \frac{\partial}{\partial z} \left[K(\vartheta) \left(1 - \frac{\partial \psi}{\partial z} \right) \right] = 0 ,$$

an highly non-linear second order partial differential equation with two dependent variables and parabolic in the major of cases (see section 2.1)[*Richards, 1931*][**147**], reducing to an ordinary differential equation for 1-D steady-state case. The equation has two terms: one expressing the contribution of the suction gradient and the other originated from the gravitational component of the total potential; whether the one or the other term predominates depends on initial and boundary conditions and on the stage of the process considered [*Hillel, 1980*][**88**]. Generally, if $\frac{\partial \psi}{\partial z} \gg 1$, capillary suction predominates, otherwise, $\frac{\partial \psi}{\partial z} \ll 1$, gravity is more relevant and if considered zero this leads to a simpler quasi-linear equation, instead of a nonlinear one. The number

Equation	Basis
1. $\frac{\partial \vartheta}{\partial t} + \frac{\partial K}{\partial z} - \frac{\partial \psi}{\partial z} \frac{\partial K}{\partial z} - K \frac{\partial^2 \psi}{\partial z^2} = 0$	<i>mixed</i>
2. $\frac{\partial \vartheta}{\partial t} - \frac{\partial}{\partial z} \left(D \frac{\partial \vartheta}{\partial z} \right) + \frac{\partial K}{\partial z} = 0$	ϑ
3. $C \frac{\partial \psi}{\partial t} - \frac{\partial}{\partial z} \left(K \frac{\partial \psi}{\partial z} \right) + \frac{\partial K}{\partial z} = 0$	ψ
4. $\frac{\partial S}{\partial t} - \frac{\partial}{\partial z} \left(D \frac{\partial S}{\partial z} \right) + \frac{\partial K}{\partial z} = 0$	S

TABLE 1.0.2. Some Richards equation formulations

- The equation 1 is the extended form of the equation 1.0.15;
- the equation 2 is the “ ϑ – based” equation where D is the *diffusivity* and $D(\vartheta) \equiv K \frac{d\psi}{d\vartheta}$, having dimension $[m^2 s^{-1}]$;
- the equation 3 is the “ ψ – based” equation where C is the *specific soil water capacity* and $C(\psi) \equiv \frac{d\vartheta}{d\psi}$, having dimension $[m^{-1}]$;
- the equation 4 is the formulation in S , linearly obtained from the 1 using the definition 1.0.7.

of dependent variables may be reduced from two to one providing a soil water characteristic relationship, in this way we may eliminate ψ and have a “ ϑ – based” equation or eliminate ϑ and have a “ ψ – based” equation. The table 1.0.2 shows some different forms of Richards equation adopted in this thesis [Celia, 1990][29].

With specific description of soil characteristics, analytical solutions of the local infiltration can be found. Some of them are approximations, other are exact solutions. In both of cases they cannot provide the profile of water content without large simplifications of the soil description: most of them assume that diffusivity is constant. Furthermore, these solutions have restrictive conditions of application: initially dry profile, constant flux at the soil surface, for instance. To deal with natural conditions, numerical tools are needed to solve the water flow movements [Varado et al., 2006][131]. However, analytical approaches for unsaturated flow are attractive and helpful for better understanding the physics of unsaturated flow in porous media for many reasons. They can be also used as screening tools for quick evaluations and for field cases where numerical simulations are not feasible. Moreover they may considered as references and benchmarks during validation

of the numerical scheme processes. Among the existing analytical solutions are those for steady-state flow [*Warrick, 1988; Salvucci, 1993; Zhu and Mohanty, 2002; Sadeghi et al., 2012; Hayek 2015*][**227, 170, 243, 120, 86**] and others for transient flow [*Zimmerman and Bodvarsson, 1989; Serrano, 1998, 2004; Hayek, 2014*][**244, 172, 173, 85**]. Analytical solutions for the transient Richards equation are restricted to specific soil water retention characteristics and hydraulic conductivity functions. These include those based on the exponential model [*Gardner, 1958; Russo, 1988*][**73, 160**] and those based on rational forms of the soil hydraulic conductivity and moisture retention functions [*Rogers et al., 1983; Broadbridge and White, 1987,1988; White and Broadbridge, 1988; Sander et al., 1988; Triadis and Broadbridge, 2010; Basha, 2011*][**24, 19, 20, 231, 212, 10**]. Linearization of the Richards equation simplify the analytical modeling and has been used in numerous studies [*Basha, 1999; Green and Ampt, 1911; Philip, 1957, 1969; Warrick, 1975; Warrick et al. 1985; Chen et al., 2001, 2003; Wang and Dooge, 1994; Menziani et al., 2007*][**9, 81, 137, 138, 226, 7, 59, 58, 224, 118**]. Solutions of Richards equation where the Brooks and Corey model [*Brooks and Corey, 1964*][**21**] and the Van Genuchten model [*Van Genuchten, 1980*][**218**] are applied, the most used models for water retention characteristic, deserve particular mention [*Nasseri et al., 2012; Hayek, 2016; Caputo and Stepanyants, 2008; Ross and Perlangue, 1994; Witelski, 1997, 2005; Zlotnik et al., 2007*][**119, 87, 27, 155, 234, 235, 215**]. Due to this nonlinearity the simplest way to get a solution is by a numerical approach. As a result, scientists in the past four decades have proposed several numerical methods for modeling unsaturated flow and infiltration problems [*Haverkamp et al., 1977; Van Genuchten, 1982; Celia et al., 1990; Huang et al., 1994; Pan et al., 1996; Kavetski et al., 2002; Farthing et al., 2003; Bause and Knabner, 2004; Miller et al., 2006; D'Haese et al., 2007; Li et al., 2007; Chen and Ren, 2008; Fahs et al., 2009; Casulli and Zanolli, 2010; Juncu et al., 2012; Ross, 1990*][**150, 75, 29, 110, 111, 44, 128, 12, 41, 32, 82, 30, 117, 28, 72, 154**].

However, nowadays, Richards equation solution strategy is still a subject to research, also because, often, it constitutes the starting point for the study of solute transport in the groundwater. Solute transport is a problem of great importance in environmental science to understand how chemical or biological

tracers and a broad range of pollutants are transported through a porous medium. Pollution of the subsurface is often considered to be either point source pollution or diffuse source pollution. Point source pollution covers a limited area, and is often caused by accidental or illegal spills. Diffuse source pollution covers a large area and is in general caused by large-scale application of compounds as fertilizer, pesticides or atmospheric deposition at the soil surface. Pollution is not necessarily man induced but may be due to geological or geohydrological causes, e.g., pollution with arsenic or salt. A distinction can be made among the polluting species that will be considered: dissolved and immiscible, conservative and reactive. Dissolved pollutants or aqueous phase pollutants will spread with groundwater due to groundwater flow, diffusion and dispersion. Immiscible pollutants will spread as a separate phase (non-aqueous phase liquids, NAPL). Conservative pollutants are those that do not react with the solid soil material or with other pollutants, and they will not be degraded by biological activity. Reactive solutes may enter or leave the water phase through adsorption or desorption, chemical reactions, dissolution or precipitation and biodegradation. For modeling such processes, the first step is to define the flow regime. If a mathematical model is developed, the approach often includes Richards equation for water flow, followed by a specific model for solute transport.

CHAPTER 2

MATERIALS AND METHODS

Soil physics was born as an empirical science and it has remained so for the most part to the present, due to the highly nonlinear nature and random components of important processes involved. As scientific discipline it is rather young with its roots barely reaching the first half of last century. Even if soil physics does not have the elegance and the formalism just like the old sciences, it is able to provide quantitative answers to various complex problems. Soil physics is a collection of often disparate theories, experiences, hypothesis and beliefs. The role of a soil physics scientist is to reflect the character of a such evolving discipline and to introduce and illustrate the tools which are currently used [Roth, 1996][157]. For this purpose, this chapter is dedicated to the main mathematical tools that have been studied in depth and used to obtain the results presented in the next chapter. The treatment does not claim to be extremely rigorous, but only to provide the necessary basis for a fluid reading of the rest of the thesis also for those who are specialist in other fields of study.

2.1. Partial differential equations

Almost always, physical models representing natural phenomena are described by a partial differential equation (PDE) or a system of PDEs. A partial differential equation is an equation linking an unknown function depending on two (or more) independent variables, usually space and time, to

its derivatives. If second order derivatives appear in the equation, the last will be a second order PDE; otherwise a first order PDE, since higher orders are very rare. The general form of a second order PDE (in two variables) is:

$$(2.1.1) \quad F(D^2u(x, y), Du(x, y), u(x, y), x, y) = 0;$$

expanding and writing only the maximum order terms:

$$(2.1.2) \quad A(x, y)u_{xx} + 2B(x, y)u_{xy} + C(x, y)u_{yy} + \dots = 0,$$

where $u_{xy} = u_{yx}$ is assumed. Depending on whether the terms are linear or not, the equation is linear or nonlinear, respectively. They can be classified according to the sign of the discriminant $\Delta = b^2 - ac$ in the following way:

- hyperbolic for $\Delta > 0$,
- elliptic for $\Delta < 0$,
- parabolic for $\Delta = 0$.

Since many problems in subsurface transport give rise to partial differential equations that belong to the class of parabolic equations, we will now focus on the PDEs of this type where the variables will be the time t and a spacial variable x , or z if the variable represents the depth. For a well-posed problem, initial and boundary conditions must be clear. By specifying particular initial conditions and boundary conditions, we try to encode mathematically the physical conditions, constraints, and external influences which are present in a particular situation. For example, in the transport, they constitutes answers about background conditions as what happens along the soil surface, lower root zone, water table and so on. For transient problems, the boundaries are with respect to the time domain as well as spatial boundaries; for steady-state problems, boundaries are only spatial (actually the equation degenerate in an ordinary differential equation, ODE, easier to treat). A solution to the differential equation, if it is unique and satisfies initial/boundary conditions, constitutes a prediction about what will occur under these physical conditions. Thus, the question of uniqueness of solution is extremely important in the general theory. It needs that the governing equations and the auxiliary (initial

and boundary) conditions are mathematically well-posed, and therefore that the following three conditions are met:

- (1) the solution exists,
- (2) the solution is unique,
- (3) the solution depends continuously on the data.

The existence does not usually create any difficulty, just like in our case. The usual cause of non-uniqueness is a failure to properly match the auxiliary conditions to the type of governing PDE. For linear problems, powerful and well-known theorems are available to guarantee the points 1 and 2, but for nonlinear conditions the basic existence and uniqueness properties are less well understood. In this case, experience, imagination and effort in defining the problem are important. The third criterion above requires that a small change in the initial or boundary conditions should cause only a small change in the solution. If the third condition is not met, the errors in the data will propagate causing the solution to blow up [*Pivato, 2010*]. [140]

The simplest example and prototype of a parabolic equation is the diffusion equation:

$$(2.1.3) \quad u_t = Du_{zz} ,$$

in heat transfer it is called the heat equation, and, in hydrogeology, it is sometimes called the dispersion equation. It models, for example, the molecular diffusion of a chemical contaminant of concentration $u = u(z, t)$, dissolved in an immobile liquid. The positive constant D , having dimensions $[L^2T^{-1}]$, is the diffusion coefficient, which measures the ability of the contaminant to diffuse through the liquid. The simplest solutions of (2.1.3) are plane wave solutions of the form:

$$(2.1.4) \quad u = \exp[i(kz + wt)] ,$$

where k is the wave number and w is the frequency. Substituting this form into (2.1.3), given the dispersion relation $w = ik^2D$, we obtain solutions of the form:

$$(2.1.5) \quad u(z, t) = \exp(-k^2 Dt) \exp(ikz) .$$

Finally, superimposing all of the plane wave solutions over all wave numbers, i.e. :

$$\int_{-\infty}^{+\infty} \exp(-k^2 Dt) \exp(ikz) dk = \frac{1}{\sqrt{4\pi Dt}} \exp(-z^2/4Dt) ,$$

we get the most important solution called the fundamental solution:

$$(2.1.6) \quad u(z, t) = \frac{1}{\sqrt{4\pi Dt}} \exp(-z^2/4Dt) .$$

Note that the right-side of this expression is just the Fourier transform of the Gaussian function $y = \exp(-k^2 Dt)$. The fundamental solution (2.1.6) is the concentration that arises from an initial, unit contaminant source localized at the origin in a one-dimensional domain. The time cross sections, or time snapshots, of the concentration for different times, have the form of a bell-shaped curve, as the figure 2.1.1 shows. Since we think of diffusion in terms of the random motion and collisions of molecules, it is not surprising that the fundamental solution is a normal probability density.

If we are interested to solve the Cauchy problem:

$$(2.1.7) \quad \begin{cases} u_t = Du_{zz} \\ u(z, 0) = \phi(z) \quad z \in \mathbb{R}, t > 0 \end{cases} ,$$

the solution is the convolution (over z) of the fundamental solution, that we indicate here with $g(z, t)$, and the initial condition:

$$(2.1.8) \quad u(z, t) = g(z, t) * \phi(z) = \int_{-\infty}^{+\infty} g(z - \xi, t) \phi(\xi) d\xi ;$$

in fact, in applied analysis, the convolution operation is usually regarded as a solution operator that maps the initial profile into the solution profile at time t . This result will be useful in many cases. In many contaminant transport

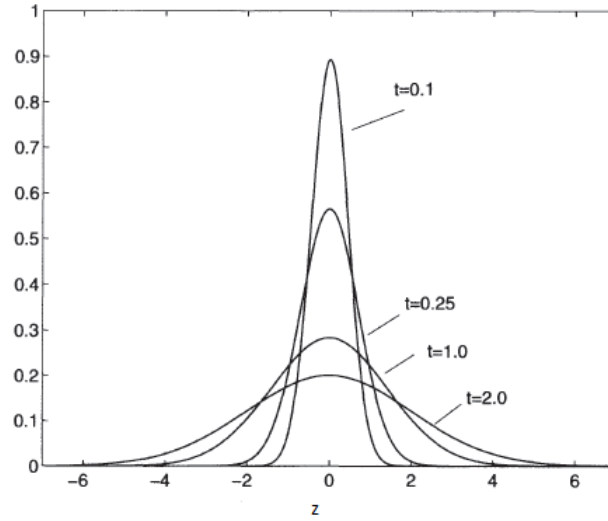


FIGURE 2.1.1. Fundamental solution of diffusive equation
Time profiles of the fundamental solution showing the diffusion of a unit amount of contaminant released initially at $z = 0$.

problems the porous domain is semi-bounded. Let us consider this example of Cauchy-Dirichlet problem, or the initial-boundary value problem, for the diffusion equation on a semi-infinite domain:

$$(2.1.9) \quad \begin{cases} u_t = Du_{zz} \\ u(z, 0) = \phi(z) \quad z \in \mathbb{R}, t > 0, \\ u(0, t) = 0 \end{cases}$$

where $t > 0$ and $z > 0$. To solve the problem, it can be used the method of reflection or the Laplace transform method. Actually, many problems on semi-infinite domains can also be solved by Laplace transform method, commonly used in hydrogeology, although, the inversion problem back from the transform domain is often impossible to perform analytically, and therefore numerical methods of inversion are often required [Logan, 2001]. [116]

The third condition of the system 2.1.9 represents the Dirichlet boundary condition, having the general form:

$$(2.1.10) \quad \begin{cases} u(a, t) = \alpha_1(t) \\ u(b, t) = \alpha_2(t) \end{cases},$$

where a and b are the eventually domain extremes. Another type of boundary condition to mention is the Neumann condition, which gives information about the derivative:

$$(2.1.11) \quad \begin{cases} u'(a, t) = \alpha_1(t) \\ u'(b, t) = \alpha_2(t) \end{cases}.$$

For instance, in water flow problems, Dirichlet conditions are conditions where the variable ϑ , S , ψ , are specified; Neumann conditions express conditions about vertical or horizontal flow (the flux q), or surface evaporation.

There is no general theory known concerning the solvability of all partial differential equations, given the rich variety of physical, geometric and probabilistic phenomena which can be modeled by PDEs. Instead, research focuses on various particular PDEs that are important for applications, with the hope of giving strategy clues for other equations. So by solving a partial differential equation in the classical sense we mean if possible to write down a formula for a classical solution [*Evans, 1998*][57]. Some analytical methods are: characteristic method, spectral method, calculus of variations [*Salsa, 2010*][169]. This is almost never feasible and it need to shrink to look for approximate solutions, analytical (e.g. through perturbation methods) or numerical. Analytical approximation methods often provide extremely useful information concerning the character of the solution for critical values of the dependent variables but tend to be more difficult to apply than the numerical methods, that will be discussed in the next section in more detail.

2.2. Numerical methods

Universal analytical techniques to solve PDEs do not exist, so, in the most cases, we need to find numerical solutions, and, even if an analytical solution exists and we are able to calculate it, often it may result useless for our purpose because it may be difficult to handle.

In literature various methods exist to solve partial differential equations. Here we will briefly discuss some of them.

- (1) Finite Difference Method: it is a numerical procedure which solves a partial differential equation by discretizing the continuous physical domain into a discrete finite difference grid, approximating the individual exact partial derivatives in the partial differential equations by algebraic finite difference approximations (FDA), substituting the FDA's into the partial differential equations to obtain an algebraic finite difference equation (FDE), and solving the resulting algebraic finite difference equations for the dependent variable.
- (2) Finite Volume Method: it is a method for representing and evaluating partial differential equations in the form of algebraic equations. Similar to the finite difference method, values are calculated at discrete places on a meshed geometry. "Finite volume" refers to the small volume surrounding each node point on a mesh. In the finite volume method, volume integrals in a partial differential equation that contain a divergence term are converted to surface integrals, using the divergence theorem. These terms are then evaluated as fluxes at the surfaces of each finite volume. Because the flux entering a given volume is identical to that leaving the adjacent volume, these methods are conservative.
- (3) Finite Element Method: the functions are represented in terms of basis functions and the partial differential equations is solved in its integral form. In the finite element method (FEM) the domain is partitioned in a finite set of elements, $\{\Omega_i\}_{i \in I}$, so that $\{\Omega_i \cap \Omega_j\}_{i,j \in I} = \emptyset$ for $i \neq j$, and $\cup \bar{\Omega}_i = \bar{\Omega}$. Then the function is approximated by $u_h = \sum a_i \Phi_i$ where Φ_i are functions that are polynomials on each Ω_i (i.e. piecewise polynomials). Usually the functions Φ_i are continuous polynomials of a low degree.

We will now examine in more detail finite differences for linear diffusion, well understood from a theoretical viewpoint and considered in many textbooks on numerical methods, which often leads towards an expression for Richards equation.

As we saw, the objective of a finite difference method for solving a partial differential equation (PDE) is to transform a calculus problem into an algebraic problem by:

- (1) Discretizing the continuous physical domain into a discrete difference grid.
- (2) Approximating the individual exact partial derivatives in the partial differential equation (PDE) by algebraic finite difference approximations (FDAs).
- (3) Substituting the FDAs into the PDE to obtain an algebraic finite difference equation (FDE).
- (4) Solving the resulting algebraic FDEs.

Consider the pure diffusive equation (2.1.3) with $0 \leq z \leq L$ (also for semi-bounded/bounded domain) and $0 \leq t \leq T$ supported by an initial condition $u(z, 0) = u_0(z)$ and boundary conditions $u(0, t) = g_1(t)$ and $u(L, t) = g_2(t)$. The differential equation, the initial and boundary conditions together form an initial boundary values problem [Quarteroni, 2000][142]. Note that, since a computer does not know “the infinite”, for a semi-infinite (or infinite too) domains (e.g. $z \geq 0$), it comes the need to decrease the size of it as much as possible by finding a good compromise between performance and calculation accuracy: L as small as possible to contain processing times but large enough to not affect (negatively) the flow.

The solution domain, $D(z, t)$ must be covered by a two-dimensional grid of lines, called the finite difference grid. The intersections of these grid lines are the grid points at which the finite difference solution of the partial differential equation is evaluated. The spatial and time grid lines are equally spaced lines perpendicular, respectively, to the z and t axis having uniform spacing Δz and Δt . The subscript i will denote the spatial grid lines, $z_i = (i - 1) \Delta z$, and the superscript n will be used to denote the time grid lines, $t^n = (n - 1) \Delta t$. Thus, grid point (i, n) corresponds to location (z_i, t^n) in the solution domain $\mathcal{D}(z, t)$.

In the development of finite difference approximations, a distinction must be made between the exact solution of a partial differential equation and the solution of the finite difference equation which is an approximated solution of the partial differential equation, for this reason let u_i^n be an approximation

of $u(z_i, t^n)$. Exact partial derivatives, which appear in the parabolic diffusion equation, can be approximated at a grid point in terms of the values of $u_i(t)$ at that grid point and adjacent grid points. It is known that the physical information propagation speed associated with second-order spatial derivatives is infinite, and that the solution at a point at a specified time level depends on the influences of the all other points in the solution domain at that time level. Consequently, second-order spatial derivatives, such as u_{zz} , should be approximated by centered-space approximations at spatial location i . The centered-space approximations can be second-order, fourth-order, etc. Simplicity of the resulting finite difference equation usually dictates the use of second-order centered-space approximations for second-order spatial derivatives. This is accomplished by writing Taylor series for $u(z_{i+1}, t^n)$ and $u(z_{i-1}, t^n)$ using grid point (i, n) as the base point:

$$(2.2.1) \quad u(z_{i+1}, t^n) = u(z_i, t^n) + u_z(z_i, t^n) \Delta z + \frac{1}{2} u_{zz}(z_i, t^n) \Delta z^2 + \frac{1}{6} u_{zzz}(z_i, t^n) \Delta z^3 + \frac{1}{24} u_{zzzz}(z_i, t^n) \Delta z^4 + \dots ,$$

$$(2.2.2) \quad u(z_{i-1}, t^n) = u(z_i, t^n) - u_z(z_i, t^n) \Delta z + \frac{1}{2} u_{zz}(z_i, t^n) \Delta z^2 - \frac{1}{6} u_{zzz}(z_i, t^n) \Delta z^3 + \frac{1}{24} u_{zzzz}(z_i, t^n) \Delta z^4 - \dots .$$

Subtracting the first one from the second one and solving for $u_z(z_i, t^n)$, it gives

$$(2.2.3) \quad u_z(z_i, t^n) = \frac{u(z_{i+1}, t^n) - u(z_{i-1}, t^n)}{2\Delta z} + \frac{1}{3} u_{zzz}(\xi) ,$$

where $z_{i-1} \leq \xi \leq z_{i+1}$. Truncating the remainder term yields the second-order centered-space approximation

$$(2.2.4) \quad \frac{\partial u}{\partial z}(z_i, t^n) \approx \frac{u_{i+1}^n - u_{i-1}^n}{2\Delta z} .$$

Adding the first Taylor series from the second one and solving for $u_{zz}(z_i, t^n)$ gives

$$(2.2.5) \quad u_{zz}(z_i, t^n) = \frac{u(z_{i+1}, t^n) - 2u(z_i, t^n) + u(z_{i-1}, t^n)}{\Delta z^2} + \frac{1}{12}u_{zzzz}(\xi) ,$$

where $z_{i-1} \leq \xi \leq z_{i+1}$ again. Truncating the remainder terms, the following second-order centered-space approximation yields

$$(2.2.6) \quad \frac{\partial^2 u}{\partial z^2}(z_i, t) \approx \frac{u(z_{i+1}, t^n) - 2u(z_i, t^n) + u(z_{i-1}, t^n)}{\Delta z^2} .$$

Note that the approximation error is $O(\Delta z^2)$. Clearly, the second-order centered-difference finite difference approximations at time level $n + 1$ are obtained simply by replacing n by $n + 1$ in the equations above.

The exact time derivative can be approximated at time level n by a first-order forward-time approximation. Writing the Taylor series:

$$(2.2.7) \quad u(z_i, t^{n+1}) = u(z_i, t^n) + u_t(z_i, t^n) \Delta t + \frac{1}{2}u_{tt}(z_i, t^n) \Delta t^2 + \dots$$

and solving for $u_t(z_i, t^n)$ yields

$$(2.2.8) \quad u_t(z_i, t^n) = \frac{u(z_i, t^{n+1}) - u(z_i, t^n)}{\Delta t} + \frac{1}{2}u_{tt}(\tau) \Delta t ,$$

where $t \leq \tau \leq t + \Delta t$. Truncating the remainder terms, the first-order forward-time approximation yields:

$$(2.2.9) \quad \frac{\partial u}{\partial t}(z_i, t^n) \approx \frac{u_i^{n+1} - u_i^n}{\Delta t} .$$

Note that, for the approximation (2.2.9), the approximation error is $O(\Delta t)$. Finite difference equations are obtained by substituting the finite difference approximations of the individual exact partial derivatives into the PDE evaluating the spatial derivative at a time level between the beginning of the time step and at the end of time step:

$$(2.2.10) \quad \frac{u_i^{n+1} - u_i^n}{\Delta t} = D\theta \frac{u(z_{i+1}, t^{n+1}) - 2u(z_i, t^{n+1}) + u(z_{i-1}, t^{n+1})}{\Delta z^2} + \\ + D(1 - \theta) \frac{u(z_{i+1}, t^n) - 2u(z_i, t^n) + u(z_{i-1}, t^n)}{\Delta z^2},$$

where $0 < \theta < 1$ is a sort of weight factor. It is convenient to introduce the ratio

$$(2.2.11) \quad \gamma \equiv \frac{D\Delta t}{\Delta z^2},$$

the so called Fourier grid number, γ , a key term in evaluating the performance of finite difference forms for the diffusion equation: the error is not amplified in time advancing, the numerical method is stable, for instance. There are four important properties of finite difference methods, for propagation problems governed by parabolic PDEs, that must be considered before choosing a specific approach. They are:

- Consistency,
- Order,
- Stability,
- Convergence.

A finite difference equation is consistent with a partial differential equation if the difference between the FDE and the PDE (i.e., the truncation error) vanishes as the sizes of the grid spacings go to zero independently. The order of a FDE is the rate at which the global error decreases as the grid sizes approach zero. A finite difference equation is stable if it produces a bounded solution for a stable partial differential equation and is unstable if it produces an unbounded solution for a stable PDE. A finite difference method is convergent if the solution of the finite difference equation (i.e., the numerical values) approaches the exact solution of the partial differential equation as the sizes of the grid spacings go to zero. However, the convergence of a finite difference method is related to the consistency and stability of the finite difference equation. The Lax equivalence theorem states:

THEOREM. “Given a properly posed linear initial-value problem and a finite difference approximation to it that is consistent, stability is the necessary and sufficient condition for convergence”.

Thus, the question of convergence of a finite difference method is answered by a study of the consistency and stability of the finite difference equation. If the finite difference equation is consistent and stable, then the finite difference method is convergent.

For this method, if $\theta = 0$, all spatial derivatives are evaluated at old time level. This is a fully explicit method and once the approximation solution at $t = t^n$ is known, we can compute the solution at the next time level $t = t^{n+1}$, directly. The main weakness of the explicit method is the requirement of the stability condition, that imposes a restriction on the relative size of Δt with respect to Δz [Hoffman, 2001][92]:

$$(2.2.12) \quad \gamma \equiv \frac{D\Delta t}{\Delta z^2} < \frac{1}{2};$$

if $\theta = 1$, we have a fully implicit method where the spatial derivative is evaluated at the new time level and generally is always stable. When $0 < \theta < 1$, we have a mixed scheme, also known as Crank-Nicholsen scheme in the particular case that $\theta = 0.5$. A fully implicit scheme and a mixed scheme have the little drawback that they need an algorithm to solving the system of equations that arises from the equation 2.2.10, the most efficient is the well-known Thomas algorithm [Von Rosenberg, 1969][153].

Unfortunately, the Lax equivalence theorem can be applied only to well-posed, linear, initial-value problems. Many problems in engineering and science are not linear, and nearly all problems involve boundary conditions in addition to the initial conditions. There is no equivalence theorem for such problems, just like for the Richards equation. Nonlinear PDEs must be linearized locally, and the FDE that approximates the linearized PDE is analyzed for stability. Experience has shown that the stability criteria obtained for the FDEs which approximates the linearized PDEs are often still useful, and that the consistent and stable FDEs generally converge, even for nonlinear initial/boundary-value problems. Therefore, nonlinear PDEs are solved iteratively after being linearized in some way. Taylor’s expansion provides a

standard way of doing this and the method is usually referred to as Newton's method [Smith, 1985][56]. Other very performing method are, e.g., the Richtmyer's method [Richtmyer and Morton, 1967][149] and the three time-level method [Lees, 1966][113]. Which one is the best depends on the type of the starting equation and on the error that is willing to accept.

2.3. Stochastic methods

In the last decades a significant number of unsaturated water flow models have been applied on a regional basis for prediction or simulation purposes. Examples include the prediction of the system flow and quality responses to given excitations, such as natural and artificial recharge, change of pumping rates and/or patterns, surface or subsurface discharge of pollutants, and salt-water intrusion in coastal aquifers. For this purpose, hydrogeological parameters must be known. However, in practice, the required distributions of system parameters are very difficult to obtain. This difficulty is recognized to be a major impediment to wider use of groundwater models and to their full utilization [Frind and Pinder, 1973][70]. Freeze called the estimation of parameters the "Achilles' heel" of groundwater models. The problem arises because of the scarcity of available direct measurements of the hydrogeological parameters, but, even in the cases where measurements exist, they cannot be considered representative of regional conditions and very often they are affect by large errors [Freeze, 1972][68]. A common approach is thus to treat them as a random field variable [Vanmarcke, 1983; Dagan, 1989; Gelhar, 1993][219, 50, 74], i.e. to use a stochastic approach based on random space functions (RFS). Consequently the governing equations for flow (and transport) are stochastic, and the resulting dependent variables are also random. One of the first stochastic analysis of groundwater flow was performed by Freeze [Freeze, 1975][69], but other many contributions were presented [Bakr et al., 1978, Gutjahr et al., 1978; Dagan, 1979, 1982b, 1984][2, 4, 45, 46, 47], overall addressed to obtain the two first spatial moments [Dagan, 1988, 1990, 1991; Neuman et al., 1987, 1990][49, 51, 52, 201, 132]. The conservative travel time can also only be known statistically, consequently. The main approach to analyze solute travel times through a field characterized by randomness is based

on repeated numerical solving of the problem, Monte Carlo method [*Suciu, 2014*][**205**].

Generally, a random field, or a stochastic process, $f(z)$ is a process for which we cannot predict the outcome of an experiment (the trial of a process), prior to performing it, contrary to the deterministic process. It can be described as a set of random variables, $f(z_i)$, where each variable corresponding to a point z_i in space and it is characterized by a probability density function (PDF). To every outcome of a probabilistic “experiment” there corresponds a set of sample values of random variables, conveniently, summarized through a function of space, denoted again by $f(z)$ and characterized by the joint probability density function. All possible realizations of the field form the ensemble, on which we can perform a statistical analysis and find statistical measures, like mean and standard deviation [*Kitanidis, 1983*][**107**]. We anticipate that, employing appropriate ergodicity assumptions (we will discuss this concept later), this ensemble variability represents spatial variability as well [*Dagan, 1987*][**48**]. The ensemble average of a random function is defined as:

$$(2.3.1) \quad E[f(z)] = \overline{f(z)} = \frac{1}{n} \sum_{i=1}^n f_i(z) ,$$

where n is the number of the samples. If the mean is not a function of the space the process is called homogenous; equivalently, if the process is a random time function and the mean is independent to the time it is called stationary. Note that the stochastic terminology does not create confusion with the terminology used above for the deterministic processes, which may be considered as a stochastic process with a single realization. The variance is defined as:

$$(2.3.2) \quad \sigma_f^2(z) = \overline{[f(z) - \overline{f(z)}]^2} = \overline{f^2(z)} - \overline{f(z)}^2 ,$$

while the square root of it, $\sigma_f(z)$, is called standard deviation, and measures the average magnitude of the deviations from the mean. Another important statistical measure is the cross-covariance between two variables, which detects if a similar trend exists:

$$(2.3.3) \quad \begin{aligned} cov_{fg}(z_i, z_j) &= \overline{[f(z_i) - \overline{f(z_i)}][g(z_j) - \overline{g(z_j)}]} = \\ &= \overline{f(z_i)g(z_j)} - \overline{f(z_i)}\overline{g(z_j)}, \end{aligned}$$

where i and j indicate two different locations. A similar quantity, the cross-correlation, is defined as:

$$(2.3.4) \quad r_{fg}(z_i, z_j) = \overline{f(z_i)g(z_j)}.$$

If the location is the same the two definitions above are, respectively, called covariance and correlation. Associated with the covariance and the correlation functions are the autocovariance and the autocorrelation, respectively, the covariance and correlation between the same quantity at different locations:

$$(2.3.5) \quad cov_{ff}(z_i, z_j) = \overline{f(z_i)f(z_j)} - \overline{f(z_i)}\overline{f(z_j)},$$

$$(2.3.6) \quad r_{ff}(z_i, z_j) = \overline{f(z_i)f(z_j)}.$$

For a homogeneous model, we assume that the autocovariance is not a function of a pair of locations, rather of the vector direction $\chi = z_1 - z_2$. We can write:

$$(2.3.7) \quad cov_{ff}(z, z + \chi) = \overline{f(z)f(z + \chi)} - \overline{f(z)}\overline{f(z + \chi)} = cov_{ff}(\chi),$$

this means that, for homogenous or stationary problems, the autocovariance, or in general the covariance, not depends on the locations but only on the vector direction. In particular if the covariance depends only on the distance between the two points, $|\chi|$, the field is isotropic; otherwise if depends on the direction as well, the field is called anisotropic and an anisotropic ratio can be defined. A length scale associated with the autocovariance of a stationary field is the integral scale, defined roughly as the distance at which $f(z_1)$ and $f(z_2)$ cease to be correlated. One of the possible definitions can be:

$$(2.3.8) \quad I_f = \frac{1}{\sigma_f^2} \int_0^\infty r_{ff}(|\xi|) d|\xi| .$$

The spatial statistics (or temporal statistic for a functions of time) differs from the ensemble statistics, presented above, in a most important way: the former is performed on a single realization. Given a single realization of a RSF, or in time, the spatial mean, respectively temporal mean, $\langle f \rangle(z)$, is defined by:

$$(2.3.9) \quad \langle f \rangle(z) = \frac{1}{L} \int_{z-L/2}^{z+L/2} f(z') dz' ,$$

where L is a length large enough such that the average is independent on the choice of it and small enough to ensure that the average may still vary with distance for non-homogeneous problems. The brackets $\langle \rangle$, are used to denote the spatial average and the spatial versions of the all respectively statistically measures described in the ensemble sense. Generally definitions 2.3.1 and 2.3.9 are not the same quantity. The first one need a knowledge on the entire population, the second one a knowledge of the joint PDF. In many cases, overall in natural processes, may occur that one of the two is impossible to calculate, and ergodicity hypothesis is essential. It may be stated as follows:

“for a stationary (homogeneous) random process, a large number of observations made on a single system, at N arbitrary instants of time (points of space), have the same statistical properties as observing N arbitrarily chosen systems, from an ensemble of similar system.”[*McQuarrie, 2000*][**125**]

Simply, with the ergodicity hypothesis we can assume that the average of a process over time or space is equal to the average of that process over its statistical ensemble. Notice that the hypothesis is possible only for homogeneous/stationary problems, so the ergodic process must be homogeneous/stationary, but not necessary the reverse. With this assumption we can state that in a homogenous ergodic process definitions 2.3.1 and 2.3.9

are equal and constant [*Bear and Cheng, 2010*][**14**]. Actually, various definitions of ergodicity can be found in hydrogeological literature, e.g. the general formulation:

“an observable of the transport process is ergodic with respect to a stochastic model if the root mean square distance from the model prediction is smaller than a given threshold.” [*Suciu et al., 2006*][**130**]

As mentioned several times, unfortunately, the practical applications of analytical methods are limited due to the facts that: usually only the first two moments (mean and covariance) of the output variables are obtained; many problems of transport are nonlinear. On the other hand, numerical methods provide the most flexible approach to evaluate the uncertainties of dependent variables using a Monte-Carlo (MC) approach. The MC method does not attempt to treat the problem as a stochastic partial differential equation, but rather computes deterministic solutions for a number of numerically generated equally likely (equiprobable) realizations of the field, and analyzes statistically the collection of outputs of the realizations [*Wen, 1995*][**229**]. There is not a single MC method, the term, instead, describes a class of approaches widely used for a wide category of problems. However, these approaches tend to follow a particular pattern:

- (1) Define a domain of possible input data;
- (2) Generate random inputs from the domain with a given probability distribution;
- (3) Perform a deterministic calculation using input data (input). The traditional finite difference or finite element methods are generally used for the solution of flow equation, while the particle tracking method or random walk method is commonly used for the solution of the mass transport equation [*Pollock, 1988*][**141**].
- (4) Aggregate the results of the individual calculations in the final result with a statistical analysis that estimate mean, variance, and possibly the joint PDF.

The MC method is completely general with few assumptions and probably the most powerful method for practical purposes. The main advantages are:

- It provides the possibility to fully evaluate the PDF of results;
- The input can have any features;
- The principle of this method is simple and easy to implement. Also a large variety of computer software is available;
- Using this method, also nonlinear problems can be easily handled.

It has been extensively used to treat problems of groundwater flow and transport [e.g. *Warren and Price, 1961; Delhomme, 1979; De Marsily, 1986; Gomez-Hernandez and Gorelick, 1989*][**225, 55, 124, 79**], however, it should be noted that MC is an approximation method, where the main source of error is the truncating error in the spatial (or time) discretization of the flow (or transport) equations.

3.1. Data mining for geostatistics

Data mining is an important activity for selecting, modelling and exploiting data in the new digital age. It is the automatic process of discovery and identification, within the data, of patterns, relationships and information not a priori notes, which, used for descriptive and/or forecasting purposes, are a valuable tool to support decisions. It releases integrated applications in decision-making processes and does not study a phenomenon like the statistics do. This type of activity is crucial in many areas of scientific research like the Geostatistics [*Journal, 1980*][104].

Etymologically, the term geostatistics designates the statistical study of natural phenomena that can be, often, characterized by the distribution in space of one or more variables. Let $z(x)$ be the value of the variable z at the point x , the problem is to represent the variability of the function $z(x)$ in space when x varies. This representation will then be used to solve such problems as the estimation of the value $z(x_0)$ at a point at which no data are available, or to estimate the proportion of values $z(x)$ within a given field that are greater than a given limit. The geostatistical solution consists of interpreting each value $z(x_i)$ as a particular realization of a random variable $Z(x_i)$ at the point x_i . The set of these auto-correlated random variables constitutes a random function. The problem of characterizing the spatial variability of $z(x)$ then

reduces to that of characterizing the correlations between the various random variables $Z(x_i)$ [Kitanidis, 1996; Goovaerts, 1997] [106, 80]. In the mining field, geostatistics provides a coherent set of probabilistic techniques like the variography, e.g. used to obtain the results presented in the following paper, published in *Procedia Computer Science* for the International Workshop on Data Mining on IoT Systems (DAMIS16) [196]. In this paper the variable $z(x)$, for which we try to catch the heterogeneity, is the α -parameter, or rather the inverse of the characteristic length (see table 1.0.1), a measure of the relevance of the capillary force with respect to the gravitational one. The study of this variable constitutes the true innovative element of the paper since the most of the efforts have been addressed to other soil properties.

Mining in geostatistics to quantify the spatial variability of certain soil flow properties.

_aGerardo Severino, _aMaddalena Scarfato, _bGerardo Toraldo

_aDepartment of Agricultural Sciences

_bDepartment of Mathematics and Applications "R. Caccioppoli"

University of Naples - Federico II, Italy

Abstract. The functional dependence of the relative unsaturated hydraulic conductivity (UHC) $K_r(\psi) \equiv \exp(\alpha\psi)$ upon the matric potential ψ , [L], via the soil-dependent parameter α , [L⁻¹], has been traditionally regarded as a deterministic process (i.e. $\alpha \sim \text{constant}$). However, in the practical applications one is concerned with flow domains of large extents where α undergoes to significant spatial variations as consequence of the disordered soil's structure. To account for such a variability (hereafter also termed as "heterogeneity") we adopt the mining geostatistical approach, which regards α as a random space function (RSF). To quantify the heterogeneity of α , estimates of local-values were obtained from ~ 100 locations along a trench where an internal drainage test was conducted. The analysis of the statistical moments of α demonstrates (in line with the current literature on the matter) that the log-transform $\zeta \equiv \ln \alpha$ can be regarded as a structureless, normally distributed, RSF. An novel implementation of the present study in the context of the "Internet of Things" (IoT) is outlined.

Introduction. The challenging and very difficult task to develop modelling of flow and transport in soils of large extents has been undertaken only in the last decades by using a mining geostatistical approach [*Comegna et al., 2010; Severino et al., 2010*][**33, 174**]. The use of data-mining methods is due to the difficulties into quantifying the spatial distribution of the soil flow properties [*Severino et al., 2006, 2009, 2012*][**177, 189, 184**]. However, while a considerable effort has been invested to quantify the heterogeneity of certain soil properties, such as the Darcy's permeability coefficient [*Rubin, 2003*][**158**], a very limited information about the spatial distribution of the α -parameter (relating the matric potential to the UHC) is available. Indeed, there have been only a limited number of studies [*Russo and Bouton, 1992; White and Sully, 1992; Ragab and Cooper, 1993; Russo et al., 1997*][**165,**

232, 145, 168] focusing on the spatial variability of α , and nevertheless they suffer from many limitations, the most important of which is about the extreme difficulty to carry out precise in situ measurements (somewhat similar to the analysis of water waves distribution [*Farina et al., 2015*][**61**]). In view of such shortcomings, the present paper aims at showing how to use a data-mining (geostatistical) approach to quantify the spatial variability of the α -parameter. In addition, we believe that the present paper provides useful hints on how to combine devices/sensors and data in order to set up a compact web-tool (such as IoT) to gain quick analyses of complex (heterogeneous) environments, similarly to other studies concerning similar problems [*Cuomo et al., 2015, 2016; Farina et al., 2015*][**43, 42, 61**].

Characterization of the spatial variability of the α -parameter by means of the mining geostatistical approach: from theory to the practical use.

THE THEORETICAL FRAMEWORK. The α -parameter is more than a curve-fitting number, since it is related to the soil's texture. Indeed, it has been demonstrated [*White and Sully, 1992*][**232**] that the characteristic length $\lambda_c \equiv \alpha^{-1}$, [L], is a measure of the importance of the capillary force relative to the gravitational one. More precisely, $\lambda_c \rightarrow 0$ implies that gravity dominates capillarity (coarse textured soils), and viceversa (fine textured soils). Since, the soil's texture is highly variable from point to point in the soil, a tantamount degree of variability is detected into the values taken by the α -parameter. This is clearly seen in the Figure 3.1.1 that shows the contour levels of λ_c (cm) along a vertical cross-section in a trench.

A detailed characterization of the spatial distribution of α (and more generally of any soil flow property) via the so-called "standard approach" (i.e. by collecting samples in the field and subsequently determining local values) requires: i) considerable time, and ii) great expense/effort, therefore rendering such an avenue practically impossible. A viable (and widely accepted) alternative is to treat α as a "stochastic process in the space" or equivalently a RSF [*Dagan, 1989; Rubin, 2003*][**50, 158**]. As a consequence, characterization of the heterogeneity of α is cast within the more general approach of the data mining methods.

Thus, the value of α at any \mathbf{x} is regarded as one out-coming related to the many possible geologic materials that might have been generated there.

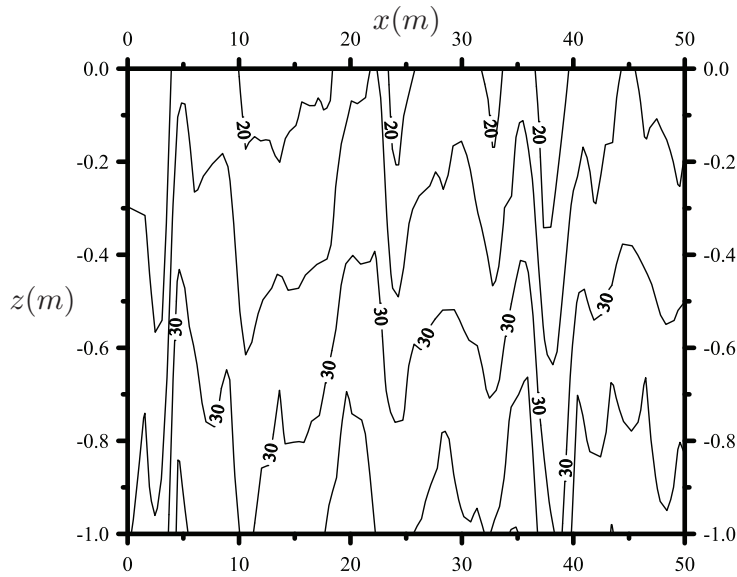


FIGURE 3.1.1. Distribution of the iso-values of λ_c (cm) along a vertical cross-section at the Ponticelli site (Naples, Italy); vertical exaggeration: 250/6

As a consequence, $\alpha \equiv \alpha(\mathbf{x}; \Omega)$ becomes a random variable. The symbol Ω refers to the sample space, which is generally dependent upon the position \mathbf{x} . Likewise, if α is measured at different positions $\mathbf{x}_1, \mathbf{x}_2, \dots, \mathbf{x}_k$ then the values $\alpha_i \equiv \alpha_i(\mathbf{x}_i; \Omega_i)$ ($i = 1, \dots, k$) are random variables, each one characterized by a (generally position dependent) probability density function (PDF). In addition, the possibility of finding any sequence of α -values at a certain \mathbf{x} depends not only upon the PDF itself, but also on those PDFs at other positions. In the context of the mining geostatistics, the probability of finding such a sequence is given by the joint probability density function. Thus, any sequence of α -values at different points is viewed as a possible out-coming of the sample space of a joint PDF, and it is usually termed as a single realization. As a matter of fact, determining the occurrence of any realization requires the knowledge of the joint PDF. Unfortunately, this latter is not an accessible information since in the practice only a single realization (the one obtained by the sampling) is available, and therefore one must resort to some simplifying assumptions, i.e. stationarity and ergodicity. Stationarity

implies that the joint PDF is translationally invariant, whereas ergodicity enables one to infer the joint PDF by means of a single realization [*Rubin, 2003*][**158**]. The pragmatic approach adopted in Hydrology, and in line with the statistical continuous theories, is to derive moments of interest for the flow variables and to check the applicability of these two assumptions only ex post. In terms of moments, stationarity requires the space invariance of “all” the moments: a very stringent assumption. Since, in the practical applications one is mainly interested into the first and second order moments of the flow/transport processes [*Severino et al., 2008, 2012, 2015; Fiori et al., 2010; Severino, 2011a, 2011b*][**191, 186, 175, 66, 180, 192**], the stationarity of the input variables is replaced by the stationarity up to the second order (weak stationarity). Thus, the pair “mean and covariance” becomes the tool to characterize the spatial variability of α . Nevertheless, it is important to emphasize that the knowledge of the mean and covariance does not specify the α -values at any \mathbf{x} , but it rather provides a way to quantify how widely the α -values spread around the mean, and how these values are spatially correlated.

RESULTS AND DISCUSSION. In the present paper local measurements of α were obtained by means of a field-scale drainage experiment [*Severino et al., 2003*][**190**] at the Ponticelli site (Naples, Italy). Along a transect (50m long) 40 verticals (1.25 m apart) were chosen, and for each of them the pair (ψ, K_r) was measured at three depths ($z = 30, 60, 90$ cm). Hence, from the 40×3 available pairs, the α -parameter was obtained via a best fitting procedure [*Gomez et al., 2009*][**78**], and the resulting spatial distribution is shown in the Figure 3.1.1. The cumulative distribution function of α (m^{-1}) (red) together with its logarithmic transform $\zeta \equiv \ln \alpha$ (black) is depicted in the Figure 3.1.2. At a first glance, it is seen that the empirical distribution (discrete symbols) exhibits a larger deviation from the normal distribution, whereas deviations from the log-normal one are smaller. This is quantitatively confirmed by inspection of Table 3.1.1 where we summarize (among the other) the result of the hypothesis (Kolmogorov-Smirnov) normality test.

The problem of quantifying the spatial structure (i.e. the covariance, in the present study) of α is rather complicated, even when measurements are

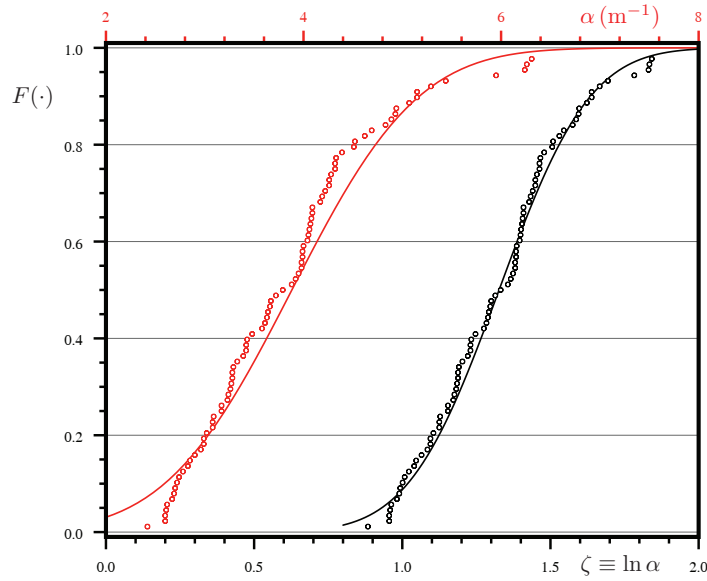


FIGURE 3.1.2. Cumulative distribution function of α (m^{-1}) (red), and its log-transform $\zeta \equiv \ln \alpha$ (black)

Discrete symbols and continuous lines refer to the empirical distribution and to the models, respectively.

statistics	α^*	$\zeta \equiv \ln \alpha$
mean	3.88	1.33
variance	1.01	$5.80 \cdot 10^{-2}$
D	1.03	$5.97 \cdot 10^{-1}$

TABLE 3.1.1. Estimates of the: i) mean, and ii) variance, together with the test (D) of normal/log-normal (null) hypothesis

*values of α are in m^{-1}

numerous. The identification process should involve several steps: i) an hypothesis about the functional model of the covariance, ii) estimates of the parameters of such a model, and iii) a model validation test. However, the problem of selecting the most appropriate model remains to some extent in the realm of the practical applications [Rubin, 2003][158]. The prevailing approach is the pragmatic one: select a model for its practicality/versatility as well as its performance in similar situations. Nevertheless, it is important

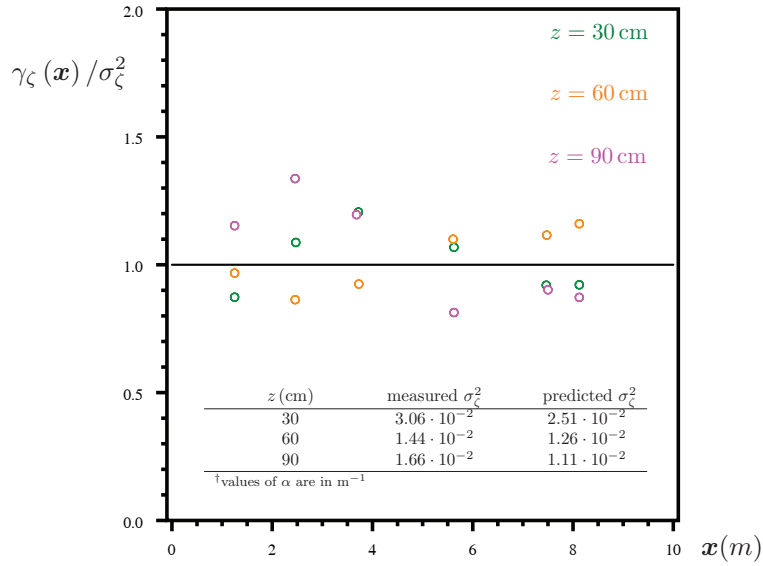


FIGURE 3.1.3. Scaled variogram $\gamma_\zeta/\sigma_\zeta^2$ at the three measuring depths along the horizontal distance \mathbf{x}

The measured vs predicted structured variances σ_ζ^2 are shown in the insert.

in view of the subsequent analysis to discuss some general properties of the covariance function $C \equiv C(\mathbf{x})$. Thus, the value $C(0)$ is the so-called “structured variance”, and it provides information about the spread of the α -values around the mean. For $|\mathbf{x}| \neq 0$, the value $C(\mathbf{x})$ is a measure of the correlation between the α -values at two points separated by the distance $|\mathbf{x}|$. More precisely, the higher is $|\mathbf{x}|$ the smaller the correlation. Of particular interest is the concept of integral scale, \mathcal{I}_α . Roughly speaking the integral scale, $[\text{L}]$, represents the distance over which two values of α cease to be correlated [Dagan, 1989][50]. A frequently encountered case is that of zero integral scale, i.e. $\mathcal{I}_\alpha \rightarrow 0$. In this case the geological formation is characterized by a complete lack of spatial correlation, i.e. $C(\mathbf{x}) \simeq 0$ for any $|\mathbf{x}| \neq 0$, and this is known as stochastic structureless process. In such a circumstance, it is convenient to deal with the variogram $\gamma \equiv \gamma(\mathbf{x})$ [Dagan, 1989; Rubin, 2003][50, 158]. Generally, the variogram γ (whose computation is straightforward) is of wider applicability as compared with the covariance, since its applicability does not require the stationarity hypothesis in a strict sense.

Nevertheless, for a stationary process one can easily demonstrate [Dagan, 1989; Rubin, 2003][50, 158] that $\gamma(\mathbf{x}) \equiv C(0) - C(\mathbf{x})$. As a consequence, for a stochastic, stationary, structureless process the variogram in practice coincides with the structured variance, i.e. $\gamma(\mathbf{x}) \simeq C(0)$. Thus, the use of the variogram is very useful to visualize whether any stochastic process is structureless. The experimental scaled-variograms γ/σ_ζ^2 at three different depths found for the transect in Figure 3.1.1 is plotted in the Figure 3.1.3. The fact that $\gamma/\sigma_\zeta^2 \sim 1$ supports the assumption of a spatial lack of correlation, and concurrently for the geological formation at stake the RSF α can be regarded as a structureless stochastic process.

Concluding remarks and highlights toward an implementation in the context of the IoT. A preliminary analysis of a field scale drainage test suggests that the log-transform $\zeta \equiv \ln \alpha$ of the parameter appearing into the relative UHC: $K_r \equiv \exp(\alpha\psi)$, characterizing the length of the capillary force acting into unsaturated porous media (soils), can be modeled as a stationary RSF of zero integral scale (i.e. a structureless stochastic process). The most important consequence in view of the applications is that the covariance of ζ can be approximated by a white noise signal in the horizontal plane.

Before concluding, we wish to highlight here an application of the presented material which can be easily implemented in the IoT-context. Indeed, data-driven agricultural technologies are rapidly becoming a tool of large use, and in particular they allow one to design a site-specific management plan (precision-agriculture). In particular, a majority of precision-agriculture strategies rely on statistical analyses (or image processing) of indirect measurements of soil conditions obtained, for example, by satellites, unmanned aircraft or other means of remote sensing. Various (above-ground) parameters related to crop conditions can be effectively monitored with wireless sensor networks. Thus, the utility of our approach comes from the use of dynamic real-time forecasting of the quantity and quality of soil water to guide the field irrigation. This forecasting will be facilitated and informed by in situ measurements of water content obtained with spatially distributed autonomous and automated sensors along an IoT-approach [Chianese et al., 2016][31].

Acknowledgements. The Authors acknowledge the support from the CAISIAL Department within the MODige-project (E72C14000170005). Gerardo Severino acknowledges the kind assistance of his students (class: Protection of environmental water resources) during the data-processing.

3.2. Nonstationary unsaturated steady flows

In this section a very interesting application example, which illustrates how simplified analytical models of heterogeneous media can be applied to field data avoiding brute force of intensive numerical modelling, is presented. More precisely, a fully three-dimensional analytical model accounting for the nonstationarity of the unsaturated flow variables influenced by the water table is described and simple (closed form) expressions for the second-order moments of the specific flux and the pressure head are derived.

Flow behavior close to the water-table was analyzed. In the majority of the cases the water-table is located at depths which are completely inaccessible for the experimental applications and solving the unsaturated flow in the vicinity of the groundwater, through a reliable model connecting information of surface to those at the very deep, is even more important.

The listed below major conclusions were achieved and published on *Water Resources Research* (on August 2017)[**193**]:

- the infiltrating flux q_0 and the integral scale I impact the stationary values of the specific flux $(q_h, q_z)^\top$, whereas they have a limited influence upon the distance from the water-table at which such stationary values are attained;
- from the application point of view, one can estimate the thickness of the flow domain where the nonstationary is dominant by means of a 1D Richards equation (i.e. valid for the vertical mean pressure head $\langle \Psi \rangle$).

The authors strongly believe that simplified analytical solutions can provide useful insights into the physical processes of the vadose zone, and also serve as useful tools for applications, all the approximations notwithstanding. The good agreement between predictions and real data confirmed the scientific consistency of the developed model and, although we have limited the discussion to the data of the Ponticelli's experiment, the vadose zone flow model derived in the present study is rather general.

Stochastic analysis of unsaturated steady flows above the water table.

^aGerardo Severino, ^aMaddalena Scarfato, ^bAlessandro Comegna

^aDepartment of Agricultural Sciences

University of Naples - Federico II, Italy

^bSchool of Agricultural Forestry Food and Environmental Science

University of Basilicata, Italy

Abstract. Steady flow takes place into a three-dimensional partially saturated porous medium where, due to their spatial variability, the saturated conductivity K_s and the relative conductivity K_r are modeled as random space functions (RSFs). As a consequence, the flow variables (FVs), i.e. pressure-head and specific flux, are also RSFs. The focus of the present paper consists into quantifying the uncertainty of the FVs above the water-table. The simple expressions (most of which in closed form) of the second-order moments pertaining to the FVs allow one to follow the transitional behavior from the zone close to the water-table (where the FVs are non-stationary), till to their far-field limit (where the FVs become stationary RSFs). In particular, it is shown how the stationary limits (and the distance from the water-table at which stationarity is attained) depend upon the statistical structure of the RSFs K_s , K_r and the infiltrating rate. The mean pressure head $\langle \Psi \rangle$ has been also computed, and it is expressed as $\langle \Psi \rangle = \Psi_0(1 + \psi)$, being ψ a characteristic heterogeneity function which modifies the zero-order approximation Ψ_0 of the pressure head (valid for a vadose zone of uniform soil properties) to account for the spatial variability of K_s and K_r . Two asymptotic limits, i.e. close (near field) and away (far field) from the water-table, are derived into a very general manner, whereas the transitional behavior of ψ between the near/far field can be determined after specifying the shape of the various input soil properties. Besides the theoretical interest, results of the present paper are useful for practical purposes, as well. Indeed, the model is tested against to real data, and in particular it is shown how it is possible for the specific case study to grasp the behavior of the FVs within an environment (i.e. the vadose zone close to the water-table) which is generally very difficult to access by direct inspection.

Introduction. Soil hydraulic properties, such as saturated conductivity, water retention and relative conductivity have been largely considered as well-defined properties of the unsaturated porous formations [Hillel, 1998][90]. However, in the majority of the hydrological applications unsaturated flows take place in a complex environment (often termed as vadose zone) whose setup changes erratically, thus undermining any attempt to characterize within a deterministic framework the flow (and transport) properties. Such a setup shows discrete and/or continuous variations over several scales, thus making hydraulic properties to do likewise. On the other side, owing to several logistic and economic limitations, hydraulic properties can be measured only at a limited number of positions where their values depend upon the size of the sample(s) as well as the procedure of measurement. Inferring parameters at points where measurements are not available entails a random error [Sinsbeck and Tartakovsky, 2015][198]. In addition to this, measured values are biased by experimental errors. As matter of fact, these errors and uncertainties render the hydraulic parameters RSFs, and the corresponding flow-equations stochastic.

It is a common tenet that an appropriate tool to deal with this uncertainty is the geostatistical approach [Rubin, 2003][158]. Thus, measurements of the hydraulic parameters are regarded as samples of random fields, which in turn are characterized by a multivariate probability density function (or alternatively by ensemble moments). If the statistical properties of the hydraulic parameters can be inferred from measurements, the stochastic flow-equations can be solved either analytically [Severino and Indelman, 2004; Severino et al., 2006, 2012][176, 177, 179] or numerically [Severino and De Bartolo, 2015][175] by Monte Carlo simulations (MCs), and results analyzed in a statistical sense [Severino et al., 2007][185]. MCs are conceptually simple, and they have the advantage to be applicable to a large variety of configurations [Barajas-Solano and Tartakovsky, 2016][8]. However, MCs pose a number of serious drawbacks and limitations. Indeed, to account for high-frequency fluctuations of the input RSFs, very fine numerical grids are required. As a consequence, each realization (sampling) may result computer-demanding, especially when one deals with three-dimensional flows. In addition, even if

MCs converge after a sufficiently large number of runs, there is not a systematic procedure to ascertain whether to consider conclusive (and therefore completed) the MCs (a deep discussion upon these issues can be found in [*Jankovic et al., 2003; Russo et al., 2009*][**100, 163**]).

To avoid the lack of accuracies attached to the MCs, analytical approaches have been also developed (see, e.g. [*Severino, 2011*][**181**] and references therein). Unlike MCs, analytical methods enable one: i) to compute the fluctuations of the FVs, and subsequently to obtain (by ensemble averaging) the various (cross)covariances, or ii) to end up with deterministic equations which are solved for the (cross)covariances. This second avenue (which will be adopted in the present study) is also known as the method of moments' equation (MME). The applicability of analytical methods generally relies upon some assumptions, the most relevant of which are: i) unbounded flow-domain, and ii) gravity-dominated mean flow [*Yeh et al., 1985a; Russo, 1993; Severino and Santini, 2005; Severino et al., 2009*][**238, 161, 178, 189**]. In particular, the latter assumption implies that the mean pressure-head is constant within the flow-domain. However, assuming that gravity is the only driving force for the mean flow is sometimes too limiting, especially when one is interested in the flow's behavior close to the water-table where, as it is well known, the mean pressure-head is not constant. This renders the problem more difficult, and it is not surprising that very few analytical studies have been carried out toward such a direction. From the stand point of the applications, solving the unsaturated flow in the vicinity of the groundwater is even more important. In fact, in the majority of the cases the water-table is located at depths which are completely unaccessible, therefore rendering direct inspection impossible (or extremely time-consuming and expensive). Within such a picture, the use of a reliable model connecting informations that can be easily acquired at the soil surface to those at the very deep (difficult to access) locations becomes of paramount relevance.

One of the first attempt to account for the impact of the water-table upon the FVs' behavior is from [*Andersson and Shapiro, 1983*][**5**] who analyzed the spatial distribution of the water content in a one-dimensional domain by means of both analytical methods (small perturbations) and MCs. They

found that the distance from the water-table to the region of “stationarity” depends upon the soil properties as well as the flux at the soil-surface. However, in the study of Andersson only the saturated hydraulic conductivity K_s was regarded as a RSF. The pressure-head behavior under the same conditions of the previous study was analyzed by Indelman [*Indelman et al., 1993*][**96**] who adopted the model of Gardner [*Gardner, 1958*][**73**] for the relative conductivity K_r . In the region of non-stationarity, the variance of the pressure-head was found sensitive to both the mean flow conditions and to the spatial variability of the soil hydraulic properties. Tartakovsky et al. [*Tartakovsky et al., 1999*][**209**] developed an alternative methodology based upon the Kirchhoff’s transformation which enables one to avoid (or delay) any approximation procedure. In order to fully take advantage of the Kirchhoff transformation, they regarded the α -parameter as a random constant. Then, by dealing with a one-dimensional domain and vertical flow conditions, they derived analytical solutions for the covariance and the second order correction to the pressure-head. A similar analysis in a three dimensional formation, relying upon MCs, has been conducted by Russo [*Russo and Fiori, 2008*][**162**], who showed that when the water-table is located at a sufficiently large depth from the soil surface, one can delineate a region where flow is essentially gravity-dominated (and concurrently the FVs are stationary).

In the present paper we solve unsaturated steady flow in three dimensional bounded heterogeneous formations by means of analytical tools, and we aim at computing second-order moments of the FVs. More precisely, we employ a general perturbation procedure to achieve simple (closed-form) results relating into a straightforward manner the statistical structure of the input soil properties to the spatial distribution of the FVs in the vicinity of the water-table. The paper is organized as follows: we begin by formulating the mathematical problem in the context of a stochastic framework (see section “Mathematical statement of the problem”), and derive second-order moments for the FVs (sections “Second-Order Moments of the Pressure-Head” and “Higher-Order Correction of the Mean Pressure-Head”). The model is calibrated against to a recently conducted flow experiment in the vadose zone (section Calibration Versus Validation”), and subsequently it is used to grasp the behavior of the

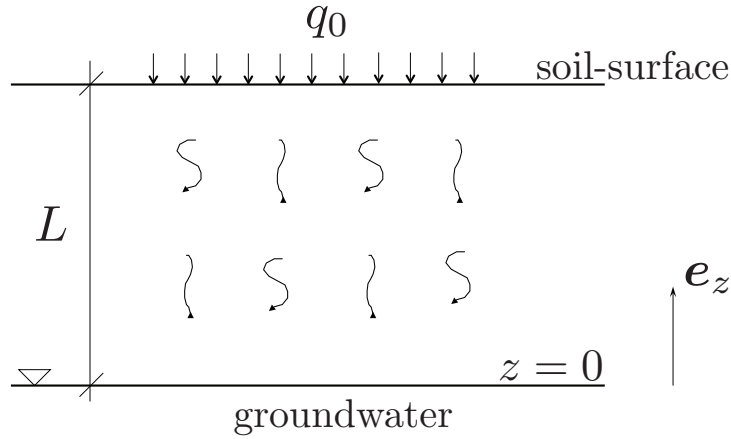


FIGURE 3.2.1. Sketch of a flow taking place into a vadose zone delimited at the bottom ($z = 0$) by the water-table and at the top ($z = L$) by the soil surface

FVs in the close vicinity of the water-table (section “Discussion”). We end up with concluding remarks (section “Conclusions”).

Mathematical Statement of the Problem. Unsaturated steady flow takes place in a three-dimensional domain Ω which is horizontally unbounded, and vertically delimited by the position of the water-table ($z = 0$) and the soil surface ($z = L$), i.e.

$$(3.2.1) \quad \Omega = \{ \mathbf{x} \equiv (x, y, z) : (x, y) \equiv \mathbf{x}_h \in \mathbb{R}^2, \quad 0 \leq z \leq L \},$$

(Figure 3.2.1). The governing equations are: i) the Buckingham-Darcy (constitutive) law, and ii) the mass-balance law

$$(3.2.2) \quad \mathbf{q}(\mathbf{x}) = -K(\Psi) \nabla(z + \Psi), \quad \nabla \cdot \mathbf{q}(\mathbf{x}) = 0,$$

respectively. In equations 3.2.2, $\mathbf{q} \equiv (q_x, q_y, q_z)^\top$ is the specific flux, $\Psi \equiv \Psi(\mathbf{x})$ is the pressure-head, and $K \equiv K(\Psi)$ is the pressure-dependent hydraulic

conductivity. Boundary conditions are determined by physical processes at the soil surface and water-table. Thus, let q_0 denote a prescribed (negative for infiltration) vertical flux at the soil surface ($z = L$) (as determined either by the rainfall or by the irrigation). This gives rise to a boundary condition:

$$(3.2.3) \quad K(\Psi) \left(1 + \frac{\partial}{\partial z} \Psi \right) \Big|_{z=L} = -\mathbf{q} \cdot \mathbf{e}_z = -q_0,$$

being $\mathbf{e}_z \equiv (0, 0, 1)$ the vertical unit pointing outward vector (Figure 3.2.1). Generally, flows occurring in the uppermost soil are largely transient as consequence of the high variability of the atmospheric conditions. However, in the close vicinity of the water-table the dependence of flow with time results of negligible impact [Wang *et al.*, 2009][223]. More precisely, Russo and Fiori [Russo and Fiori, 2008][162] have demonstrated that, when the water-table is deep, the vadose zone can be conceptually decomposed into two distinct zones: a highly transient near-surface zone, and a deeper one where practically steady state flow conditions occur. Within such a zone, an equivalent constant flux q_0 (obtained by averaging the cumulative flux of the net applied water over the relevant time period) provides a good approximation of the cumulative water flux arriving to the water-table.

Although the pressure head may fluctuate in the zone close to the water-table, the numerical analysis of Russo and Fiori demonstrates that, when the water-table is located at sufficiently large depth from the soil surface, a steady spatially uniform head is worth to reconstruct not only the flow regime but also the mass arrivals at the groundwater. Such an approximation applies to very general vadose zones (i.e. of largely different textures) in the presence or absence of vegetation [Russo and Fiori, 2009][167]. Thus, we assume that the water-table ($z = 0$) is at rest, and it separates the unsaturated zone ($\Psi < 0$) from the phreatic one ($\Psi > 0$). Before proceeding further, it is worth also clarifying why, for the present study, the capillary fringe can be neglected. Thus, its thickness is significant when the water-table: i) largely fluctuates in the time [Li and Yeh, 1998][115], and ii) when the water-table is shallow [Gillham, 1984][76]. In addition, such fluctuations are particularly relevant in the coarser soils, and in this case they significantly affect the flow and

transport regimes [*Russo and Fiori, 2009*][**167**]. However, under steady state conditions (which apply in the present study), the situation is completely reversed, since in the structureless sandy soils (like the one considered in the sequel), the water's raise due to the capillarity-mechanism is highly contrasted by the macropores [*Zhang and Winter, 1998; Zhang 2002*][**242, 241**]. Hence, a boundary condition at the water-table reads as:

$$(3.2.4) \quad \Psi(\mathbf{x}) \Big|_{z=0} = 0.$$

In order to solve the system of the two equations 3.2.2, a functional dependence for $K \equiv K(\Psi)$ must be specified. Several models for K are available in the literature [*Brooks and Corey, 1964; Mualem, 1976; Van Genuchten, 1980*][**21, 127, 217**]. In the context of the present study we shall adopt the exponential model of Gardner [*Gardner, 1958*][**73**]:

$$(3.2.5) \quad K(\Psi) \equiv K_s K_r(\Psi), \quad K_r(\Psi) = \exp(\alpha \Psi),$$

where K_s and α are the saturation conductivity and a pore-size distribution parameter, respectively. Generally, other conductivity curves have been proved to better reproduce the hydrological soil behavior. However, such curves require a very detailed characterization which is typically carried out at laboratory scale [*Romano et al., 2011*][**152**]. Instead, at formation (and even larger) scales the uncertainty of the soil hydraulic properties and the limitations of the in situ sampling devices do not allow gaining a very detailed resolution of the conductivity curve. Thus, owing to these limitations (and wishing to reduce the computational burden), we have adopted, similarly to [*Indelman et al., 1993; Tartakovsky et al., 1999, 2004; Severino and Tartakovsky, 2015*][**96, 209, 206, 194**], the Gardner's model. Last, the main difference between the Gardner's and any other model is at the saturation, i.e. $\Psi \sim 0$. Instead, for $\Psi < 0$ (which in the vadose zone is the rule rather than the exception) the hydraulic response of the Gardner's model does not significantly differ from that of any other ones [*Comegna et al., 1996; Tartakovsky et al., 2003*][**37, 208**].

Due to their erratic variations [White and Sully, 1992; Russo and Bouton, 1992; Severino et al., 2003, 2010, 2016; Fallico et al., 2016][232, 165, 190, 174, 196, 60], the log-transformed parameters $\zeta = \ln \alpha$ and $Y = \ln K_s$ are modelled as stationary RSFs. As a consequence, their geometric means: $\alpha_G = \exp \langle \zeta \rangle$ and $K_G = \exp \langle Y \rangle$ are constant with zero-mean fluctuations, i.e., $\langle \zeta' \rangle = \zeta - \langle \zeta \rangle = 0$ and $\langle Y' \rangle = Y - \langle Y \rangle = 0$. Since the conductivity curve (3.2.5) depends upon the two RSFs K_s and α , the cross covariance $C_{Y\zeta}$ has to be provided, as well. In line with field-data [Rubin, 2003], we assume that covariances of the RSFs have axisymmetric structure, i.e.,

$$(3.2.6) \quad C_\gamma(x_h, z) = \sigma_\gamma^2 \rho_h \left(\frac{x_h}{I_\gamma} \right) \rho_v \quad \gamma = Y, Y\zeta, \zeta,$$

being I_γ and λ_γ the horizontal integral scale and the anisotropy-ratio, respectively. The asymmetric (spatial) structure equation 3.2.6 is rather general feature accounting for the typical statistical anisotropies of a vadose zone (a wide survey can be found in Rubin [Rubin, 2003][158]). We adopt α_G^{-1} and K_G as scales for the length and the flux, respectively. As a consequence, equations 3.2.2 write as (for simplicity we retain the same notations):

$$(3.2.7) \quad \begin{cases} \mathbf{q}(\mathbf{x}) = -\exp(Y') \exp[\Psi \exp(\zeta')] \nabla(z + \Psi) \\ \nabla \cdot \mathbf{q}(\mathbf{x}) = 0. \end{cases}$$

Due to the random nature of Y' and ζ' , the system 3.2.7 becomes stochastic, and we aim at computing the statistical moments of the FVs. To solve 3.2.7, we expand Ψ , \mathbf{q} , $\exp(Y')$ and $\exp(\zeta')$ in asymptotic-series as follows

$$(3.2.8) \quad \begin{aligned} \Psi &= \Psi_0 + \Psi_1 + \Psi_2 + \dots; \quad \mathbf{q} = \mathbf{q}^{(0)} + \mathbf{q}^{(1)} + \mathbf{q}^{(2)} + \dots; \\ \exp(Y') &= 1 + \frac{Y'}{1!} + \frac{Y'^2}{2!} + \dots; \quad \exp(\zeta') = 1 + \frac{\zeta'}{1!} + \frac{\zeta'^2}{2!} + \dots \end{aligned}$$

The non-linear term $f(\Psi, \zeta') \equiv \exp[\Psi \exp(\zeta')]$ appearing into the first of 3.2.7 is likewise expanded up to the second-order, i.e.,

$$\begin{aligned}
(3.2.9) \quad f(\Psi, \zeta') &= f(\Psi_0, 0) + \frac{1}{1!} \left[\left. \frac{\partial}{\partial \Psi_1} f(\Psi, \zeta') \right|_{(\Psi_0, 0)} \Psi_1(\mathbf{x}) + \left. \frac{\partial}{\partial \zeta'} f(\Psi, \zeta') \right|_{(\Psi_0, 0)} \zeta'(\mathbf{x}) \right] + \\
&\quad + \frac{\partial}{\partial \Psi_2} f(\Psi, \zeta') \Big|_{(\Psi_0, 0)} \Psi_2(\mathbf{x}) + \frac{\partial}{\partial \zeta'^2} f(\Psi, \zeta') \Big|_{(\Psi_0, 0)} \zeta'^2(\mathbf{x}) + \\
&\quad + \frac{1}{2!} \left[\left. \frac{\partial}{\partial \Psi_1} f(\Psi, \zeta') \right|_{(\Psi_0, 0)} \Psi_1(\mathbf{x}) + \left. \frac{\partial}{\partial \zeta'} f(\Psi, \zeta') \right|_{(\Psi_0, 0)} \zeta'(\mathbf{x}) \right]^{(2)} + \dots
\end{aligned}$$

To compute the first-order derivatives of $f(\Psi, \zeta')$ at the right-hand side of 3.2.9, we employ the chain-rule of derivation, i.e.,

$$\begin{aligned}
(3.2.10) \quad \left. \frac{\partial}{\partial \Psi_1} f(\Psi, \zeta') \right|_{(\Psi_0, 0)} &= \left[\frac{d}{d\Psi} f(\Psi, \zeta') \cdot \frac{\partial \Psi}{\partial \Psi_1} \right]_{(\Psi_0, 0)} = \\
&= [\exp(\zeta') f(\Psi, \zeta') \cdot 1]_{(\Psi_0, 0)} = K_r(\Psi_0),
\end{aligned}$$

$$\begin{aligned}
(3.2.11) \quad \left. \frac{\partial}{\partial \zeta'} f(\Psi, \zeta') \right|_{(\Psi_0, 0)} &= \left[\frac{df(\Psi, \zeta')}{d \exp(\zeta')} \cdot \frac{\partial \exp(\zeta')}{\partial \zeta'} \right]_{(\Psi_0, 0)} = \\
&= \left[\Psi f(\Psi, \zeta') \cdot \frac{1}{1!} \right]_{(\Psi_0, 0)} = \Psi_0(z) K_r(\Psi_0),
\end{aligned}$$

$$\begin{aligned}
(3.2.12) \quad \left. \frac{\partial}{\partial \Psi_2} f(\Psi, \zeta') \right|_{(\Psi_0, 0)} &= \left[\frac{d}{d\Psi} f(\Psi, \zeta') \cdot \frac{\partial \Psi}{\partial \Psi_2} \right]_{(\Psi_0, 0)} = \\
&= [\exp(\zeta') f(\Psi, \zeta') \cdot 1]_{(\Psi_0, 0)} = K_r(\Psi_0),
\end{aligned}$$

$$\begin{aligned}
(3.2.13) \quad \left. \frac{\partial}{\partial \zeta'^2} f(\Psi, \zeta') \right|_{(\Psi_0, 0)} &= \left[\frac{df(\Psi, \zeta')}{d \exp(\zeta')} \cdot \frac{\partial \exp(\zeta')}{\partial \zeta'^2} \right]_{(\Psi_0, 0)} = \\
&= \left[\Psi f(\Psi, \zeta') \cdot \frac{1}{2!} \right]_{(\Psi_0, 0)} = \frac{1}{2} \Psi_0(z) K_r(\Psi_0),
\end{aligned}$$

where hereafter we shall set: $K_r(\Psi_0) \equiv \exp(\Psi_0)$. The second-order derivatives are computed by means of 3.2.10 and 3.2.11, the final result being:

$$(3.2.14) \quad \left. \frac{\partial^2}{\partial \Psi_1^2} f(\Psi, \zeta') \right|_{(\Psi_0, 0)} = \left[\frac{\partial}{\partial \Psi_1} \frac{\partial}{\partial \Psi_1} f(\Psi, \zeta') \right]_{(\Psi_0, 0)} = \\ = \left[\exp(\zeta') \frac{\partial}{\partial \Psi_1} f(\Psi, \zeta') \right]_{(\Psi_0, 0)} = K_r(\Psi_0) ,$$

$$(3.2.15) \quad \left. \frac{\partial^2 f(\Psi, \zeta')}{\partial \Psi_1 \partial \zeta'} \right|_{(\Psi_0, 0)} = \left\{ \frac{\partial}{\partial \Psi_1} \left[\frac{\partial}{\partial \zeta'} f(\Psi, \zeta') \right] \right\}_{(\Psi_0, 0)} = \\ = \left\{ \frac{\partial}{\partial \Psi_1} [\Psi f(\Psi, \zeta')] \right\}_{(\Psi_0, 0)} = \left[f(\Psi, \zeta') \frac{\partial \Psi}{\partial \Psi_1} + \Psi \frac{\partial}{\partial \Psi_1} f(\Psi, \zeta') \right]_{(\Psi_0, 0)} = \\ = f(\Psi_0, 0) + \Psi_0 \left[\frac{\partial}{\partial \Psi_1} f(\Psi, \zeta') \right]_{(\Psi_0, 0)} = K_r(\Psi_0) + \Psi_0 K_r(\Psi_0) ,$$

$$(3.2.16) \quad \left. \frac{\partial^2}{\partial \zeta'^2} f(\Psi, \zeta') \right|_{(\Psi_0, 0)} = \left[\frac{\partial}{\partial \zeta'} \frac{\partial}{\partial \zeta'} f(\Psi, \zeta') \right]_{(\Psi_0, 0)} = \\ = \Psi_0 \left[\frac{\partial}{\partial \zeta'} f(\Psi, \zeta') \right]_{(\Psi_0, 0)} = \Psi_0^2 K_r(\Psi_0) .$$

To summarize, the asymptotic-expansion of the constitutive-law reads as:

$$(3.2.17) \quad \mathbf{q}(\mathbf{x}) = -K_r(\Psi_0) \nabla [z + \Psi_0(z) + \Psi_1(\mathbf{x}) + \Psi_2(\mathbf{x}) + \dots] \cdot \\ \cdot \left[1 + Y'(\mathbf{x}) + \frac{1}{2} Y'^2(\mathbf{x}) + \dots \right] \times \left\{ 1 + \Psi_2(\mathbf{x}) + \Psi_1(\mathbf{x}) + \Psi_0(z) \zeta'(\mathbf{x}) + \right. \\ \left. + \Psi_1(\mathbf{x}) \zeta'(\mathbf{x}) + \frac{\Psi_0(z)}{2} \zeta'^2(\mathbf{x}) + \frac{1}{2} [\Psi_1(\mathbf{x}) + \Psi_0(z) \zeta'(\mathbf{x})]^2 + \dots \right\} .$$

We wish to note that a more general result, i.e. accounting for any functional shape $K_r \equiv K_r(\Psi)$, can be found in [Indelman, 1993][96]. However, for the functional model 3.2.5 one easily recovers from [Indelman, 1993] the same linearized expression 3.2.17.

THE LEADING-ORDER APPROXIMATION. At the zero-order the system 3.2.7 writes as

$$(3.2.18) \quad \begin{cases} \mathbf{q}^{(0)}(\mathbf{x}) = -K_r(\Psi_0) \nabla (z + \Psi_0) \\ \nabla \cdot \mathbf{q}^{(0)}(\mathbf{x}) = 0 \end{cases} \Rightarrow \nabla \cdot [K_r(\Psi_0) \nabla \Psi_0] + \frac{\partial}{\partial z} K_r(\Psi_0) = 0 ,$$

with the following boundary conditions:

$$(3.2.19) \quad \Psi_0(\mathbf{x})|_{z=0} = 0, \quad K_r(\Psi_0) \left(1 + \frac{\partial}{\partial z} \Psi_0 \right) \Big|_{z=L} = -q_0.$$

To solve the boundary-value problem 3.2.18-3.2.19, we employ a modified Kirchhoff transformation

$$(3.2.20) \quad \mathcal{F}(\mathbf{x}) = \exp\left(\frac{z}{2}\right) \int_{-\infty}^{\Psi_0} ds K_r(s) = \exp\left(\frac{z}{2}\right) K_r(\Psi_0) ,$$

[*Severino and Tartakovsky, 2015*][**194**] to map the second of 3.2.18 into an Helmholtz-type equation

$$(3.2.21) \quad \nabla^2 \mathcal{F}(\mathbf{x}) - \frac{1}{4} \mathcal{F}(\mathbf{x}) = 0,$$

whereas the boundary-conditions 3.2.19 become:

$$(3.2.22) \quad \mathcal{F}(\mathbf{x})|_{z=0} = 1, \quad \frac{\partial}{\partial z} \mathcal{F}(\mathbf{x}) + \frac{1}{2} \mathcal{F}(\mathbf{x}) \Big|_{z=L} = -q_0 \exp(L/2).$$

Skipping the straightforward algebraic derivations, one ends up with

$$(3.2.23) \quad \mathbf{q}^{(0)} = q_0 \mathbf{e}_z, \quad \Psi_0(z) = \ln \{ -q_0 [1 - \kappa \exp(-z)] \}, \quad \kappa = 1 + q_0^{-1}.$$

Note that the zero-order terms $\mathbf{q}^{(0)}$ and Ψ_0 are function of the vertical coordinate z solely, since the boundary conditions 3.2.22 do not depend upon the planar coordinate $\mathbf{x}_h \equiv (x, y) \in \mathbb{R}^2$. Moreover, one can easily check that: $0 \leq -q_0 [1 - \kappa \exp(-z)] \leq 1$ (it is reminded that $-1 \leq q_0 \leq 0$, and

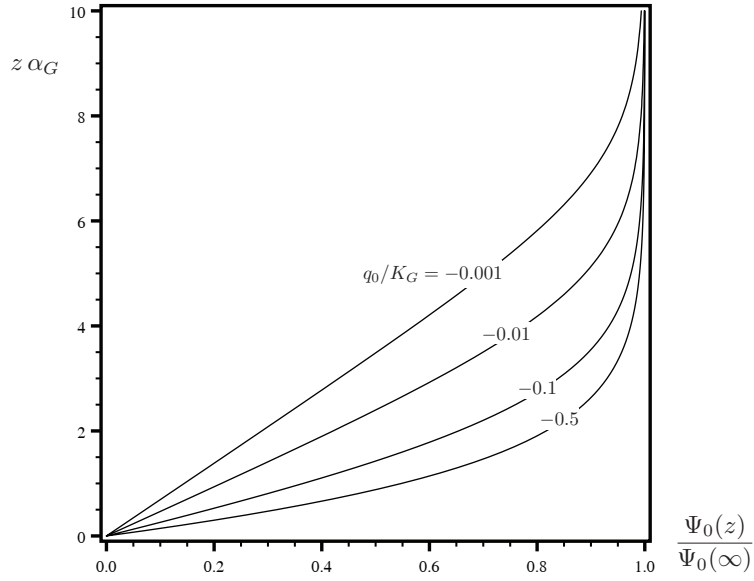


FIGURE 3.2.2. The normalized leading order pressure head $\Psi_0(z)/\Psi_0(\infty)$ as function of the scaled depth $z \alpha_G$, and different values of the non dimensional flux q_0/K_G

concurrently $-\infty < \kappa \leq 0$), therefore implying that $\Psi_0 \in]-\infty, 0]$ [Severino and Coppola, 2012][184]. Finally, away from the water-table it yields: $\Psi_0 \approx \ln(-q_0) \equiv \Psi_0(\infty)$, in agreement with previous studies dealing with an unbounded flow-domain [Russo, 1993; Severino and Santini, 2005; Severino et al., 2009][161, 178, 189].

In the Figure3.2.2 the leading order pressure $\Psi_0(z)$ relative to its far field $\Psi_0(\infty)$ has been depicted along $z \alpha_G$ for several values of the normalized flux q_0/K_G . The high sensitivity of Ψ_0 to the infiltrating flux q_0 is clearly seen. In particular, the smaller q_0/K_G , the larger the distance (from the water-table $z = 0$) of attainment the far field, and viceversa.

THE FIRST-ORDER APPROXIMATION. At the first order the mass-conservation and the constitutive law write as

$$(3.2.24) \quad \nabla \cdot \mathbf{q}^{(1)}(\mathbf{x}) = 0 \quad ,$$

$$\mathbf{q}^{(1)}(\mathbf{x}) = -K_r(\Psi_0)\nabla\Psi_1(\mathbf{x}) + q_0 [\Psi_1(\mathbf{x}) + Y'(\mathbf{x}) + \Psi_0(z)\zeta'(\mathbf{x})] \mathbf{e}_z ,$$

where we have accounted for the fact that $-K_r(\Psi_0)\nabla(z + \Psi_0) \equiv q_0\mathbf{e}_z$. By combining equations 3.2.24, one obtains the governing equation for the fluctuation Ψ_1 of the pressure-head, i.e.,

$$(3.2.25) \quad \nabla [K_r(\Psi_0)\nabla\Psi_1(\mathbf{x})] - q_0\frac{\partial}{\partial z}\Psi_1(\mathbf{x}) = q_0\frac{\partial}{\partial z} [Y'(\mathbf{x}) + \Psi_0(z)\zeta'(\mathbf{x})] ,$$

which, due to the deterministic nature of the pressure head at the water-table, is solved with zero-boundary conditions.

Equation 3.2.25 represents the starting point to obtain the statistical moments of interest. In particular, moments can be computed by either solving for Ψ_1 (and subsequently averaging) or via the MME. In the present study, it was found easier in terms of mathematical derivations to follow this second avenue. Note that for large z it yields $K_r(\Psi_0) \approx -q_0$, and one recovers from 3.2.25 the same equation of [Severino and Santini, 2005][178] valid for an unbounded domain.

THE SECOND-ORDER APPROXIMATION. The second-order correction to the flux is derived similarly to the previous case, the final result being:

$$\nabla \cdot \mathbf{q}^{(2)}(\mathbf{x}) = 0 ,$$

$$(3.2.26) \quad \begin{aligned} \mathbf{q}^{(2)}(\mathbf{x}) = & -K_r(\Psi_0)\nabla\Psi_2(\mathbf{x}) + q_0\Psi_2(\mathbf{x})\mathbf{e}_z + \\ & -K_r(\Psi_0) [\Psi_1(\mathbf{x}) + Y'(\mathbf{x}) + \Psi_0(z)\zeta'(\mathbf{x})] \nabla\Psi_1(\mathbf{x}) + \\ & + q_0 \left\{ \frac{1}{2} [\Psi_1(\mathbf{x}) + \Psi_0(z)\zeta'(\mathbf{x})]^2 + \Psi_1(\mathbf{x})Y'(\mathbf{x}) + \Psi_1(\mathbf{x})\zeta'(\mathbf{x}) + \right. \\ & \left. + \frac{1}{2} Y'^2(\mathbf{x}) + \Psi_0(z)Y'(\mathbf{x})\zeta'(\mathbf{x}) + \frac{\Psi_0(z)}{2}\zeta'^2 \right\} \mathbf{e}_z . \end{aligned}$$

Elimination of $\mathbf{q}^{(2)}$ into 3.2.26 leads to the following equation for the second-order approximation Ψ_2 of the pressure-head:

$$(3.2.27) \quad \nabla \cdot [K_r(\Psi_0)(z) \nabla \Psi_2(\mathbf{x})] - q_0 \frac{\partial}{\partial z} \Psi_2(\mathbf{x}) = q_0 \frac{\partial}{\partial z} \mathcal{L}_2(\mathbf{x}) - \mathcal{L}'_2(\mathbf{x}),$$

where we have set

$$(3.2.28) \quad \mathcal{L}_2(\mathbf{x}) \equiv \Psi_1(\mathbf{x}) Y'(\mathbf{x}) + \Psi_0(z) Y'(\mathbf{x}) \zeta'(\mathbf{x}) +$$

$$+\frac{1}{2} \Psi_0(z) \zeta'^2(\mathbf{x}) + \Psi_1(\mathbf{x}) \zeta'(\mathbf{x}) + \frac{1}{2} Y'^2(\mathbf{x}) + \frac{1}{2} [\Psi_1(\mathbf{x}) + \Psi_0(z) \zeta'(\mathbf{x})]^2 +$$

$$-q_0^{-1} K_r(\Psi_0) [\Psi_1(\mathbf{x}) + Y'(\mathbf{x}) + \Psi_0(z) \zeta'(\mathbf{x})] \frac{\partial}{\partial z} \Psi_1(\mathbf{x}),$$

$$(3.2.29) \quad \mathcal{L}'_2(\mathbf{x}) \equiv K_r(\Psi_0) \nabla_h \{[\Psi_1(\mathbf{x}) + Y'(\mathbf{x}) + \Psi_0(z) \zeta'(\mathbf{x})] \nabla_h \Psi_1(\mathbf{x})\},$$

$$\nabla_h \equiv \left(\frac{\partial}{\partial x}, \frac{\partial}{\partial y} \right).$$

It is important to notice that, since all the RSFs appearing into 3.2.29 are stationary in horizontal plane, it results $\langle \mathcal{L}'_2(\mathbf{x}) \rangle = 0$.

Second order moments of the pressure-head. Before proceeding with the derivation of the second-order moments of Ψ , it is worth noting that, due to the linear dependence (see equation 3.2.25) of Ψ_1 upon Y' and ζ' in the plane of isotropy, the various moments will result stationary RSFs there. Furthermore, since we are interested in the unsaturated flow close to the water-table ($z = 0$), we can regard the soil surface ($z = L$) sufficiently far away from such a zone, so that one can let $L \rightarrow \infty$. Note that this latter assumption does not modify the leading-order expressions 3.2.23 of the FVs. In addition, away from the water-table $z = 0$ the lower boundary condition does not impact anymore, and consequently the FVs tend to become stationary, unless the upper boundary condition (i.e. the soil's surface) is approached (in this latter case the flow would again result nonstationary).

We start from the two-point covariances $C_{\Psi_\gamma}(\mathbf{x}, \mathbf{x}')$ whose governing equation is obtained by multiplying 3.2.25 by γ evaluated at $\mathbf{x}' \neq \mathbf{x}$ and averaging, i.e.,

$$(3.2.30) \quad \mathcal{L} C_{\Psi\gamma}(\mathbf{x}, \mathbf{x}') = q_0 \frac{\partial}{\partial z} [C_{Y\gamma}(\mathbf{x} - \mathbf{x}') + \Psi_0(z) C_{\zeta\gamma}(\mathbf{x} - \mathbf{x}')] ,$$

$$\mathcal{L} \equiv \nabla \{K_r [\Psi_0(z)] \nabla\} - q_0 \frac{\partial}{\partial z} ,$$

where, by virtue of the stationarity of the soil-properties, we have set $\langle Y'(\mathbf{x}) \gamma(\mathbf{x}') \rangle \equiv C_{Y\gamma}(\mathbf{x} - \mathbf{x}')$ and similarly for $\langle \zeta'(\mathbf{x}) \gamma(\mathbf{x}') \rangle$. Hereafter, we shall assume that the ensemble average $\langle \mathcal{A} \rangle$ of any RSF \mathcal{A} is interchangeable with its spatial counterpart $\bar{\mathcal{A}}$, i.e. $\langle \mathcal{A} \rangle \simeq \bar{\mathcal{A}}$ (ergodic hypothesis). We also adopt in the sequel the following convention: $Y\gamma \equiv Y$ for $\gamma = Y$, and $\zeta\gamma \equiv \zeta$ for $\gamma = \zeta$. To facilitate the successive derivations, it is useful to introduce the transformation

$$(3.2.31) \quad C_{\Psi\gamma}(\mathbf{x}, \mathbf{x}') = \sqrt{-q_0} \frac{\exp(-z/2)}{K_r[\Psi_0(z)]} \Phi(\mathbf{x}, \mathbf{x}') ,$$

which converts 3.2.30 into an Helmholtz-type problem:

$$(3.2.32) \quad \begin{aligned} \nabla^2 \Phi(\mathbf{x}, \mathbf{x}') - \frac{1}{4} \Phi(\mathbf{x}, \mathbf{x}') = \\ = -\sqrt{-q_0} \exp\left(\frac{z}{2}\right) \frac{\partial}{\partial z} [C_{Y\gamma}(\mathbf{x} - \mathbf{x}') + \Psi_0(z) C_{\zeta\gamma}(\mathbf{x} - \mathbf{x}')] . \end{aligned}$$

For the sake of simplicity, we limit to quote the final result

$$(3.2.33) \quad \begin{aligned} C_{\Psi\gamma}(r_h, z, z') = \\ = g(z) \int_0^\infty dk k J_0(kr_h) \int_0^\infty d\xi \chi_\gamma(\xi) \frac{d}{d\xi} \left[\exp\left(\frac{\xi}{2}\right) G_\beta(z, \xi) \right] , \end{aligned}$$

$$g(z) \equiv \frac{\exp(-z/2)}{1 - \kappa \exp(-z)},$$

(3.2.34)

$$\chi_\gamma(\xi) = \sigma_{Y\gamma} \tilde{\rho}_h(k I_{Y\gamma}) \rho_v \left(\frac{\xi - z'}{\bar{\lambda}_{Y\gamma}} \right) + \sigma_{\zeta\gamma} \tilde{\rho}_h(k I_{\zeta\gamma}) \Psi_0(\xi) \rho_v \left(\frac{\xi - z'}{\bar{\lambda}_{\zeta\gamma}} \right),$$

(3.2.35)

$$G_\beta(z, \xi) = \beta^{-1} \left[\exp\left(-\frac{z + \xi}{2}\beta\right) - \exp\left(-\frac{|z - \xi|}{2}\beta\right) \right], \beta = \sqrt{1 + 4k^2},$$

and address the interested reader to the Appendix A for details. In equation 3.2.33 J_0 is the zero-order Bessel function of the first kind, r_h is the magnitude of the vector $(x - x', y - y')$, and $\bar{\lambda}_\mu \equiv \lambda_\mu I_\mu$ (no summation-convention). The expression 3.2.33 is a general representation of the cross-covariances $C_{\Psi\gamma}$, and its computation is achieved by carrying out two quadratures. The cross-variance $\sigma_{\Psi\gamma}(z)$ is derived by setting $r_h = 0$ and $z \equiv z'$ into 3.2.33.

The head covariance C_Ψ is obtained multiplying 3.2.25 by $\Psi_1(\mathbf{x}')$, and averaging:

$$(3.2.36) \quad \mathcal{L} C_\Psi(\mathbf{x}, \mathbf{x}') = q_0 \frac{\partial}{\partial z} [C_{\Psi Y}(\mathbf{x}', \mathbf{x}) + \Psi_0(z) C_{\Psi \zeta}(\mathbf{x}', \mathbf{x})].$$

Notice that the cross-covariances $C_{\gamma\Psi}(\mathbf{x}, \mathbf{x}')$ were replaced by $C_{\Psi\gamma}(\mathbf{x}', \mathbf{x})$ since maintaining the order between \mathbf{x} and \mathbf{x}' is crucial due to the non-stationarity of $C_{\gamma\Psi}$ along the depth. The solution for C_Ψ is achieved similarly to the previous case, and the final result is (Appendix A):

$$(3.2.37) \quad C_\Psi(r_h, z, z') = g(z) g(z') \int_0^\infty dk k J_0(k r_h) \int_0^\infty \int_0^\infty d\xi d\eta \cdot$$

$$\cdot \Sigma(\xi, \eta) \frac{\partial^2}{\partial \xi \partial \eta} \left[\exp\left(\frac{\xi + \eta}{2}\right) G_\beta(z, \xi) G_\beta(z', \eta) \right],$$

$$(3.2.38) \quad \Sigma(\xi, \eta) = \sigma_Y^2 I_Y \tilde{\rho}_h(k I_Y) \rho_v \left(\frac{\xi - \eta}{\bar{\lambda}_Y} \right) +$$

$$\begin{aligned}
& +\sigma_{Y\zeta} I_{Y\zeta} \tilde{\rho}_h(kI_{Y\zeta}) [\Psi_0(\xi) + \Psi_0(\eta)] \rho_v \left(\frac{\xi - \eta}{\bar{\lambda}_{Y\zeta}} \right) + \\
& +\sigma_\zeta^2 I_\zeta \tilde{\rho}_h(kI_\zeta) \Psi_0(\xi) \Psi_0(\eta) \rho_v \left(\frac{\xi - \eta}{\bar{\lambda}_\zeta} \right) .
\end{aligned}$$

Likewise, the head variance $\sigma_\Psi^2 \equiv \sigma_\Psi^2(z)$ is obtained by setting $r_h = 0$, and $z \equiv z'$ into 3.2.37.

Higher-order correction of the mean pressure-head. To compute the higher-order correction $\langle \Psi \rangle = \Psi_0 + \langle \Psi_2 \rangle$ of the mean head, one has to solve the equation 3.2.27 for the second-order correction Ψ_2 . Like before, such a task is easily achieved by means of the transformation $\Psi_2(\mathbf{x}) = \sqrt{-q_0} \frac{\exp(-z/2)}{K_r[\Psi_0(z)]} \Phi_2(\mathbf{x})$ which casts 3.2.27 into an Helmholtz equation, i.e.,

$$(3.2.39) \quad \nabla^2 \Phi_2 - \frac{1}{4} \Phi_2 = -\sqrt{-q_0} \exp\left(\frac{z}{2}\right) \left[\frac{\partial}{\partial z} \mathcal{L}_2(\mathbf{x}) - q_0^{-1} \mathcal{L}'_2(\mathbf{x}) \right].$$

Taking the ensemble average into 3.2.39 provides the equation for $\langle \Phi_2 \rangle$, i.e.,

$$(3.2.40) \quad \frac{d^2}{dz^2} \langle \Phi_2(z) \rangle - \frac{1}{4} \langle \Phi_2(z) \rangle = -\sqrt{-q_0} \exp\left(\frac{z}{2}\right) \frac{d}{dz} \langle \mathcal{L}_2(z) \rangle,$$

$$(3.2.41) \quad \begin{aligned} \langle \mathcal{L}_2(z) \rangle = & \frac{1}{2} \sigma_Y^2 + \Psi_0(z) \sigma_{Y\zeta} + \frac{\Psi_0(z)}{2} [1 + \Psi_0(z)] \sigma_\zeta^2 + \\ & + \sigma_{\Psi Y}(z) + [1 + \Psi_0(z)] \sigma_{\Psi \zeta}(z) + \frac{1}{2} \sigma_\Psi^2(z) + \end{aligned}$$

$$-\frac{1}{q_0} K_r(\Psi_0) \left[\frac{1}{2} \frac{d}{dz} \sigma_\Psi^2(z) + \left\langle Y'(\mathbf{x}) \frac{\partial}{\partial z} \Psi_1(\mathbf{x}) \right\rangle + \Psi_0(z) \left\langle \zeta'(\mathbf{x}) \frac{\partial}{\partial z} \Psi_1(\mathbf{x}) \right\rangle \right],$$

where we have accounted for the fact that $\langle \mathcal{L}'_2(\mathbf{x}) \rangle = 0$. Notice that, due to the stationarity of the term \mathcal{L}_2 in the horizontal-plane (see eq. 3.2.28), the function $\langle \Phi_2 \rangle$ (and concurrently $\langle \Psi_2 \rangle$) depends upon the depth z , solely. A similar conclusion was drawn both by [Zhang and Winter, 1998][242] via

extensive MCs, and by [Indelman *et. al.*, 1993][**96**] by means of analytical tools. Thus, solving for $\langle \Phi_2 \rangle$ and back substitution leads to

$$(3.2.42) \quad \langle \Psi_2(z) \rangle = \frac{1}{f_\kappa(z)} \left\{ \langle \mathcal{L}_2(\infty) \rangle [1 - \exp(-z)] - \exp(-z) \int_0^z d\xi \exp(\xi) \langle \mathcal{L}_2(\xi) \rangle \right\},$$

$$f_\kappa(z) = 1 - \kappa \exp(-z).$$

It is convenient to represent the mean pressure-head as $\langle \Psi(z) \rangle = \Psi_0(z) + \langle \Psi_2(z) \rangle = \Psi_0(z) \Theta(z)$, where we have set $\Theta(z) = 1 + \psi(z)$ with

$$(3.2.43) \quad \psi(z) = \frac{\langle \Psi_2(z) \rangle}{\Psi_0(z)} = q_0 \frac{\exp[-\Psi_0(z)]}{\Psi_0(z)} \cdot \left\{ \exp(-z) \int_0^z d\xi \exp(\xi) \langle \mathcal{L}_2(\xi) \rangle - \langle \mathcal{L}_2(\infty) \rangle [1 - \exp(-z)] \right\}.$$

The utility of such a representation is that $\langle \Psi \rangle$ is expressed via the product between Ψ_0 (valid for a homogeneous formation) and a characteristic function Θ which "modifies" Ψ_0 according to the medium's heterogeneity. One advantage related to the representation $\langle \Psi(z) \rangle = \Psi_0(z) \Theta(z)$ is that it is instrumental to identify the statistical properties of a vadose zone. Indeed, once $\langle \Psi \rangle$ has been estimated by the measurements of the pressure-heads at different locations, one can identify the statistical parameters pertaining to the RSFs $Y, Y\zeta$, and ζ by matching against to it.

The general expression of the normalized correction ψ allows one to investigate the flow behavior in the near and far field. More precisely, at large depths one has $\psi(\infty) = 0$, and concurrently $\langle \Psi(\infty) \rangle \equiv \Psi_0(\infty)[1 + \psi(\infty)] = \ln(-q_0)$, which coincides with the result obtained by Russo [Russo, 1993][**161**] and Severino [Severino and Santini, 2005][**178**] in the case of an unbounded domain. Instead, at the water-table ($z = 0$) it is easily shown from 3.2.43 (we omit the algebraic derivations) that: $\psi(0) = [\langle \mathcal{L}_2(\infty) \rangle - \langle \mathcal{L}_2(0) \rangle] / \kappa < \infty$, and therefore we recover that: $\langle \Psi(0) \rangle \equiv \Psi_0(0)[1 + \psi(0)] = 0$. This result is explained by noting that the boundary condition at $z = 0$ requires a fixed head, and thus the heterogeneity does not affect the value of the pressure-head there [Severino and Coppola, 2012][**184**]. These two asymptotics can be useful: i)

in the practical applications (to design proper sampling-strategies), and ii) in the modeling aspects (to validate more involved numerical codes).

Calibration versus Validation. We wish here to illustrate the application/use of the theoretical results obtained so far. In particular, it is seen that a relatively large number of input parameters, i.e. geometric means of the saturated conductivity and the alpha-parameter as well as the related (cross)-covariances, has to be preliminarily selected. While the statistical characterization of Y and ζ has been largely discussed and assessed (see e.g. the survey exploited in [Rubin, 2003][158], and references therein), the cross-correlation Y - ζ is still a matter of debate, and it deserves a thorough analysis. To this end, we refer to a recently conducted unsaturated flow experiment in a field [Severino et al., 2010, 2016a, 2016b][174, 195, 196], which is described briefly herein with special care to the identification of the statistical quantities which are relevant for the present study.

The field is located at the Ponticelli-site (Naples, Italy). The soil texture was analyzed by sampling at several (randomly selected) locations across the field. The resulting structure is that of a typical “andosol”: a structureless sand with a small (lesser than a coarse-textured soil) bulk density $\rho = (1.0 \pm 0.1) \text{ g/cm}^3$ [Terribile et al., 2007; Comegna et al., 2013][211, 34]. Prior to any analysis concerning the spatial distribution, it is instrumental to examine the measurements of Y and ζ by means of conventional (univariate) statistics.

UNIVARIATE ANALYSIS OF Y AND ζ . The saturated conductivity K_s was measured (by a permeameter working at constant head) upon ~ 80 samples taken at two depths along a transect 50 m-long (1.25 m horizontal step) excavated parallel to the experimental site. The measure of α was instead acquired in the field by means of an internal test drainage (a general description about such a test as well as the identification procedure can be found in [Severino et al., 2003; Gomez et al., 2009][190, 78]). More precisely, the field was ponded by applying water in excess of the infiltration rate. After two days of continuous ponding (when steady state conditions were almost reached) water’s application was halted, and monitoring initiated. This latter consisted of simultaneous measurements of the water content ϑ and the pressure head Ψ (taken by TDR-probes and tensiometers, respectively) at three depths, $z = 0.30, 0.60, 0.90$ m (from the soil surface), along the transect. Monitoring

statistics	$Y \equiv \ln K_s$	$\zeta \equiv \ln \alpha$
mean	2.30	-3.31
standard deviation	1.38	$2.76 \cdot 10^{-1}$
coefficient of variation	$6.01 \cdot 10^{-1}$	$8.35 \cdot 10^{-2}$
D	0.882	0.715

TABLE 3.2.1. Estimates of the: i) mean, ii) standard deviation, and iii) coefficient of variation together with the D - test of normal (null) hypothesis

For comparison purposes, the reference value at the 5%-level of confidence is in the circular brackets. Values of K_s and α are expressed in cm/h and cm^{-1} .

was interrupted 77 days later, when drainage was evolving too slowly to make it impossible to further collect significantly different pairs of (ϑ, Ψ) . The experimental hydraulic conductivity curve $K^{(ex)} \equiv K^{(ex)}(\Psi)$ was determined by following the method suggested by [Basile et al., 2003][11]. Hence, the value of α was determined by matching the theoretical curve $K_r \equiv K_r(\Psi)$ (second of eq. 3.2.5) against to $K^{(ex)}(\Psi)$ divided by the K_s -value measured upon the sample taken at the same depth (details can be found in [Comegna et al., 2006][35]).

The empirical (symbols) cumulative distribution function (CDF) of $Y \equiv \ln K_s$ (blue) and $\zeta \equiv \ln \alpha$ (red) along with the theoretical (continuous) fitted normal (CDF)s are shown in the Figure 3.2.3. The observed good agreement between empirical and theoretical CDFs is quantitatively confirmed by the Kolmogorov-Smirnov test (Table 3.2.1). To summarize, both ζ and Y can be considered as normally distributed with the latter exhibiting a larger variability than the former. It is worth noting that the intervals of (5%)-confidence of the quantity $(\sigma_u/\mu_u)^2$ (being u either K_s or α) as determined i) by the raw u -data, and ii) by the expression $\exp(\sigma_{\ln u}^2) - 1$ (which is known to apply to log-normally distributed random variables) are:

Thus, the overlapping between the intervals of confidence further demonstrates that the log-transforms of K_s and α can be regarded (up to the experimental errors) as normally distributed random variables.

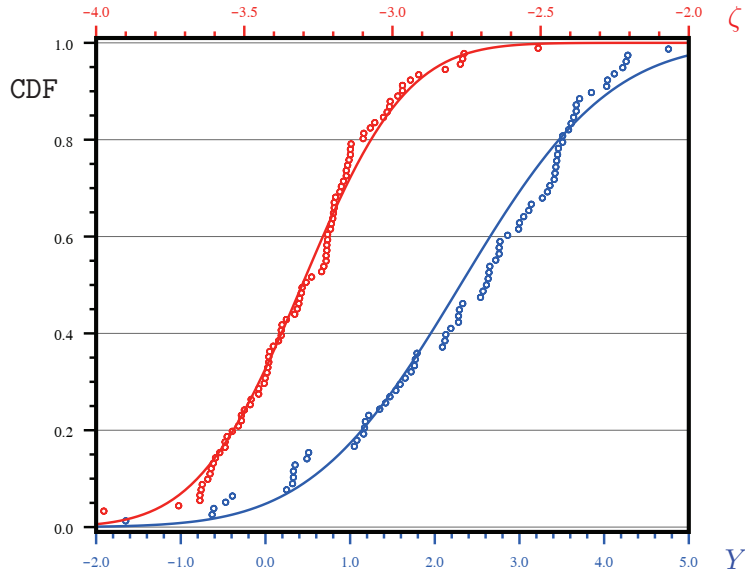


FIGURE 3.2.3. Cumulative distribution functions of measured (symbols) $Y \equiv \ln K_s$ (blue) and $\zeta \equiv \ln \alpha$ (red)

Continuous lines represent the respective fitted theoretical CDFs. The saturated conductivity K_s and the α -parameter are expressed in cm/h and cm^{-1} , respectively.

$(\sigma_u/\mu_u)^2$	$\ln K_s$	$\ln \alpha$
u -data	[0.697; 2.32]	$[5.27; 10.4] \cdot 10^{-2}$
$\exp(\sigma_{\ln u}^2) - 1$	[1.59; 9.85]	$[5.38; 10.5] \cdot 10^{-2}$

TABLE 3.2.2. Intervals of (5%)-confidence of $(\sigma_u/\mu_u)^2$ as determined by the u -data, and by the expression $\exp(\sigma_{\ln u}^2) - 1$

In order to investigate possible scale-issues the saturated conductivity K_s was measured in the field (Auger-hole device), as well. The intervals of 5%-confidence (see Table 3.2.3) for the estimates of the mean and variance of $Y \equiv \ln K_s$ demonstrate that there is no statistical difference between the characterization of Y at laboratory and at field scale. This is explained by recalling that the sampling volume of the Auger-hole device is approximately of the same size (details are in [Severino et al., 2010][174]) of the soil samples

Scale	$\langle Y \rangle$	σ_Y^2	Number of data
laboratoy	$(199; 261) \cdot 10^{-2}$	$(142; 267) \cdot 10^{-2}$	82
field	$(227; 293) \cdot 10^{-2}$	$(150; 287) \cdot 10^{-2}$	70

TABLE 3.2.3. Intervals of 5%-confidence for the estimates of the mean and variance of Y at laboratory and field scale

(see also discussion in [Fallico *et al.*, 2016][60]). The usefulness of using laboratory K_s -measurements stems from the fact that these were more numerous than those at field scale (Table 3.2.3).

Likewise, the support volumes attached to the devices (i.e. time domain reflectometry, and piezometers) used in situ to detect the pairs (θ, Ψ) at the several locations are approximately of the same size of the soil samples taken from the site [Comegna *et al.*, 2013][34]. As a consequence, the measurements of the α -parameter can be regarded de facto as local ones (comparable with those of K_s at laboratory scale). Of course, matters would result completely different if one aims at inferring the statistics of α (or of any other random variable) by using the ensemble average of the flow variables [Severino *et al.*, 2003][190]. In this case, due to the completely different size of the involved volume support, the comparison between local and field scale measurements should also account for the proper upscaling [Russo, 2003; Severino and Santini, 2005; Severino and Coppola, 2012][164, 178, 184].

To investigate whether ζ and Y can be considered cross-correlated, we have used the t -Student test with $t \simeq r_{\zeta Y} \sqrt{(n-2)/(1-r_{\zeta Y}^2)}$, being $r_{\zeta Y}$ the estimate of the correlation coefficient, i.e.,

$$(3.2.44) \quad r_{\zeta Y} \equiv \frac{\sigma_{\zeta Y}}{\sigma_{\zeta} \sigma_Y} \simeq \frac{\sum_i (\zeta_i - \bar{\zeta})(Y_i - \bar{Y})}{\sqrt{(\sum_i \zeta_i^2)(\sum_i Y_i^2)}} = 0.143, \quad (i = 1, \dots, 82).$$

Since it yields $t = 1.292$ ($n = 82$), the null hypothesis ($H_0: \rho_{\zeta Y} \equiv 0$) can not be rejected till to the 10% of confidence (it is remained that $1.292 \simeq t_{0.10}$). The residuals (ζ', Y') along with the regression-line and the 95% confidence-limits are displayed in Figure 3.2.4. The weak correlation, which is detected at a first glance (by the modest slope of the regression-line), is also confirmed by the Fisher-test (p -value $\sim 5.72\%$). However, for the experiment at stake, such a correlation is not statistically significative (at the 5% of confidence).

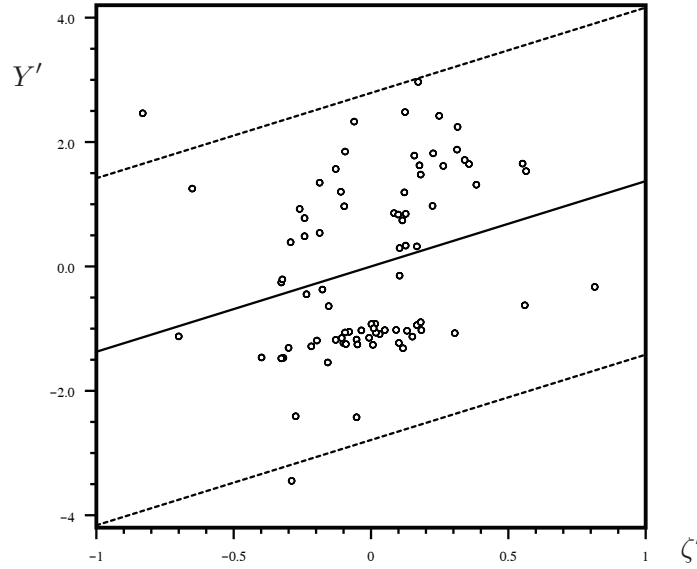


FIGURE 3.2.4. Residuals of Y versus residuals of ζ . The linear regression and the associated 95% confidence-limits are represented by solid and dashed lines, respectively.

The same findings were observed into similar previous studies [*Wierenga et al., 1991; Russo and Bouton, 1992; Russo et al., 1997*][**233, 165, 168**].

More generally, even if a positive correlation may result important for the variance of the unsaturated conductivity $K \equiv K(\Psi)$ [*Russo et al., 1997*][**168**], it is worth noting here that, into studying the impact upon the flow and transport processes, one can still regard (along the lines suggested by Russo [*Russo and Bouton, 1992*][**165**]) $Y \equiv \ln K_s$ and $\zeta \equiv \ln \alpha$ as uncorrelated random fields (the weak positive correlation notwithstanding). More important is the fact that in coarser-textured soils (like the one at the Ponticelli site) the cross-correlation is found of scarce importance [*Ragab and Cooper, 1993a, 1993b; Tartakovsky et al., 1999*][**145, 144, 209**]. Finally, in the case of the Ponticelli site the α -parameter can be regarded as a given constant (see below), and this further underpins the neglect of the Y - ζ correlation. Thus, for all these reasons we feel comfortable disregarding the cross correlation between K_s and α .

Though our general theory allows one dealing with a variance of ζ of the same order of that of Y , the soil properties of the Ponticelli site (see Table 3.1.1) show that $\sigma_\zeta^2/\sigma_Y^2 = \mathcal{O}(10^{-2})$, and therefore one can disregard the variability of the former as compared with that of the latter. This is tantamount to assume α everywhere equal to α_G . Hence, we can limit our analysis to the zero-order approximation in σ_ζ , and to the second-order approximation in σ_Y .

SPATIAL HETEROGENEITY-STRUCTURE OF Y . The problem of quantifying the spatial structure (autocorrelation) of Y is rather complicated, even when measurements are numerous. The procedure should involve several steps: i) an hypothesis about the functional model of the covariance, ii) estimates of the parameters of such a model, and iii) a model validation test [*Russo and Bouton, 1992; Russo et al., 1997*][**165, 168**]. The problem of selecting the most appropriate model remains to some extent in the realm of the practical applications [*Rubin, 2003*][**158**]. The prevailing approach is the pragmatic one: select a model for its practicality/versatility as well as its performance in similar situations, determine the parameter(s), and check subsequently its usefulness by matching against to real data. Thus, by adopting this stand point, and in line with the model structure 3.2.6, for the horizontal autocorrelation (for simplicity hereafter denoted by ρ_h) we select the Gaussian model, i.e.,

$$(3.2.45) \quad \rho_h(x_h) \equiv \exp \left[-\pi \left(\frac{x_h}{2I} \right)^2 \right],$$

with $I_Y \equiv I$. Hence, the horizontal integral scale was estimated by considering the two sampling depths, separately (Figure 3.2.5). The results were nevertheless quite similar leading to $I \sim 20$ m. Note that the relatively large value of the horizontal integral scale I is not surprising due to the stratified nature of the vadose zone at stake, and it significantly differs from its other counterparts [*Russo and Bouton, 1992; Russo et al., 1997*][**165, 168**]. It has to be noted that, given the ratio $L/I \simeq (50 \text{ m})/(20 \text{ m})$ between the transect length-scale L and I , the flow domain can not be regarded “into a strict sense” as ergodic. In fact, only when the flow domain is large enough with respect to the integral scales of the RSF, the spatial average of the single (available) realization can be replaced with the ensemble mean. Otherwise, the spatial

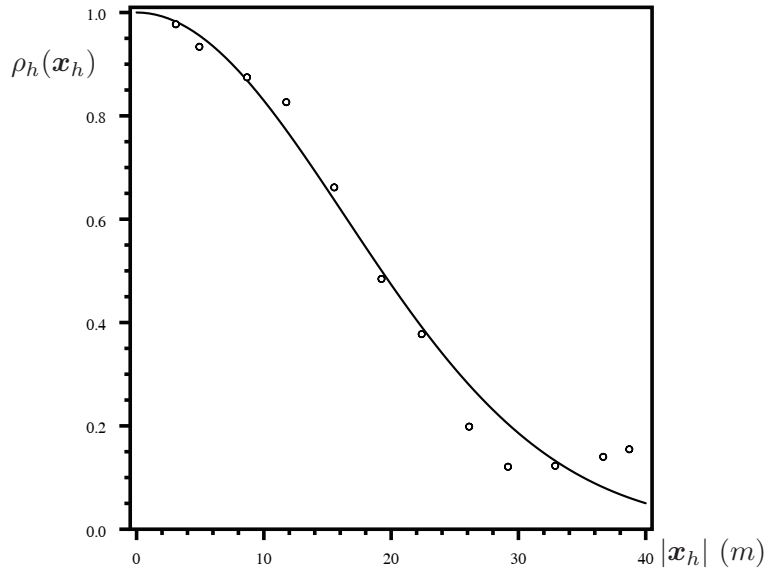


FIGURE 3.2.5. Horizontal autocorrelation function for the log-conductivity Y

. Symbols pertain to the measured values, whereas the continuous line refers to the Gaussian model 3.2.45 with $I \equiv 20.5\text{m}$.

average is only an estimate of the ensemble mean, which in turn is affected by uncertainty. In particular, for a domain of finite size such an uncertainty increases with both the coefficient of variation and the size of the integral scales of the spatially variable hydraulic properties.

However, a previous study conducted [*Comegna and Basile, 1994*][**36**] about the spatial distribution of the soil hydraulic properties in the same site (and involving a much larger domain) has lead to a similar statistical characterization. Thus, given this extra information, we feel comfortable about the fact that the domain at the Ponticelli site can be regarded as approximately ergodic. Last, as it will be clearer later on, the good matching between theoretical and experimental values provides (among the others) a posteriori justification of the presumed ergodicity (the numerous approximations, source of uncertainties and measurement-errors notwithstanding).

To complete the spatial characterization of Y at the Ponticelli site, the vertical autocorrelation (hereafter denoted by ρ_v) has to be identified. However, the scarce availability of K_s -measurements along the vertical does not enable one to identify ρ_v by the same procedure which we used for the horizontal autocorrelation. Thus, we used geological information to gain insight about the shape of ρ_v . More precisely, the analysis of the texture suggests that the soil is a sedimentary structureless sand [Severino *et al.*, 2010][174]. This is also confirmed by the geological pattern of the formation: subsequent depositions of different (erupted) materials [Comegna *et al.*, 2010][33], and therefore the soil can be sought as a collection of sedimentary lenses each one exhibiting different Y -values from one lense to the other. This is a typical feature of those formations where the vertical correlation scale is found to be much lesser than the horizontal one [Russo and Bresler, 1981][166]. In this case the soil property is characterized by a complete lack of vertical correlation, thus authorizing to replace the vertical autocorrelation with a Dirac distribution, i.e. $\rho_v \sim \delta$. Such an approximation (also known as δ -correlation) was adopted in previous studies pertaining to both the vadose zone [Indelman *et al.*, 1993; Severino and Santini, 2005; Severino and Coppola, 2012][96, 178, 184], and the aquifers [Fiori *et al.*, 1998; Indelman and Dagan, 1999; Severino, 2011; Severino *et al.*, 2012; Severino and Bartolo, 2015][65, 97, 181, 179, 175]. We apply the statistical characterization obtained by dealing with the first meters to the entire flow domain (~ 40 m). Such a choice is justified on the basis of the available geological information [Terribile *et al.*, 2007][211] suggesting that the soil at stake can be thought as a continuous sequence of thin stratified (mainly erupted) materials of the same type of those detected at the shallow depths. At any rate, from a general point of view, it is reminded that any statistical characterization of the soil's hydraulic properties based upon shallow measurements is not enough for the entire flow domain. A rigorous (methodological) approach would require a dense sampling campaign at all the depths (similarly to [Russo and Bouton, 1992; Russo *et al.*, 1997][165, 168]).

With the input parameters and the autocorrelation functions identified so far, we are in position to compute the (cross)-variances $\sigma_{\Psi Y}$ and σ_{Ψ}^2 . By omitting the (very lengthy) algebraic derivations, the final result is:

$$(3.2.46) \quad \sigma_{\Psi Y}(z) = \sigma_{\Psi Y}(\infty) \frac{\mathcal{F}_{\Psi Y}(z)}{f_{\kappa}(z)}, \quad \sigma_{\Psi}^2(z) = \sigma_{\Psi}^2(\infty) \frac{\mathcal{F}_{\Psi}(z)}{f_{\kappa}^2(z)}$$

$$(3.2.47) \quad \mathcal{F}_{\Psi Y}(z) = 1 - \frac{\Lambda(2z)}{\Lambda(0)}(1 + 2\pi z^2) + \frac{2z}{\Lambda(0)} \exp(-z),$$

$$(3.2.48)$$

$$\mathcal{F}_{\Psi}(z) = 1 - \frac{\Lambda(2z)}{\Lambda(0)} \{1 + 2\pi z[1 - \exp(-z)]\} + \frac{2}{\Lambda(0)} [\exp(-z) - \exp(-2z)],$$

being

$$\Lambda(a) = \exp \left[\frac{1 + (\pi a)^2}{4\pi} \right] \operatorname{erfc} \left(\frac{1 + \pi a}{2\sqrt{\pi}} \right),$$

whereas

$$\sigma_{\Psi Y}(\infty) = -\frac{\Lambda(0)}{2} \lambda I \sigma_Y^2,$$

$$\sigma_{\Psi}^2(\infty) = \frac{\Lambda(0)}{2} \lambda (I \sigma_Y)^2,$$

are the far field (large z) values of 3.2.46. Note that we have set $\lambda_Y \equiv \lambda$, for simplicity.

It is seen that the functions $\omega_{\Psi Y}(z) \equiv \sigma_{\Psi Y}(z)/\sigma_{\Psi Y}(\infty)$ and $\omega_{\Psi}(z) \equiv \sigma_{\Psi}^2(z)/\sigma_{\Psi}^2(\infty)$ are weights driving the transition (see 3.2.6) of the (cross) variance 3.2.46 from the water-table, where $\omega_{\Psi Y}(0) = \omega_{\Psi}(0) = 0$, to the far field, where $\omega_{\Psi Y}(\infty) = \omega_{\Psi}(\infty) = 1$. Note that the rate of the transition from the water-table to the far field with the infiltration flux q_0 is regulated by the term $f_{\kappa} \equiv f_{\kappa}(z)$, solely. Due to its multiplicative structure, the quantity $\kappa \exp(-z)$ is significantly different from zero only when $z \ll 1$, i.e. close to the water-table. To the contrary, away from the water-table (i.e. $z \gg 1$) one has $f_{\kappa} \sim 1$, in agreement with Severino and Santini [*Severino and Santini, 2005*][178].

We are now in position to complete the characterization of the heterogeneity structure of the field at stake by identifying the anisotropy ratio λ by means of the variance σ_{Ψ}^2 of the pressure head. This implies that the steady state Ψ -measurements are required, and therefore before going further it is worth exploiting the experimental data set which has been used for such a purpose. Indeed, during another stage of the experimental campaign (aiming

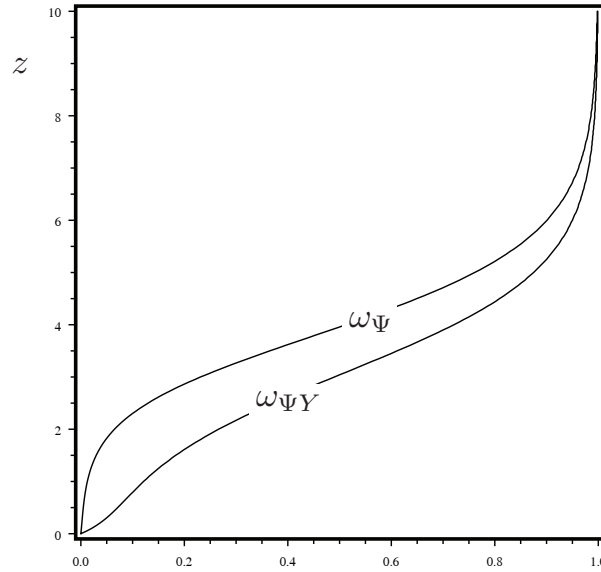


FIGURE 3.2.6. Dependence of the weight-functions (horizontal axe) $\omega_{\Psi Y}$ - ω_{Ψ} upon the depth z (normalized by $\alpha_G^{-1} = 27.4\text{cm}$)

- . The parameter κ associated to the infiltrating non dimensional flux ($q_0 = -4.21 \cdot 10^{-2}$) is $\kappa = 1 + q_0^{-1} = -22.8$.

to monitor a solute transport process), the plot was irrigated ($4.2 \cdot 10^{-1} \text{ cm/h}$) until stationary (steady) values of the pressure head Ψ (and water content, as well) were detected at the sampling depths along the trench. By this time, pressure-head values were read at the tensiometers along the trench, and the statistical (dimensionless) moments, which are of interest for the present study, are summarized in the Table 3.2.4.

Since the sampling depths lie very far from the water-table (details are in the caption of Table 3.2.4), it yields from 3.2.6 that $\omega_{\Psi}(z) \simeq \omega_{\Psi}(\infty) \equiv 1$, and concurrently one can use the asymptotic value of the head variance to estimate the anisotropy ratio λ .

The legitimacy of using the asymptotic $\sigma_{\Psi}^2(\infty)$ for calibration purposes is corroborated by the fact that the far field $\Psi_0(\infty)$ of the mean head lies within the interval of confidence of the mean pressure-heads (Table 3.2.5). The anisotropy ratio λ is approximately $2.4 \cdot 10^{-3}$. It is interesting to note

z	$\bar{\Psi}(-)$	$\bar{\sigma}_{\Psi Y}(-)$	$\bar{\sigma}_{\Psi}^2(-)$	N
145	-3.60	$-6.88 \cdot 10^{-2}$	7.60	35
144	-2.87	$-9.55 \cdot 10^{-2}$	12.3	37
143	-2.52	$-1.30 \cdot 10^{-2}$	15.5	36

TABLE 3.2.4. Steady-state values of the experimental spatial variables

- i) mean, $\bar{\Psi}$, of the pressure head;
- ii) cross-variance, $\bar{\sigma}_{\Psi Y}$;
- iii) head-variance, $\bar{\sigma}_{\Psi}^2$;
- iv) number of samples, N ;

at the three sampling depths lying at: i) $z = 40.0 - 0.9 = 39.1\text{m}$ (the deepest), ii) $z = 40.0 - 0.6 = 39.4\text{m}$ (intermediate), and iii) $z = 40.0 - 0.9 = 39.7\text{m}$ (the shallowest) above the water-table which is 40 m deep. Moments, i.e. $\bar{\sigma}_{\Psi Y} - \bar{\sigma}_{\Psi}^2$, and depths, i.e. z , have been made dimensionless by adopting $\alpha_G^{-1} = 27.4\text{ cm}$ as length-scale.

z	$\bar{\Psi}_{\text{lower}}$	$\Psi_0(\infty)$	$\bar{\Psi}_{\text{upper}}$
145	-4.1	-3.2	-3.1
144	-3.5	-3.2	-2.3
143	-3.2	-3.1	-1.9

TABLE 3.2.5. Lower and upper limit of the interval of confidence of the mean pressure head

Lower, i.e. $\bar{\Psi}_{\text{lower}} \equiv \bar{\Psi} - \bar{\sigma}_{\Psi}/\sqrt{N}$, and upper, i.e. $\bar{\Psi}_{\text{upper}} \equiv \bar{\Psi} + \bar{\sigma}_{\Psi}/\sqrt{N}$, limit of the interval of confidence of the mean pressure head as determined from data at the three sampling depths (Table 3.2.2), along with the asymptotic mean value $\Psi_0(\infty) \equiv \ln(-q_0) = \ln(4.21 \cdot 10^{-2})$. Pressure-head values and depths have been made dimensionless by adopting $\alpha_G^{-1} = 27.4\text{ cm}$ as length-scale.

that such an estimate implies that $I_v = \lambda I \sim 5\text{ cm}$, a value which is in line with the geological information [*Comegna et al., 2010*][**33**] about the thickness of the strata, i.e. $\mathcal{O}(10\text{ cm})$, detected at the experimental site.

In the Figure 3.2.7 we have depicted the far field value of the pressure-head variance (continuous red line) as calibrated by means of the experimental (red symbols) values. In the same figure we also compare the far field cross variance (continuous black line) against to the experimental (black symbols)

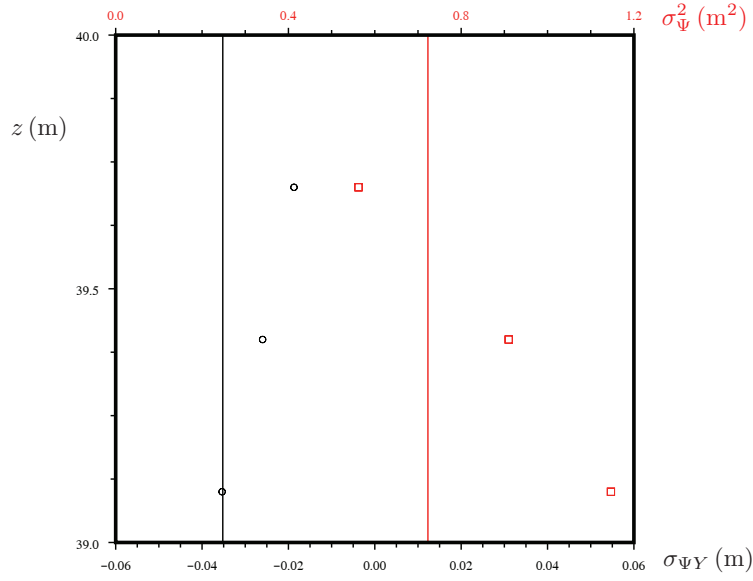


FIGURE 3.2.7. Distribution of the cross-variance $\sigma_{\Psi Y}$ (black), and the head-pressure variance σ_{Ψ}^2 (red) along the depth z (from the water-table)

Symbols refer to the experimental measurements, whereas continuous lines pertain to the far field values of equation 3.2.46.

values which were not used for the above calibration. Note that the deviations of the experimental far field $\sigma_{\Psi Y}$ and σ_{Ψ}^2 from their theoretical (i.e. constant) counterparts lie within the errors of measurements of the tensiometers [Comegna *et al.*, 2006, 2010][35, 33]. Thus, the matching between theoretical and experimental $\sigma_{\Psi Y}$ represents a satisfactory validating benchmark.

After determining all the relevant quantities required by the flow model, we are in position to make predictions upon the behavior of the FVs in the close vicinity of the water-table. To this end, we wish to point out here that direct measurements would have been tremendously time consuming and expensive, and most of them probably even impossible since the water-table is 40 m deep. This further underpins the usefulness of our model to predict the behavior of flow (and transport) variables by relating shallow measurements (which can be carried out with a relatively ease) to depths of the vadose zone which are practically inaccessible.

Discussion. We wish to illustrate how the developed stochastic model can be used to grasp the behavior of the flow variables close to the water-table. The input parameters are those determined by the set of real data pertaining to the Ponticelli site (Naples, Italy).

Due to its importance in the applications (e.g. quantifying the recharge of the aquifers and/or determining the solute mass arrivals at the water-table), we mainly concentrate the present discussion upon the uncertainty qualification of flux \mathbf{q} along the depth z . To compute the variance of this latter, the starting point is the first-order approximation 3.2.24, which is re-written here as

$$(3.2.49) \quad \mathbf{q}^{(1)}(\mathbf{x}) \simeq -K_r(\Psi_0)\nabla\Psi_1(\mathbf{x}) + q_0 [\Psi_1(\mathbf{x}) + Y'(\mathbf{x})] \mathbf{e}_z,$$

to account for the approximations which we have shown to be valid for the Ponticelli-site. To derive the variance of the flux in the horizontal plane, we take advantage from the stationarity of the flow variables there. Thus, we write the horizontal component $\mathbf{q}_h^{(1)}$ of the fluctuation 3.2.49 by means of its spectral (Fourier transform) representation, i.e.,

$$(3.2.50) \quad \mathbf{q}_h^{(1)}(\mathbf{x}_h, z) = \int \frac{d\mathbf{k}}{2\pi} \mathbf{k} \tilde{\Psi}_1(\mathbf{k}, z) \exp(-j\mathbf{k} \cdot \mathbf{x}_h),$$

being

$$(3.2.51) \quad \tilde{\Psi}_1(\mathbf{k}, z) = -q_0 \frac{\exp(-z/2)}{K_r(z)} \int_0^\infty d\xi \tilde{Y}'(\mathbf{k}, \xi) \frac{d}{d\xi} \left[\exp\left(\frac{\xi}{2}\right) G_\beta(z, \xi) \right],$$

the horizontal (2D) Fourier transform of the pressure-head fluctuation. For ease of notation we have set $K_r(\Psi_0) \equiv K_r(z)$. Taking the square of 3.2.50, and accounting for the property

$$(3.2.52) \quad \left\langle \tilde{Y}'(\mathbf{k}_1, z_1) \tilde{Y}'(\mathbf{k}_2, z_2) \right\rangle = 2\pi\lambda \sigma_Y^2 \delta(\mathbf{k}_1 + \mathbf{k}_2) \tilde{\rho}_h(k_2) \delta(z_1 - z_2),$$

leads (after introducing polar coordinates) to:

$$(3.2.53) \quad \sigma_{q_h}^2(z) = \lambda (q_0 \sigma_Y)^2 \exp(-z) \int_0^\infty dk k^3 \tilde{\rho}_h(k) \mathcal{G}_\beta(z, z),$$

$$(3.2.54) \quad \mathcal{G}_\beta(z, \zeta) \equiv \int_0^\infty d\xi \frac{d}{d\xi} \left[\exp\left(\frac{\xi}{2}\right) G_\beta(z, \xi) \right] \frac{d}{d\xi} \left[\exp\left(\frac{\xi}{2}\right) G_\beta(\zeta, \xi) \right].$$

Note that, due to the stationarity of the flux in the isotropy (horizontal) plane, the variance 3.2.53 does not depend upon x_h . To compute $\mathcal{G}_\beta(z, z)$, we preliminarily note that upon integrating by parts in 3.2.54 it yields

$$(3.2.55) \quad \mathcal{G}_\beta(z, \zeta) = - \int_0^\infty d\xi \exp\left(\frac{\xi}{2}\right) G_\beta(z, \xi) \frac{d^2}{d\xi^2} \left[\exp\left(\frac{\xi}{2}\right) G_\beta(\zeta, \xi) \right].$$

Then, by recalling that $G_\beta(\zeta, \xi)$ is such that $\frac{d^2}{d\xi^2} G_\beta(\zeta, \xi) - \frac{\beta^2}{4} G_\beta(\zeta, \xi) = \delta(\xi - \zeta)$, one has

$$(3.2.56) \quad \begin{aligned} & \frac{d^2}{d\xi^2} \left[\exp\left(\frac{\xi}{2}\right) G_\beta(\zeta, \xi) \right] = \\ & = \exp\left(\frac{\xi}{2}\right) \left[\frac{\beta^2 + 1}{4} G_\beta(\zeta, \xi) + \frac{d}{d\xi} G_\beta(\zeta, \xi) + \delta(\xi - \zeta) \right], \end{aligned}$$

and therefore substitution into the last of 3.2.55 gives

$$(3.2.57) \quad \begin{aligned} \mathcal{G}_\beta(z, \zeta) &= - \exp(\zeta) G_\beta(z, \zeta) - \frac{\beta^2 + 1}{4} \int_0^\infty d\xi \exp(\xi) G_\beta(z, \xi) G_\beta(\zeta, \xi) + \\ & - \int_0^\infty d\xi \exp(\xi) G_\beta(z, \xi) \frac{d}{d\xi} G_\beta(\zeta, \xi). \end{aligned}$$

The function $\mathcal{G}_\beta(z, z)$ is now computed by taking the limit $\zeta \rightarrow z$ into 3.2.57, i.e.,

$$(3.2.58) \quad \begin{aligned} \mathcal{G}_\beta(z, z) &= \lim_{\zeta \rightarrow z} \mathcal{G}_\beta(z, \zeta) = - \exp(z) G_\beta(z, z) + \\ & - \frac{\beta^2 + 1}{4} \int_0^\infty d\xi \exp(\xi) G_\beta^2(z, \xi) - \frac{1}{2} \int_0^\infty d\xi \exp(\xi) \frac{d}{d\xi} G_\beta^2(z, \xi), \end{aligned}$$

and carrying out integration by parts in the last integral, to have

$$(3.2.59) \quad \mathcal{G}_\beta(z, z) = -\exp(z)G_\beta(z, z) - \frac{\beta^2 - 1}{4} \int_0^\infty d\xi \exp(\xi)G_\beta^2(z, \xi).$$

Evaluation of the straightforward integral on the right hand side of 3.2.59 leads to

$$(3.2.60) \quad \mathcal{G}_\beta(z, z) = \frac{1}{2} \{ \exp(z)[\beta + 2 - 2\exp(-\beta z)] - \beta \exp(-\beta z) \}.$$

Hence, the variance 3.2.53 reads as

$$\sigma_{q_h}^2(z) = \sigma_{q_h}^2(\infty) \omega_{q_h}(z),$$

$$(3.2.61)$$

$$\omega_{q_h}(z) \equiv 1 - \exp(-z) + 2z \frac{(4\pi^2 z^2 + 6\pi - 1)\Lambda(2z) + 2(1 - 2\pi z)\exp(-z)}{14 + (6\pi - 1)\Lambda(0)},$$

being $\sigma_{q_h}^2(\infty) = \frac{\pi}{8} [14 + (6\pi - 1)\Lambda(0)] \lambda (q_0 \sigma_Y)^2$ the far field (large z). Like above, it is seen (Figure 3.2.8) that the function $\omega_{q_h} \equiv \omega_{q_h}(z)$ is a depth dependent weight describing the transition of $\sigma_{q_h}^2(z)$ from the water-table, where $\omega_{q_h}(0) \equiv 0$, till to its far field, corresponding to $\omega_{q_h}(\infty) \equiv 1$. It is interesting to note that $\sigma_{q_h}^2 \neq 0$ (for $z > 0$) although the mean flux is purely vertical everywhere in the flow domain. This is due to the fact that, unlike the mean, the fluctuation of the flux (and therefore the variance) has a three dimensional structure. Instead, the vanishing of $\sigma_{q_h}^2$ at the water-table ($z = 0$) is explained by the deterministic nature of the head there which requires $\tilde{\Psi}_1(\mathbf{k}, 0) \equiv 0$ (see 3.2.50-3.2.51).

The variance $\sigma_{q_z}^2 \equiv \langle q_z^{(1)2} \rangle$ of the vertical flux is computed by the same token. Thus, starting from the fluctuation

$$(3.2.62) \quad q_z^{(1)}(\mathbf{x}) = -K_r(z) \frac{\partial}{\partial z} \Psi_1(\mathbf{x}) + q_0 [\Psi_1(\mathbf{x}) + Y'(\mathbf{x})],$$

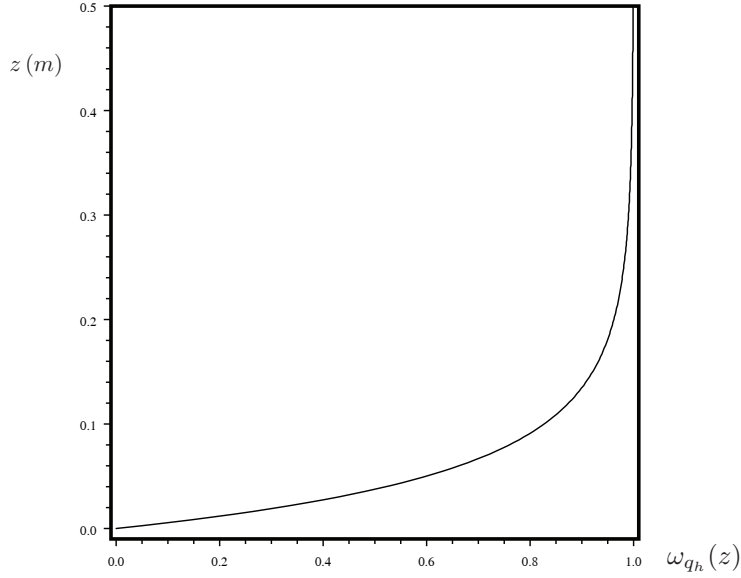


FIGURE 3.2.8. Dependence of the weight function $\omega_{q_h} \equiv \omega_{q_h}(z)$ (horizontal axe) upon the dimensional depth z (vertical axe)

the variance of the vertical flux reads as

(3.2.63)

$$\begin{aligned} \sigma_{q_z}^2(z) = & K_r^2(z) \left\langle \frac{\partial}{\partial z} \Psi_1(\mathbf{x}) \frac{\partial}{\partial z} \Psi_1(\mathbf{x}) \right\rangle + q_0^2 [\sigma_Y^2 + 2\sigma_{\Psi Y}(z) + \sigma_{\Psi}^2(z)] + \\ & -2q_0 K_r(z) \left[\frac{1}{2} \frac{d}{dz} \sigma_{\Psi}^2(z) + \left\langle Y'(\mathbf{x}) \frac{\partial}{\partial z} \Psi_1(\mathbf{x}) \right\rangle \right]. \end{aligned}$$

To compute the two still left ensemble averages, we make use of the spectral representation of 3.2.51, i.e.,

$$\begin{aligned} (3.2.64) \quad \Psi_1(\mathbf{x}_h, z) & \equiv \int \frac{d\mathbf{k}}{2\pi} \exp(-j\mathbf{k} \cdot \mathbf{x}_h) \tilde{\Psi}_1(\mathbf{k}, z) = \\ & = g(z) \int_0^\infty d\xi \int \frac{d\mathbf{k}}{2\pi} \exp(-j\mathbf{k} \cdot \mathbf{x}_h) \tilde{Y}'(\mathbf{k}, \xi) \frac{d}{d\xi} \left[\exp\left(\frac{\xi}{2}\right) G_\beta(z, \xi) \right], \end{aligned}$$

leading to

$$(3.2.65) \quad \left\langle \frac{\partial}{\partial z} \Psi_1(\mathbf{x}) \frac{\partial}{\partial z} \Psi_1(\mathbf{x}) \right\rangle =$$

$$= \lambda \sigma_Y^2 g^2(z) \left[\mathcal{L}^2(z) \Upsilon(z, \zeta) + 2 \mathcal{L}(z) \frac{\partial}{\partial \zeta} \Upsilon(z, \zeta) + \frac{\partial^2}{\partial z \partial \zeta} \Upsilon(z, \zeta) \right]_{\zeta=z},$$

$$(3.2.66) \quad \left\langle Y'(\mathbf{x}) \frac{\partial}{\partial z} \Psi_1(\mathbf{x}) \right\rangle = \frac{\lambda \sigma_Y^2}{4 f_\kappa(z)} \mathcal{F}(z),$$

$$(3.2.67) \quad \mathcal{F}(z) = [4 + \Lambda(2z) - \Lambda(0)] \mathcal{L}(z) +$$

$$+ \pi [(1 + 2z + 2\pi z^2) \Lambda(2z) + \Lambda(0)] - (1 + 2\pi z) \exp(-z) - 5,$$

where

$$\mathcal{L}(z) \equiv \frac{d}{dz} \ln [g(z)] = - \frac{1 + \kappa \exp(-z)}{2[1 - \kappa \exp(-z)]},$$

and

$$\Upsilon(z, \zeta) \equiv \int_0^\infty dk k \rho_h(k) \mathcal{G}_\beta(z, \zeta).$$

It is therefore clear that the crux of the matter to derive the variance 3.2.63 is the computation of the Υ -function as well as its derivatives. With the details in the Appendix B, eq. 3.2.63 reads as

$$(3.2.68) \quad \frac{\sigma_{q_z}^2(z)}{(q_0 \sigma_Y)^2} = 1 + 2 \frac{\sigma_{\Psi Y}(z)}{\sigma_Y^2} + \frac{\sigma_\Psi^2(z)}{\sigma_Y^2} \left[1 + f_\kappa(z) \frac{d}{dz} \ln \sigma_\Psi^2(z) \right] +$$

$$- \frac{\lambda}{8} [4 \mathcal{L}^2(z) \Upsilon_1(z) + 4 \mathcal{L}(z) \Upsilon_2(z) + \Upsilon_3(z) - 4 \mathcal{F}(z)],$$

being the Υ_i -functions given in eqs 3.2.81-3.2.82 of the Appendix B. In particular, the far and near field of $\sigma_{q_z}^2$ are:

$$(3.2.69) \quad \frac{\sigma_{q_z}^2(\infty)}{(q_0 \sigma_Y)^2} = 1 - \frac{\lambda}{4} \left[11 + 7\pi + \frac{3}{2} (2\pi^2 - \pi + 1) \Lambda(0) \right],$$

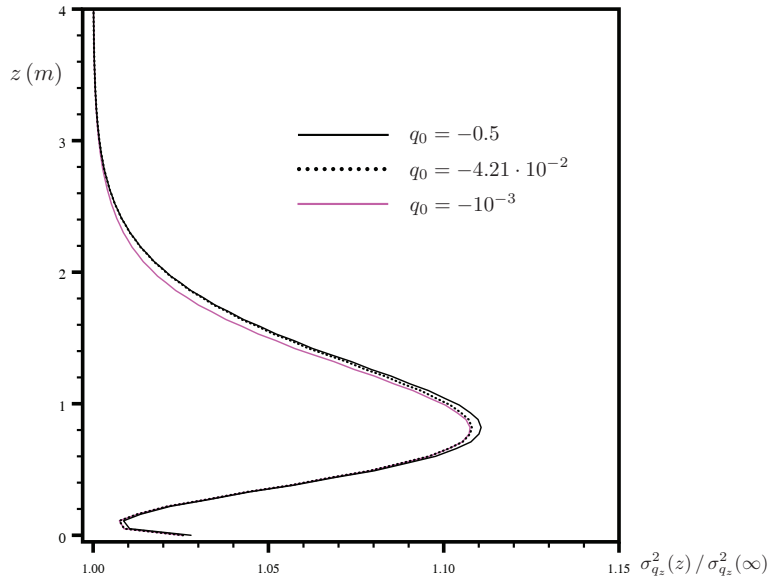


FIGURE 3.2.9. Normalized variance $\sigma_{q_z}^2(z)/\sigma_{q_z}^2(\infty)$ of the vertical specific flux as a function of the (dimensional) depth from the water-table under a few values of the dimensionless infiltration rate q_0

Thick dot-line pertains to the normalized infiltration rate during the experiment at the Ponticelli site.

$$\frac{\sigma_{q_z}^2(0)}{(q_0 \sigma_Y)^2} = 1 - \frac{\lambda}{4} [14 - \pi \Lambda(0)] ,$$

respectively. It is seen that $\sigma_{q_z}^2(\infty) < \sigma_{q_z}^2(0)$ which is due to the fact that at the groundwater ($z = 0$) particles move much more freely (due to the absence of retention there) as compared with the unsaturated zone, and concurrently particles experience larger deviation from the mean vertical velocity, therefore giving raise to a larger variance. The normalized variance $\sigma_{q_z}^2(z)/\sigma_{q_z}^2(\infty)$ of the vertical specific flux along z (expressed in m) is depicted in the Figure 3.2.9.

Close to the water-table the fluctuation $\Psi^{(1)}$ of the pressure head undergoes to the largest variations, as it is clearly detected by the pattern of ω_Ψ in the Figure 3.2.6, and concurrently so does (see 3.2.49) the fluctuation $q_z^{(1)} \equiv q_z - q_z^{(0)}$. This explains why the major source of uncertainty (i.e. large

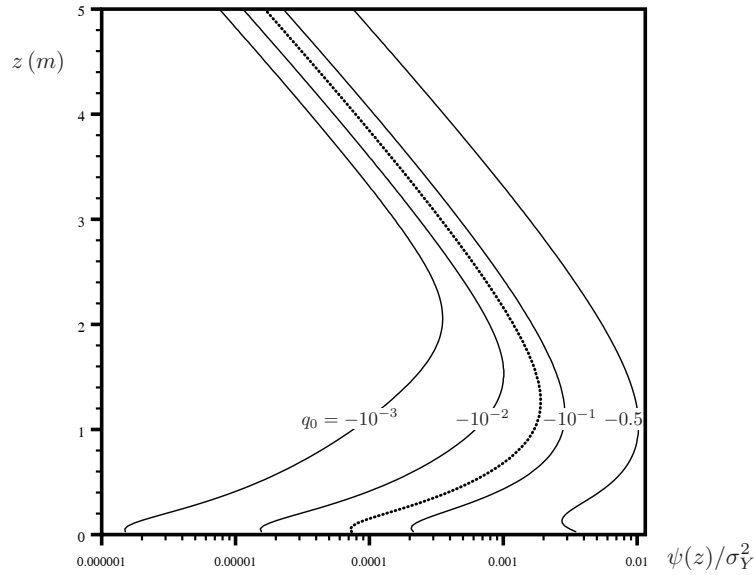


FIGURE 3.2.10. Distribution of the scaled head-factor $\psi(z)/\sigma_Y^2$ as computed from equation 3.2.43, and accounting for the data of the Ponticelli site along the dimensional depth z from the water-table ($z = 0$), and a few values of the dimensionless infiltration rate q_0

Thick dot-line pertains to the normalized infiltration rate (i.e. $q_0 = -4.21 \cdot 10^{-2}$) during the experiment at the Ponticelli site.

$\sigma_{q_z}^2$) of the vertical flux is concentrated next above the water-table. Such an out-coming is also in agreement with the large time limit of the numerical results of Ferrante and Yeh [Ferrante and Yeh, 1999][64]. Furthermore, it is worth reminding that the infiltrating flux q_0 is the upper boundary condition that, being at $z \rightarrow \infty$, does not significantly impact the behavior of the variance of the vertical specific flux at $z = 0$. This explains the scarce sensitivity of $\sigma_{q_z}^2$ to the infiltrating flux q_0 close to the water-table (see also the discussion in [Wang et al., 2009][223]).

To quantify the distortion effect upon the mean head $\langle \Psi \rangle$ as determined by the heterogeneity of the Ponticelli's soil, in the Figure 3.2.10 we have depicted the quantity $\psi(z)/\sigma_Y^2$ versus the (dimensional) depth from the water-table. Results show that ψ decreases with decreasing q_0 . In particular, the result:

$$(3.2.70) \quad \psi(0) = -\sigma_Y^2 \frac{\lambda}{2\kappa} \left[\pi\Lambda(0) + \frac{1+\kappa}{1-\kappa} \right] > \psi(\infty) \equiv 0,$$

(it is reminded that $\kappa \leq 0$) is explained by the fact that close to the water-table the pressure head attains the highest values, and therefore ψ results larger than its far field. It is worth reminding that a utility of the definition 3.2.43 is that one can filter out from the second-order correction $\langle \Psi_2(z) \rangle$ the impact of the zero-order one Ψ_0 , this latter being highly sensitive to the influx q_0 (see Figure 3.2.2), and concurrently ψ accounts exclusively for the heterogeneity of the vadose zone. This explains the slight dependence of $\psi \equiv \psi(z)$ (Figure 3.2.10) upon the magnitude q_0 . Of course, to recover the effective dependence of $\langle \Psi_2(z) \rangle$ upon the infiltration flux, the depth, and the medium's heterogeneity, one has to consider the product $\psi(z)\Psi_0(z)$.

The distance at which stationarity is reached is roughly $3m$, similarly to σ_{qz}^2 (see Figure 3.2.9). An analogous conclusion was achieved by [Zhang and Winter, 1998][242]. An important (often overlooked) question is about the asymptotic nature of the perturbation expansions 3.2.8. In fact, for the perturbation expansion $\langle \Psi \rangle = \Psi_0 + \langle \Psi_2 \rangle$ to be asymptotic, it is necessary that $\langle \Psi_2 \rangle \ll \Psi_0$, a condition which, from eq. 3.2.43, is equivalent to $\psi \ll 1$. Hence, it is seen (Figure 3.2.10) that $\psi/\sigma_Y^2 \lesssim 10^{-2}$ (any z and q_0), and therefore, as far as the heterogeneity of Y is accounted for, our solution for $\langle \Psi \rangle$ is accurate till to $\sigma_Y^2 = \mathcal{O}(1)$. In other words, although the perturbation expansion 3.2.8 is nominally restricted to mildly heterogeneous vadose zones, it works de facto quite well for relatively highly heterogeneous unsaturated porous formations (in analogy to what is observed in the aquifers, see e.g. [Fiori et al., 2010][66]). Similar conclusions were drawn by [Tartakovsky et al., 1999][209] for a one dimensional vadose zone.

Conclusions. We have developed a stochastic model for three dimensional steady flows in the vadose zone accounting for the presence of the water-table. The system the governing equations is solved at first-order of approximation in the variances of the log-transforms of: i) the saturated conductivity K_s , and ii) the α -parameter of the Gardner model. Very general expression of the statistical (second-order) moments of the pressure head and specific flux are then obtained. These moments are expressed into analytical (closed form)

expression which can be easily evaluated once the statistical structure of the above soil parameters is specified. One of the main result of the present paper is the general representation $\langle \Psi \rangle = \Psi_0(z)\Theta(z)$ with $\Theta(z) = 1 + \psi(z)$. The term ψ has been derived in a closed form which is easily evaluated after specifying the shape of the various correlation functions 3.2.6. In particular, it is shown that at large distances one has $\psi(\infty) = 0$, and concurrently $\langle \Psi(\infty) \rangle \equiv \ln(-q_0)$, which coincides with the result valid for an unbounded vadose zone. Instead, at the water-table it yields $\psi(0) < \infty$, and therefore we recover $\langle \Psi(0) \rangle \equiv 0$, that is understandable due to the deterministic nature of the pressure head at the water-table. The overall utility of the proposed model is that it enables one to assess, into a simple and quick manner, the impact of the water-table upon the nonstationary behavior of the FVs, by providing, in particular, explicit relationships between the input parameters and the model output.

Besides the general relevance, results of the present paper are shown to be useful toward the practical applications. Indeed, the model is tested against a recently conducted flow experiment in the vadose zone [Comegna *et al.*, 2010; Severino *et al.*, 2010, 2016][**33, 196, 174**]. We use independent (no calibration) univariate analysis to identify the mean, and variance of $Y = \ln K_s$ and $\zeta = \ln \alpha$. In particular, the significantly small (~ 2 two orders of magnitude) variance of ζ as compared with that of Y authorizes limiting our analysis to the zero-order approximation in σ_ζ , and to the second-order approximation in σ_Y . By using the same data set, we determine the horizontal integral scale I pertaining to Y , whereas to identify the anisotropy ratio λ we have used three batteries of (shallow) steady state measurements of the pressure head Ψ . To check the realibility of the estimated value of λ , we have compared the experimental cross-variance Ψ - Y as determined by independent (i.e. not used for calibration purposes) data against to the theoretical asymptotic cross-variance $\sigma_{\Psi Y}(\infty)$. The very satisfactory comparison (combined with prior geological informations) with the measurements corroborates the achieved results.

Once the input soil properties are identified, we have analyzed the flow behavior close to the water-table. The listed below major conclusions were achieved:

- (1) the infiltrating flux q_0 and the integral scale I impact the stationary values of the specific flux $(q_h, q_z)^\top$, whereas they have a limited influence upon the distance from the water-table at which such stationary values are attained;
- (2) from the application point of view, one can estimate the thickness of the flow domain where the nonstationary is dominant by means of a 1D Richards equation (i.e. valid for the vertical mean pressure head $\langle \Psi \rangle$).

Although we have limited the discussion to the data of the Ponticelli's experiment, the vadose zone flow model derived in the present study is rather general. Thus, one can assess the impact of: i) the spatial variability of the ζ -parameter, ii) the cross-correlation Y - ζ that in some circumstances may result relevant [Russo et al., 1997][168], and iii) the various correlation length-scales. These studies are topics of ongoing researches. Finally, we also hope that our results will be beneficial for other theoretical/experimental studies dealing with flow (and transport) under similar conditions.

APPENDIX A: derivation of $C_{\Psi\gamma}$ and C_Ψ . We preliminarily switch into 3.2.32 to the new variable $\mathbf{r}_h = \mathbf{x}_h - \mathbf{x}'_h \equiv (x - x', y - y') \in \mathbb{R}^2$, and subsequently take the (2-D) Fourier transform:

$$\tilde{f}(\mathbf{k}) = (2\pi)^{-1} \int d\mathbf{r}_h \exp(j\mathbf{k} \cdot \mathbf{r}_h) f(\mathbf{r}_h) ,$$

in the horizontal plane $\mathbf{r}_h \in \mathbb{R}^2$, to have:

$$(3.2.71) \quad \mathcal{L}_{k^2} \tilde{\Phi}(k, z, z') = -\sqrt{-q_0} \exp\left(\frac{z}{2}\right) \frac{d}{dz} \left[\bar{\sigma}_{Y\gamma} \tilde{\rho}_h(kI_{Y\gamma}) \rho_v \left(\frac{z - z'}{\bar{\lambda}_{Y\gamma}} \right) + \bar{\sigma}_{\zeta\gamma} \Psi_0(z) \tilde{\rho}_h(kI_{\zeta\gamma}) \rho_v \left(\frac{z - z'}{\bar{\lambda}_{\zeta\gamma}} \right) \right] ,$$

where we have set $\mathcal{L}_\alpha \equiv \frac{d^2}{dz^2} - (\alpha + \frac{1}{4})$, $\bar{\sigma}_{\eta\gamma} \equiv \sigma_{\eta\gamma} I_{\eta\gamma}$ and $\bar{\lambda}_{\eta\gamma} \equiv \lambda_{\eta\gamma} I_{\eta\gamma}$ ($\eta = Y, \zeta$). Thus, in the mixed domain $\{(\mathbf{k}, z) : \mathbf{k} \in \mathbb{R}^2, z \geq 0\}$ the resulting ODE is solved by the Green function 3.2.35, solution of the problem: $\mathcal{L}_{k^2} G_\beta(z, z') = \delta(z - z')$, to end up (after integrating by parts) with

$$(3.2.72) \quad \tilde{C}_{\Psi\gamma}(k, z, z') = g(z) \int_0^\infty d\xi \left[\bar{\sigma}_{Y\gamma} \tilde{\rho}_h(kI_{Y\gamma}) \rho_v \left(\frac{\xi - z'}{\bar{\lambda}_{Y\gamma}} \right) + \bar{\sigma}_{\zeta\gamma} \Psi_0(\xi) \tilde{\rho}_h(kI_{\zeta\gamma}) \rho_v \left(\frac{\xi - z'}{\bar{\lambda}_{\zeta\gamma}} \right) \right] \frac{d}{d\xi}$$

In order to calculate the inverse of 3.2.72 we need to evaluate the following integral:

$$(3.2.73) \quad \mathcal{I}(r) = \int \frac{d\mathbf{k}}{2\pi} \exp(-j\mathbf{k} \cdot \mathbf{r}) \tau(k),$$

being τ any integrable function depending only upon the modulus of the wave-number \mathbf{k} . Thus, we first adopt polar coordinates: $k(\cos\theta, \sin\theta)$, and subsequently choose the polar axis \mathbf{k} in the direction of \mathbf{r} , so that $\mathbf{k} \cdot \mathbf{r} = kr \cos\theta$. By noting that $\int_0^{2\pi} d\theta \exp(-jk r \cos\theta) = 2\pi J_0(kr)$, 3.2.73 writes as $\mathcal{I}(r) = \int_0^\infty dk k J_0(kr) \tau(k)$. This together with (3.2.72) leads to (3.2.33).

To compute the head-covariance C_Ψ , we proceed into a similar manner. Thus, we first apply the transformation 3.2.31 (with $C_{\Psi\gamma}$ replaced by C_Ψ) to convert 3.2.36 into the following:

$$(3.2.74) \quad \nabla^2 \Phi(\mathbf{x}, \mathbf{x}') - \frac{1}{4} \Phi(\mathbf{x}, \mathbf{x}') = -\sqrt{-q_0} \exp\left(\frac{z}{2}\right) \frac{\partial}{\partial z} [C_{\Psi Y}(\mathbf{x}', \mathbf{x}) + \langle \Psi(z) \rangle C_{\Psi \zeta}(\mathbf{x}', \mathbf{x})] .$$

Then, we apply the 2-D Fourier transform to 3.2.74 and solve for the Fourier transform of the function Φ (we omit the straightforward derivations). Hence, the Fourier transform of the head-covariance

$$\tilde{C}_\Psi(k, z, z') = \sqrt{-q_0} \frac{\exp(-z/2)}{K_r[\Psi_0(z)]} \tilde{\Phi}(k, z, z') ,$$

reads as

$$(3.2.75) \quad \tilde{C}_\Psi(k, z, z') =$$

$$= g(z) \int_0^\infty d\xi \left[\tilde{C}_{\Psi Y}(k, z', \xi) + \Psi_0(\xi) \tilde{C}_{\Psi \zeta}(k, z', \xi) \right] \frac{d}{d\xi} \left[\exp\left(\frac{\xi}{2}\right) G_\beta(z, \xi) \right].$$

Substitution of 3.2.72, and taking the inverse Fourier-transform of 3.2.75, leads to 3.2.37.

APPENDIX B: computation of the variance $\sigma_{q_z}^2$ of the vertical flux. To this aim, we preliminary observe that

$$(3.2.76) \quad \left. \frac{\partial}{\partial \zeta} \mathcal{G}_\beta(z, \zeta) \right|_{\zeta=z} = \frac{1}{4} (2\beta - 1) \exp(-z\beta) + \\ - \frac{\exp(z)}{4\beta} [\beta^2 + 6\beta - 2 + (\beta^2 - 3\beta + 2) \exp(-z\beta)],$$

$$(3.2.77) \quad \left. \frac{\partial^2}{\partial z \partial \zeta} \mathcal{G}_\beta(z, \zeta) \right|_{\zeta=z} = \frac{1}{8} (\beta^3 - 2\beta^2 + 2\beta - 2) \exp(-z\beta) + \\ - \frac{\exp(z)}{8\beta} [\beta^4 + 2\beta^3 + 4\beta^2 + 4\beta - 2 - 2(\beta^3 - 2\beta^2 + 4\beta - 1) \exp(-z\beta)].$$

The derivatives 3.2.76-3.2.77 have been obtained (we omit the very lengthy algebraic derivations) by: i) differentiating 3.2.57, ii) accounting for 3.2.59, and iii) making use of the straightforward identities

$$(3.2.78) \quad -\frac{\partial}{\partial z} G_\beta(z, \xi) = \frac{\partial}{\partial \xi} G_\beta(z, \xi) + \exp\left[-\frac{1}{2}(z + \xi)\beta\right],$$

$$(3.2.79) \quad -\frac{\partial^2}{\partial z \partial \xi} G_\beta(z, \xi) = \frac{\beta^2}{4} G_\beta(z, \xi) + \delta(\xi - z) - \frac{\beta}{2} \exp\left[-\frac{1}{2}(z + \xi)\beta\right].$$

By recalling that:

- (1) $\Upsilon(z, \zeta) \equiv \int_0^\infty dk k \rho_h(k) \mathcal{G}_\beta(z, \zeta)$,
- (2) $\frac{\partial}{\partial \zeta} \Upsilon(z, \zeta) \equiv \int_0^\infty dk k \rho_h(k) \frac{\partial}{\partial \zeta} \mathcal{G}_\beta(z, \zeta)$,
- (3) $\frac{\partial^2}{\partial z \partial \zeta} \Upsilon(z, \zeta) \equiv \int_0^\infty dk k \rho_h(k) \frac{\partial^2}{\partial z \partial \zeta} \mathcal{G}_\beta(z, \zeta)$,

one ends up (after taking the limit $\zeta \rightarrow z$, and carrying out the quadrature over k) with

$$(3.2.80) \quad \Upsilon(z, \zeta) \Big|_{\zeta \equiv z} = -\frac{1}{2} \exp(z) \Upsilon_1(z), \quad \frac{\partial}{\partial \zeta} \Upsilon(z, \zeta) \Big|_{\zeta \equiv z} = \\ = -\frac{1}{4} \exp(z) \Upsilon_2(z), \quad \frac{\partial^2}{\partial z \partial \zeta} \Upsilon(z, \zeta) \Big|_{\zeta \equiv z} = -\frac{1}{8} \exp(z) \Upsilon_3(z),$$

$$(3.2.81) \quad \Upsilon_1(z) = \pi(2\pi z^2 - 2z + 1)\Lambda(2z) - \pi\Lambda(0) + \\ + 2 \exp(-z) - (2\pi z - 1) \exp(-2z) - 3,$$

$$(3.2.82) \quad \Upsilon_2(z) = (\pi - 1)\Lambda(0) - (2\pi^2 z^2 - 2\pi z + \pi - 1)\Lambda(2z) + \\ + (4\pi z - 1) \exp(-2z) - 2(\pi z + 1) \exp(-z) + 7,$$

$$(3.2.83) \quad \Upsilon_3(z) = (6\pi^2 + 4\pi - 1) \Lambda(0) + \\ - [8\pi^4 z^4 - 8\pi^3 z^3 + 4\pi^2 (6\pi - 1) z^2 - 6\pi (2\pi + 1) z + 6\pi^2 - 2\pi - 1] \Lambda(2z) + \\ + [8\pi^3 z^3 + 4\pi^2 z^2 + 2\pi(10\pi + 1)z + 2\pi + 1] \exp(-2z) + \\ - 8 (2\pi^2 z^2 + 2\pi + 1) \exp(-z) + 14\pi + 11.$$

Acknowledgments. The first author acknowledges support from: (i) “Programma di scambi internazionali per mobilita’ di breve durata” (Naples University, Italy), and (ii) “OECD Cooperative Research Programme: Biological Resource Management for Sustainable Agricultural Systems” (contract JA00073336). The constructive comments from the three anonymous Referees and Xavier Sanchez-Vila were deeply appreciated. All data can be found in the supporting information.

3.3. Geostatistics for IoT in hydrology

The following paper, published on May 2018 by *Future Generation Computer System*, is a valuable contribution to the literature on the application of the IoT (Internet of Things)[187]. With the neologism IoT, we indicate a set of technologies that allow us to connect to the Internet any type of device. The purpose of this type of solutions is essentially to monitor, control and transfer information and then carry out consequent actions. In order to function properly and be really useful, the IoT needs to collect, store and process a large amount of data in real time [Ashton, 2009][6]. There are several fields of application: industrial applications (production processes), logistics, energy efficiency, remote assistance and environmental protection for instance. In particular, nowadays, Precision farming or Smart Agriculture, also called Agrifood, is one of the sectors with the highest development opportunities and with the lowest penetration of digitized solutions. It is a sector which requires digital solutions at the level of environmental and territorial sensors, of applications for the weather, of automation of equipment for the increasingly precise management of water, fertilizers, fertilizers and agrochemicals.

The paper is an example of how the geostatistical (stochastic) approach to the soil hydrology can be combined with the IoT, in fact, we have illustrated a protocol which can be easily implemented in the IoT-context. This work present a very interesting case study to the effective benefits of IoT frameworks in smart cities and environments and demonstrates how achieving simple tools is beneficial for quick estimates or for the cost effective investigations. Our aim is to present a protocol to increase both water supply and to decrease water consumption, to improve the efficiency of irrigation technologies by using in situ soil saturation measurements, precipitation forecast and modelling predictions to guide their operations. It designs an IoT framework to assess and control the environmental risks associated with the use of treated water. The main contribution are: the design of an autonomous network of environmental sensors that collect data on soil moisture and contaminants; a predictive models of soil moisture dynamics and contaminant migration; optimization of the irrigation practices while minimizing their environmental impact.

A majority of precision-agriculture strategies rely on statistical analysis of indirect measurements of soil conditions obtained, for example, by satellites,

unmanned aircraft or other means of remote sensing. Hence, the need for a geostatistical approach arises, in fact the paper makes extensive use, basically, of the data-mining methods, to overcome the difficulties into quantifying the spatial distribution of the soil flow properties.

The IoT as a tool to combine the scheduling of the irrigation with the geostatistics of the soils.

^aGerardo Severino, ^aGuido D'Urso, ^aMaddalena Scarfato, ^bGerardo Toraldo

^aDepartment of Agricultural Sciences

^bDepartment of Mathematics and Applications "R. Caccioppoli"

University of Naples - Federico II, Italy

Abstract. Persistent droughts, population growth, and consequences of the climate change put sever constraints on agriculture in many Regions. This emergence can be ameliorated by: i) either increasing the water supply, or ii) reducing the water demand. One viable avenue is to enhance the irrigation's efficiency by both increasing the water supply (via the use of recycled water), and decreasing the water consumption (via the use of drip irrigation, autonomous network of environmental sensors and predictive environmental models). To this aim, we propose an IoT-framework to assess and control the environmental risks associated with the use of treated water. Overall, the IoT-framework is organized along the following main streams: i) design an autonomous network of environmental sensors that collect data on remote about soil moisture and concentration of dissolved contaminants; ii) assimilate these data together with precipitation forecast into predictive models of soil moisture dynamics and contaminant migration; iii) use these data-driven models to optimize the irrigation practices while minimizing their environmental impact. The fundamental pre-requisite common to i)-iii) is the proper processing of the soil data. The present paper will focus on such a topic.

Introduction. The need of enhancing food security with a simultaneous save of water is drastically affecting the irrigation practices. Countries (both developed and developing) are changing from a purely supply based to a demand based methodology. Indeed, most of the existing irrigation practices are such that the system is designed for equal distribution. Nevertheless, this latter remains the biggest challenge for the new irrigation approach [*Calera et al., 2017*][25]. New technologies, such as data-driven devices as well as wireless sensors networks have enhanced the impact of information, computation, communication and control. On the top of this, the *Internet of Things* (IoT)

is replacing the manual practices in many agricultural applications [*Vuolo et al., 2015*][**221**].

In most of the Countries, water resources are operated manually. This provides a huge potential to the IoT to overcome problems related to the scarce availability of water, as well as to its delivery. The frequency of anomalous events such as the absence of water supply when a particular distributary is scheduled to receive water; or the presence of significant flow in a distributary when it is not scheduled to receive water; or sharp rises and falls in water levels can be reported using smart water metering. Wireless real-time monitoring of water quantity/quality can capture temporal changes and provide broader spatial coverage. Thus, questions about the efficiency and systematic ways to address them can be reported using smart metering approach. This challenge, which has economic, societal and environmental facets, can be ameliorated by either increasing water supply or reducing water demand. A long-term goal of the implementation of the IoT is to significantly enhance irrigation efficiency via data-driven simulation-based optimization of these two strategies.

Our aim is to present a protocol to increase both water supply (via the use of recycled water, e.g., treated sewage water) and to decrease water consumption (via the use of drip irrigation, autonomous network of environmental sensors and predictive environmental models). The tools we propose to develop for the latter strategy will also be used to assess and control the environmental risks associated with the use of treated water, e.g., the risk of contamination and salinization of the underlying soil and phreatic aquifers.

Agricultural water of good quality can be augmented by deploying “supplemental irrigation technologies”, such as rain harvesting [*Boers and Ben Ashers, 1982; Jones and Hunt, 2010*][**17, 103**] and use of marginal-quality (e.g. saline) [*Glenn et al., 2013; Hirich et al., 2014*][**77, 91**] and/or grey [*Coppola et al., 2004; Maimon et al., 2010; Pinto et al., 2010*][**38, 123, 139**] water. While rain harvesting is largely conned to the developing world [*Oweis and Hacum, 2006*][**135**], marginal-quality water is increasingly used around the world [*Suarez, 2013*][**204**]. The latter practice might cause appreciable degradation of soil health and groundwater quality , and lead to significant decline in crop yield [*Hanjra et al., 2012; Pedrero et al., 2012; Singh Grewal and Maheshwari, 2013*][**84, 136, 197**]. Our IoT-aim is to provide a site-specific

optimal irrigation schedule of the alternating use of good and marginal waters; such a schedule would rely on simulation-based forecasting of contaminants migration in the vadose zone, guided by in-situ real-time observations of soil-water quality and short-term weather predictions.

Advanced agricultural practices, e.g., deployment of drip irrigation or micro sprinkles [*De Pascale et al., 2011; Kanety et al., 2014*][**54, 105**] and development of drought-resistant plant varieties [*Lawlor, 2013; Yang et al., 2010*][**112, 237**], can provide significant reduction in water demand while maintaining (or even increasing) a field's yield. The present study focuses on optimization of irrigation practices and their effects on plant growth and crop yield. These effects are known to be nonlinear and, hence, often counterintuitive. For example, mild water stress applied to (part of) the root zone was shown to have no adverse affects on (and might prove to be beneficial for) the yield of citrus trees [*Hutton and Loveys, 2011*][**93**] and maize [*Couto et al., 2013*][**40**]. One of our aims is to dramatically improve the efficiency of irrigation technologies by using in situ soil moisture measurements, precipitation forecast and modeling predictions to guide their operations.

The challenging and very difficult task to develop modelling of flow and transport in soils of large extents has been undertaken only in the last decades by using a mining geostatistical approach [*Severino et al., 2010, 2016; Comegna et al., 2010*][**174, 196, 33**]. The use of data-mining methods is due to the difficulties into quantifying the spatial distribution of the soil flow properties [*Severino et al., 2006, 2009; Severino and Coppola, 2012*][**177, 189, 184**]. Indeed, there have been only a limited number of studies [*Russo and Bouton, 1992; White and Sully, 1992; Ragab and Cooper, 1993; Russo et al., 1997*][**165, 232, 145, 168**] focusing on the spatial variability of the log-hydraulic conductivity $Y = \ln K_S$ (by far the most important hydraulic property), and nevertheless they suffer from many limitations, the most important of which is about the extreme difficulty to carry out precise in situ measurements (somewhat similar to the analysis of other extremely variables quantities) [*Farina et al., 2015*][**61**]. In view of such shortcomings, the present paper aims at showing how to use a data-mining (geostatistical) approach to quantify the spatial variability of the Y -parameter, and to combine such an information within the target of the irrigation's efficiency.

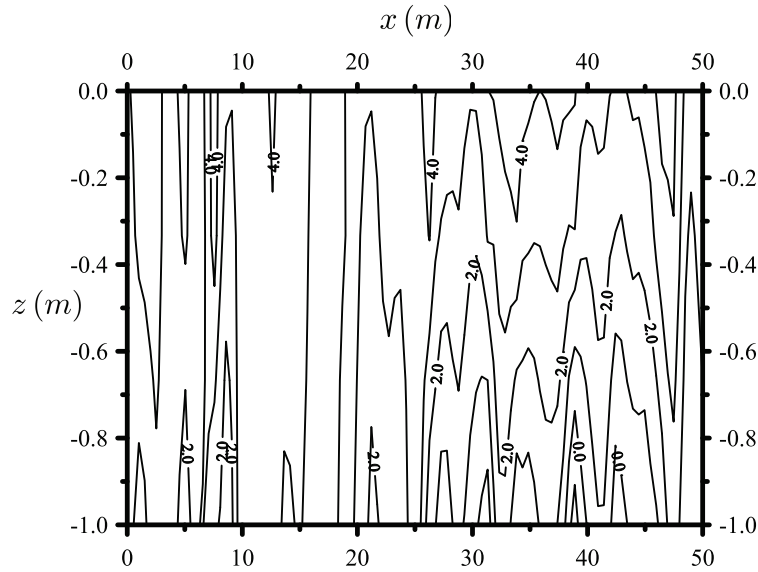


FIGURE 3.3.1. Distribution of the iso-values of $Y \equiv \ln K_s$ along a vertical cross-section at the Ponticelli site (Naples, Italy); vertical exaggeration: 250/6

The conductivity K_s is expressed in cm/h.

Characterization of the spatial variability of the log-conductivity by means of the mining geostatistical approach: from theory to the practical use.

THE PROBABILISTIC FRAMEWORK. The Y -parameter is highly related to the soil's structure. Indeed, the commonly accepted dependence $K_S \equiv \kappa\gamma/\mu$ (being γ and μ the specific weight and the viscosity, respectively), relating K_S to the intrinsic permeability κ , is largely affected by the spatial variability of κ . Since this latter strongly depends upon the effective porosity n_e (see e.g. [Illman, 2005][95]), it is clear that the spatial variability of n_e is, de facto, the main source of the spatial variability of K_S [Severino et al., 2010; Fallico et al., 2016][174, 60]. This is clearly seen in the Figure 3.3.1 that shows the contour levels of Y (being K_S in cm/h) along a vertical cross-section in a trench at the Ponticelli site (Naples, Italy).

A detailed characterization of the spatial distribution of Y (and more generally of any soil flow property) via the so-called "standard approach" (i.e. by

collecting samples in the field and subsequently determining local values) requires: i) considerable time, and ii) great expense/effort, therefore rendering such an avenue practically impossible. A viable (and widely accepted) alternative is to treat Y as a “stochastic process in the space”, or equivalently as a random space function (RSF) [Dagan, 1989; Rubin, 2003][**50, 158**]. As a consequence, the characterization of the heterogeneity of Y is cast within the more general approach of the data mining methods. Thus, the value of Y at any position x is regarded as one possible out-coming related to the many geologic materials that might have been deposited there. Hence, $Y \equiv Y(x; \Omega)$ becomes a random variable. The symbol Ω refers to the sample space, which is generally dependent upon x . If Y is measured at different positions x_1, x_2, \dots, x_k then the values $Y_i \equiv Y_i(x_i; \Omega_i)$ ($i = 1, 2, \dots, k$) are random variables, each one characterized by a (generally position dependent) probability density function (PDF). The probability of finding any sequence of Y -values at a certain x depends not only upon the PDF itself, but also on those PDFs at other positions. In the context of the mining geostatistics, the probability of finding such a sequence is given by the joint probability density function. Thus, any sequence of Y -values at different points is viewed as a possible out-coming of the sample space of a joint PDF, and it is usually termed as single realization. As a matter of fact, determining the occurrence of any realization requires the knowledge of the joint PDF. Unfortunately, this latter is not an accessible information since in the practice only a single realization (the one obtained by sampling) is available, and therefore one must resort to some simplifying assumptions, such as stationarity and ergodicity. Stationarity implies that the joint PDF is translationally invariant, whereas ergodicity enables one to infer the joint PDF by means of a single realization [Rubin, 2003][**158**]. The pragmatic approach adopted in hydrology, and in line with the statistical continuous theories, is to derive moments of interest for the flow variables and to check the applicability of these two assumptions only ex post. In terms of moments, stationarity requires the space invariance of “all” the moments (a very stringent assumption). Since, in the practical applications one is mainly interested into the first and second order moments of the flow/transport processes [Severino et al., 2008, 2012; Fioriet al., 2010; Severino, 20112011a, 20122b; Severino and De Bartolo,

2015],[191, 186, 66, 182, 180, 192, 175] the stationarity of the input variables is replaced by the stationarity up to the second order (weak stationarity). Thus, the pair “mean and covariance” becomes the tool to characterize the spatial variability of Y . Nevertheless, it is important to emphasize that the knowledge of the mean and covariance does not specify the Y -values at any x , but rather it provides a way to quantify how widely the Y -values spread around the mean, and how these values are spatially correlated.

RESULTS. For illustration purposes, we deal with local measurements of Y obtained by means of the saturated hydraulic conductivity K_s measured along 40 profiles in the field [Comegna et al., 2006][35]. The PDF of the Y -values was normal, as underlined by the good agreement between empirical and theoretical CDF as well as by the Kolmogorov-Smirnov D -test (Figure 3.3.2). The problem of quantifying the spatial structure (i.e. the covariance in the present study) of Y is rather complicated, even when measurements are numerous. The identification process should involve several steps: i) an hypothesis about the functional model of the covariance, ii) the estimate of the parameters of such a model, and iii) a model validation test. In particular, the problem of selecting the most appropriate model remains to some extent in the realm of the practical applications [Rubin, 2003][158]. The prevailing approach is the pragmatic one: select a model for its practicality/versatility as well as its performance in similar situations.

In view of the subsequent analysis, it is important to discuss some general properties of the covariance function $C \equiv C(\mathbf{x})$. Thus, the value $C(0)$ is the variance σ_Y^2 and it provides information about the spread of the Y -values around the mean. For $|\mathbf{x}| \neq 0$, the value $C(\mathbf{x})$ is a measure of the correlation between values at two points separated by the distance $|\mathbf{x}|$. Specifically, the higher $|\mathbf{x}|$ the smaller the correlation. Of particular interest is the concept of integral scale, \mathcal{I}_Y [L]. Roughly speaking, \mathcal{I}_Y is the distance over which two values of Y cease to be correlated [Dagan, 1989][50].

A frequently encountered case is that of small integral scale. In this case the soil is characterized by a complete lack of spatial correlation (stochastic structureless process). In such a circumstance, it is convenient to deal with the variogram $\gamma_Y \equiv \gamma_Y(\mathbf{x})$. Generally, the variogram γ_Y (whose computation is straightforward) is of wider applicability as compared with the

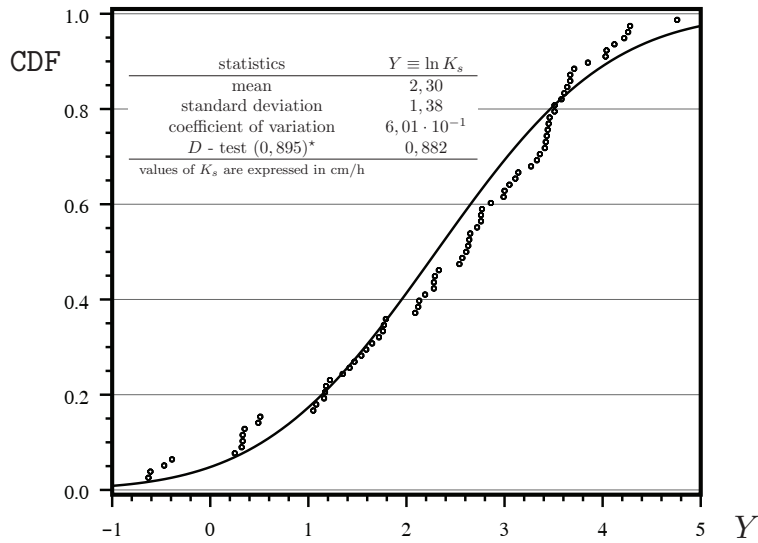


FIGURE 3.3.2. Cumulative distribution functions of measured (symbols) $Y \equiv \ln K_s$ and theoretical CDF with the D -test of normal (null) hypothesis

covariance, since its applicability does not require the stationarity hypothesis in a strict sense. Nevertheless, for a stationary process one can easily demonstrate [Dagan, 1989; Rubin, 2003][50, 158] that $\gamma_Y(\mathbf{x}) \equiv \sigma_Y^2 - C(\mathbf{x})$. As a consequence, for a stochastic, stationary, structureless process the variogram in practice coincides with the structured variance, i.e. $\gamma_Y(\mathbf{x}) \simeq \sigma_Y^2$. To establish whether the Y -process is structureless, it suffices to plot the scaled-variograms γ_Y/σ_Y^2 , and check that $\gamma_Y/\sigma_Y^2 \sim 1$. To this end, the experimental (symbols) variogram together with the theoretical (line) one at the two sampling depths ($z = 30, 90$ cm) for the transect of Figure 3.3.1 is plotted in the Figure 3.3.3. The fact that for $z = 30$ cm one has $\gamma_Y/\sigma_Y^2 \sim 1$ supports the assumption of a spatial lack of correlation, and concurrently for the soil at stake the RSF Y should be regarded as a structureless stochastic process from the surface $z = 0$ till to $z = 30$ cm. To the contrary, at $z = 90$ cm (blue face) the soil clearly exhibits a spatial correlation characterized by $\mathcal{I}_Y = 23.1$ m. A

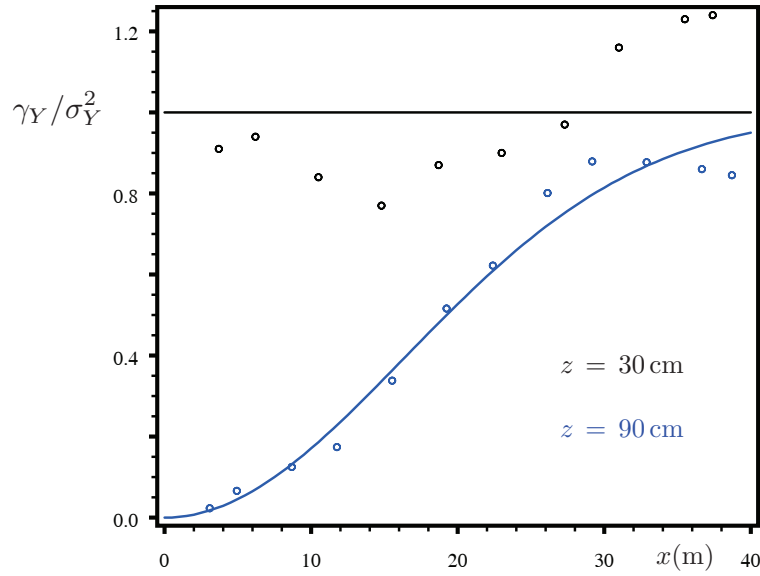


FIGURE 3.3.3. Normalized variograms

Experimental (symbols) together with the theoretical (continuous line) normalized variograms γ_Y/σ_Y^2 at the two sampling depths z along the horizontal distance x (m) of the plot shown in the Figure 3.3.1

reasonable explanation for such an out coming is that the upper most layers underwent to tillage practices which have significantly altered the soil's structure.

Implementation of the geostatistical information in the context of the IoT. A goal of optimal monitoring-network design is to select the sensor locations and sampling frequency such that a specified criterion is optimized subject to a set of constraints (e.g., the costs of individual sensors, their deployment and operation). One can choose between several optimality criteria such as the D -optimality, A -optimality, E -optimality, G -optimality and I_λ -optimality [Yeh, 1992][240]. Following Tsai et al. [Tsai et al., 2003][213], one can employ the A -optimality criterion that maximizes the trace of a weighted Fisher's information matrix of the estimated water content and solute concentrations.

Then, a goal of an optimal irrigation design and scheduling is to decrease the consumption of good-quality water while maintaining acceptable crop yields and minimizing the environmental costs of using its marginal-quality

substitutes. Such decisions have to be made in the presence of uncertainty about the soil properties and precipitation forecast. This task can be accomplished within one of the two conceptual frameworks of the IoT, optimization under uncertainty and decision analysis. While these two frameworks are sometimes viewed as opposite (e.g. [Mylopoulos, 1999][129]), they are closely related (e.g. [Freeze and Gorelick, 1999][67]) rendering this subdivision somewhat artificial.

Optimal field-specific irrigation design and scheduling depends on multiple factors, such as crop type, the type of irrigation system employed, and quality of the irrigation water. Consider a field equipped with a modern irrigation system (e.g., a drip irrigation system or a micro-sprinkler irrigation system), which enables targeted, user-controlled, and high-frequency application of water. Assume, that the irrigation system has access to the water of two distinct origins: fresh water (FW) and treated water (TW), e.g., treated sewage effluents. The two waters have different unit costs $a^{(\text{FW})}$ and $a^{(\text{TW})}$. Our goal is to minimize the amount of water and irrigation cost while maintaining desired levels of crop yield and salt leaching. An optimal irrigation scheduling problem is formulated as follows:

For a given number N of irrigation devices (i.e., micro-sprinklers or drippers) and their spatial locations $\{\mathbf{x}_i\}_{i=1}^N$ in the field, minimize the operational cost of the irrigation system,

$$(3.3.1) \quad \min_{\forall Q_{i,t}^{(\text{FW})}, Q_{i,t}^{(\text{TW})}} \sum_{t=1}^{t_{\text{op}}} \sum_{i=1}^N \left\{ a_{i,t}^{(\text{FW})} Q_{i,t}^{(\text{FW})} + a_{i,t}^{(\text{TW})} Q_{i,t}^{(\text{TW})} \right\}.$$

Here the decision variables $Q_{i,t}^{(\text{FW})}$ and $Q_{i,t}^{(\text{TW})}$ (such that $Q_{i,t}^{(\text{FW})} \equiv 0$ if $Q_{i,t}^{(\text{TW})} > 0$ and viceversa) represent amounts of the fresh and treated waters released by the i -th irrigation device during the t -th stress period; $a_{i,t}^{(\text{FW})}$ and $a_{i,t}^{(\text{TW})}$ are the unit costs of the fresh and treated waters during the t -th stress period; and t_{op} is the operation horizon. Depending on the physical constraints imposed by the irrigation equipment, decision variables $Q_{i,t}$ and $Q_{k,t}$ can be either continuous or binary such that $Q_{i,t} = 1$ if the i -th sprinkle operates during t -th stress period and $= 0$ if it remains idle. Minimization of the cost function 3.3.1 is subject to water quantity and quality constraints

$$(3.3.2) \quad \mathcal{T} \geq \mathcal{T}^* \quad \text{and} \quad \mathcal{M} \leq \mathcal{M}^*.$$

The water quantity constraint $\mathcal{T} \geq \mathcal{T}^*$ ensures that plant transpiration \mathcal{T} (which is proportional to yield) stays above its critical level \mathcal{T}^* . The transpiration is defined as $\mathcal{T} = \iint s_w(\mathbf{x}, t) d\mathbf{x}dt$, where $s_w = s_w(\mathbf{x}, t)$ is the rate of soil water extraction by the plant roots [Severino, 2015][194]. The latter depends on the spatio-temporal distributions of both hydraulic and osmotic pressures of the soil water, i.e., on the spatio-temporal distributions of both water content $\theta(\mathbf{x}, t)$ and salt (chloride) concentration $c(\mathbf{x}, t)$. The water quality constraint $\mathcal{M} \leq \mathcal{M}^*$ enforces the requirement that the mass fraction of the solute leaching below the root zone, \mathcal{M} , does not exceed its critical (maximum allowable) limit \mathcal{M}^* . This quantity is defined as $\mathcal{M} = M_{\text{lea}}/M_{\text{tot}}$, where M_{lea} is the cumulative solute mass discharged through a prescribed horizontal control plane located at vertical distance $x_3 = L$ from the soil surface, and the total solute mass $M_{\text{tot}} = M_{\text{sur}} + M_{\text{ini}} - M_{\text{ext}}$, represents a balance between cumulative mass of solute applied through the soil surface (M_{sur}), initial solute mass stored in the soil of depth L (M_{ini}), and cumulative mass of solute extracted from the soil (from the soil surface to soil depth L) by plant roots and lost to solute transformations (M_{ext}). The tight, two-way coupling of water flow and solute transport in the vadose zone suggests that there is a tradeoff between water uptake and the drainage flux, and, concurrently, solute discharge below the root zone. The latter, in turn, may be controlled by irrigation water quality/irrigation water quantity substitutions.

This problem formulation assumes that the irrigation system is already in place and aims to determine its optimal operating schedule. We can also investigate an optimal irrigation design problem, which treats the number (N) and locations ($\{\mathbf{x}_i\}_{i=1}^N$) of the irrigation devices as additional decision variables in the optimization problem. In the case of an orchard, the positions $\{\mathbf{x}_i\}_{i=1}^N$ are determined by the tree planting geometry, with the irrigation devices placed in the trees' vicinity and their laterals located along the trees' rows. In the case of crops planted in rows (e.g., corn, cotton, vegetables), the laterals are located along the crop rows. The distance between the MS or the D along the laterals, however, should be determined in the optimization

process. In the case of crops grown over the entire area of a field (e.g., grass), the locations $\{\mathbf{x}_i\}_{i=1}^N$ do not have geometrical constraints.

For a given set of the flow rates $Q_{i,t}^{(\text{FW})}$ and $Q_{i,t}^{(\text{TW})}$, the constraints 3.3.2 have to be satisfied probabilistically since $\theta(\mathbf{x}, t)$ and $c(\mathbf{x}, t)$ are random fields whose statistical distributions (probability density functions) satisfy the flow and transport problems with uncertain (random) coefficients and driving forces (e.g., precipitation). Let p^* denote an acceptable probability for predictions of both \mathcal{T} and \mathcal{M} . Then the proper formulation of the chance constraint 3.3.2 is $\Pr[\mathcal{T} \geq \mathcal{T}^*] \geq p^*$ and $\Pr[\mathcal{M} \leq \mathcal{M}^*] \geq p^*$.

Optimization under uncertainty is a rapidly developing field with applications in many fields of science and engineering. State-of-the-art and comprehensive reviews of various approaches to optimization under uncertainty, including various flavors of stochastic and fuzzy programming, [*Infanger, 2010; Verderame et al., 2010*][**98, 220**]. The use of such techniques in subsurface hydrology is surveyed in [*Tartakovsky, 2013*][**207**]. Application of stochastic optimization techniques to real-world problems is hampered by (often prohibitive) computational costs that arise from i) a large number of degrees of freedom, ii) a large number of decision variables, and iii) the need to propagate full statistical distributions of θ and c through the modeling process.

Although within the proposed framework flow and transport processes are intended as “black boxes”, we believe it is worth briefly discussing the type of the output which is expected in order to let the entire framework to properly work. Thus, flow and transport simulations are performed for a number of numerical (typically Monte Carlo) realizations of the soil-parameters [*Severino et al., 2016*][**196**]. Generally, such simulations are tightly coupled: flow velocity affects both solute transport [*Severino, 2006; Bellini, 2011; Severino et al., 2012, 2017*][**177, 15, 179, 183**], and water uptake by plant roots [*Severino, 2015*][**194**]; water uptake is coupled to both water flow and solute transport through its dependence on hydraulic and osmotic pressure heads [*Severino et al., 2017*][**188**]. The resulting system of nonlinear equations is solved by numerical methods.

Given the ubiquity of both soil heterogeneity and data scarcity [*Comegna, 2010*][**33**], each realization of soil’s properties, and hence quantitative forecasting of moisture redistribution and solute migration, are merely “educated

guesses”. Repeating the modeling effort multiple times (for multiple realizations of parameter fields conditioned on data) and carrying out a statistical analysis of the multiple modeling forecasts allows one to assign a probability (or the likelihood of occurrence) to such “educated guesses”. The level of intrusiveness is a key feature that determines whether to adopt a particular probabilistic technique [Severino, 2015][175].

Concluding remarks. We have illustrated a procedure which can be easily implemented in the IoT-context. Indeed, data-driven agricultural technologies are rapidly becoming a tool of large use, and in particular they allow one to design a site-specific management plan (precision-agriculture). In particular, a majority of precision-agriculture strategies rely on statistical analyses (or image processing) of indirect measurements of soil conditions obtained, for example, by satellites, unmanned aircraft (drones) or other means of remote sensing. Various (aboveground) parameters related to crop conditions can be effectively monitored by wireless sensor networks. Thus, the utility of our approach comes from the use of dynamic real-time forecasting of the quantity and quality of soil water to guide the field irrigation. This forecasting will be facilitated and informed by in situ measurements obtained with spatially distributed autonomous and automated sensors along an IoT-framework.

The steps of the present framework can be summarized as follows: i) design an autonomous network of environmental sensors that collect data on soil moisture and concentration of dissolved contaminants; ii) assimilate these data, and precipitation forecast, into predictive models of soil-moisture dynamics and contaminant migration; iii) Use these data-driven models to optimize the irrigation practices while minimizing their environmental impact; iv) introduce best management practices to the farming community and public decision-makers.

Before concluding, it is worth noting that the soil conductivity $K(\psi) \equiv K_r(\alpha\psi) \exp Y$ depends not only upon the spatially variable parameter Y but also upon the relative conductivity $K_r(\alpha\psi)$ that, being a function of the stress ψ , de facto, depends upon the soil moisture [Gomez, 2009][78]. The functional dependence of K_r upon ψ , [L], via the soil-dependent parameter α , [L⁻¹], has been traditionally regarded as a deterministic process (i.e. $\alpha \sim \text{constant}$). However, in the practical applications one is concerned with

domains of large extents where α undergoes to significant spatial variations as consequence of the disordered soil's structure. This is due to the fact that α is more than a fitting parameter: it depends upon the soil's texture [*White and Sully, 1992*][**232**]. Since, the soil's texture is highly variable from point to point in the soil, a tantamount degree of variability is expected to be recovered in the α -parameter [*Severino, 2016*][**195**]. As a consequence, a spatial characterization of the α -parameter has to be provided along the same lines adopted for Y .

Acknowledgments. This study was supported by grants "Programma di scambi internazionali per mobilità di breve durata", Naples University (Italy).

Unsaturated water flow has become one of the major concerns in environmental studies. The traditional deterministic approach or sensitivity analysis techniques can not effectively quantify the complicated spatial variability of the hydraulic properties. This is the reason why the stochastic approach has taken hold in the last decade, where the heterogeneous aquifer parameters are modeled by space random functions and the resulting prediction is in the form of a probabilistic distribution function. Given the stochastic representation, the prediction can be obtained using analytical or numerical methods.

The numerical methods, specifically Monte-Carlo method in this thesis, require generating a large number of equiprobable realizations of hydraulic parameters honoring the same geostatistical features and available field data. These realizations have been constructed by using geostatistical approach (3.1 and 3.3). Other widely used numerical methods are the random walk methods and the particle tracking. The first approach accounts for hydrodynamic dispersion and the second one does not, but both of them are free of numerical dispersion and oscillation. It would be very interesting, for future research, to develop these methods and to compare the results with those presented in this thesis.

On the other hand, analytical methods are basically focused on the method of moments which provide closed form of first and second moments that can

be easily evaluated once the statistical structure of the soil parameters is specified. An example of application has been provided in the 3.2.

This thesis is based on a number of separate studies and is an attempt to quantitatively analyze the above discussed features of water transport and uncertainty related to water transport in heterogeneous media. To summarize, it was obtained:

- The hydraulic parameter α is a structureless process, so it can be fully described only by mean and variance. In other words, the covariance (spatial structure) of the log-transform of α can be approximated by a white noise in horizontal plane, i.e. a disturbance signal during the information transmission. Mathematically speaking it is a vector having zero mean and diagonal auto-correlation matrix;
- Analytical expressions of the statistical moments of the pressure head and specific flux, which allow to quantifying the uncertainty of these two FVs above the water table. In particular:

$$(4.0.3) \quad \begin{cases} \psi(\infty) = 0 & \text{far field} \\ \psi(0) < \infty & \text{water table} \end{cases},$$

and

$$(4.0.4) \quad \begin{cases} \langle \Psi(\infty) \rangle \equiv \ln(-q_0) & \text{far field} \\ \langle \Psi(0) \rangle \equiv 0 & \text{water table} \end{cases};$$

- The infiltrating flux q_0 and the integral scale I impact the stationary values of the specific flux and have a limited influence upon the distance from the water-table at which such stationary values are attained;
- It is possible estimate the thickness of the flow domain where the nonstationary is dominant by means of a 1D Richards equation;
- An optimal irrigation scheduling problem which can be easily implemented in the IoT-context.

Besides the theoretical interest, conclusions of the present thesis can be useful for practical purposes.

From theory to the applications

Nowadays, the uncontrolled action of man on the territory can also trigger degradation processes, which alter, progressively, the water cycle, soil fertility and biodiversity. Water and soil conservation has become an economic asset of considerable value and its correct management is now one of the most compelling problems. In the most modern agricultural systems, water management must be the result of a compromise between the strategies adopted by Local Authorities, which must consider both environmental problems and alternative use of water resources, and the immediate needs of farmers, which have to satisfy the crop water demand in qualitative and quantitative terms. There is a need to provide more detailed information to farmers about the applicability of new irrigation methods, in particular the "water-saving" methods, determining very high irrigation efficiency and optimization. This is the purpose of some examples of irrigation protocols presented in the previous section.

For all these reasons, the need to model and predict unsaturated water transport is increasing and to understand the nature of the aquifer through which the flow and transport take place is one of the problems of the environmental science. Soils are heterogeneous in terms of hydraulic parameters and flow variables, that vary erratically from point to point in the space. The stochastic approach is an important tool to evaluate both the uncertainty quantification of hydrological properties and model predictions, even for complex and hard to study systems where direct measures are missing. The first allows to decide, optimally, how many measures are needed and where to concentrate them or to design elaborate field experiments; the second one allows an aquifer management under risk (in contrast with the deterministic model). Unfortunately, stochastic modelling has not yet become a popular tool used by the hydrological community. The geostatistical approach, developed in this thesis, represents a step forward in making hydraulic properties estimation methods cheaper, in terms of money and time, and more representative of real conditions, where the heterogeneity is the main source of uncertainty. In general, there are a lot of factors that may determine uncertainty, for instance the choice of the model (e.g. discrete versus continuous, two-dimensional versus three-dimensional, etc.) or the possibility of rains. It would be interesting,

for future research, to integrate the developed methodology with these sources as well.

All the innovative techniques and methodologies require a very big amounts of data, in order to be correctly applied even on extended areas. This requirement, on one hand, has encouraged the entry of the hydrology in the IoT-framework, widely explained above; on the other hand, it has increased the acquisition of remote sensing data with the support of Geographic Information Systems (GIS). This field of study was not taken in account for the writing of this thesis, but it would be interesting to discover this area of research in the future. Both of them make possible to collect, store, manage and process a large amount of data in real time very easily.

One never grow tired of repeating that the importance of water management is closely linked to the problem of pollution and transport of contaminant. They can sediment in the root zone and may be absorbed by plants that we are going to eat. The measurements on the soils are used to evaluate the trend of the concentrations of the pesticides, some highly toxic to humans. The contact can take place both directly and indirectly; the first case can occur during the production phases in factories and use in field treatments, the second case concerns the intake, by humans, of water and food contaminated by pesticides. The determination of toxicity criteria takes into account these data to set quality standards suitable to contain the aforementioned risks of infection. But, one should not forget that the frequent practice that uses waste water from urban sources for irrigation, even in countries traditionally not affected by water crises, and a new large spectrum of pollutants (chlorinated products, heavy metals, pesticides, organic compounds), that are only partially removed during purification treatments, are able to reach the ground with irrigation. Both areas, root zone and groundwater, if contaminated, constitute a serious risk to human and animal health. The technologies and scientific knowledge available to clean up the waters are quite advanced, although local governments are not always available to support the economic commitments that may be in some cases very expansive. This is the reason why, the keyword is to “prevent”, also through an important and frequent risk analysis, in order to avoid polluting sources of ending up in the water

table or contaminating the crops, with actions supported by clearer and more stringent legislation, especially in the repression of abuses.

ACKNOWLEDGMENTS

Ringraziamenti. Ringrazio il coordinatore della Scuola di Dottorato, Professore Guido D'Urso, sempre gentile e disponibile verso noi dottorandi. Ringrazio il mio tutor, Professore Gerardo Severino, che mi ha dato l'opportunità di vivere questa esperienza. Un' esperienza nella quale ho avuto la fortuna di incontrare dei veri amici: Nicoletta, Fabio, Caterina, Giuseppe e Paolo. Ringrazio i miei amici, quelli di una vita e quelli più recenti ma ugualmente indispensabili, su cui ho sempre potuto contare. Fortunatamente sono tanti, troppi per poter fare una lista, ma sono sicura che ognuno di loro saprà riconoscersi leggendo queste poche ma sincere righe. Ringrazio mia sorella per la sua pazienza. Ringrazio Peppe, per il suo amore che rende sempre tutto molto più semplice. Ringrazio Michele, per non lasciarmi, letteralmente, mai sola. Ma soprattutto, ringrazio mia madre per il suo quotidiano sostegno e ringrazio mio padre per la sua fiducia incondizionata. Senza voi due nulla sarebbe stato possibile.

BIBLIOGRAPHY

- [1] *Hydrodynamica*. Britannica Online Encyclopedia, UK, 2008.
- [2] A.L. Gutjahr A.A. Bakr, L.W. Gelhar and J.R. MacMillan. Stochastic analysis of spatial variability in subsurface flows, 1. *Water Resources Research*, 14:263–271, 1978.
- [3] P.J. Wierenga A.F. Toorman and R.G. Hills. Determining soil hydraulic properties from onestep outflow experiments by parameter estimation:ii. *Water Resource Research*, 28:3021–3028, 1992.
- [4] A.A. Bakr A.L. Gutjahr, L.W. Gelhar and J.R. MacMillan. Stochastic analysis of spatial variability in subsurface flows, 2. *Water Resources Research*, 14:953–959, 1978.
- [5] J. Andersson and A. Shapiro. Stochastic analysis of one-dimensional steady state unsaturated flow: A comparison of monte carlo and perturbation methods. *Water Resources Research*, 19(1):121–133, 1983.
- [6] K. Ashton. That 'internet of things' thing. *RFID Journal*, 2009.
- [7] D.O. Lomen A.W. Warrich and S.R. Yates. A generalizied solution to infiltration. *Soil Sci. Soc. Am. J.*, 49:34–38, 1985.
- [8] D. A. Barajas-Solano and D. M. Tartakovsky. Stochastic collocation methods for non-linear parabolic equations with random coefficients. *SIAM/ASA J. Uncert. Quant.*, 4(1):475–494, 2016.
- [9] H.A. Basha. Multidimensional linearized nonsteady infiltration with prescribed boundary conditions at the soil surface. *Water Resour. Research*, 35:75–83, 1999.
- [10] H.A. Basha. Infiltration models for semi-infinite soil profiles. *Water Resources Research*, 47, 2011.
- [11] Angelo Basile, Guido Ciollaro, and Antonio Coppola. Hysteresis in soil water characteristics as a key to interpreting comparisons of laboratory and field measured hydraulic properties. *Water Resources Research*, 39(12), 2003.
- [12] M. Bause and P. Knabner. Computation of variably saturated subsurface flow by adaptive mixed hybrid finite element methods. *Adv. Water Resour.*, 27:565–581, 2004.

- [13] J. Bear. *Dynamics of fluids in porous media*. Dover Publications, 1972.
- [14] J. Bear and A.H.D. Cheng. *Modeling groundwater flow and contaminant transport*. Springer, New York, 2010.
- [15] A Bellin, G Severino, and A Fiori. On the local concentration probability density function of solutes reacting upon mixing. *Water Resources Research*, 47(1), 2011.
- [16] A. Belsito. *L'acqua nel terreno, in chimica agraria*. Zanichelli, Bologna, 1988.
- [17] Th. M. Boers and J. Ben-Asher. A review of rainwater harvesting. *Agr. Water Manage.*, 5(2):145–158, 1982.
- [18] G.H. Bolt. Soil physics terminology. *Bull. International Society Soil Science*, 49:26–36, 1976.
- [19] P. Broadbridge and I. White. Time to ponding: comparison of analytical, quasi-analytical and approximate predictions. *Water Resources Research*, 23:2302–2310, 1987.
- [20] P. Broadbridge and I. White. Constant rainfall rate infiltration: A versatile nonlinear model: 1. analytic solution. *Water Resources Research*, 24:145–154, 1988.
- [21] P. M. Brooks and A. T. Corey. Hydraulic properties in porous media. *Hydrology Paper 3, Fort Collins*, 1964.
- [22] W. Brutsaert. *Hydrology-An introduction*. Cambridge University Press, Cambridge, UK, 2005.
- [23] E. Buckingham. Studies on the movement of soil moisture. *U.S. Department of Agriculture Bureau of soils*, 38, 1907.
- [24] M.P.Stallybrass C. Rogers and D.L. Clements. On two phase filtration under gravity and with boundary infiltration-application of a backlund transformation. *Nonlinear Anal. Theory Methods Appl.*, 7:785–799, 1983.
- [25] Alfonso Calera, Isidro Campos, Anna Osann, Guido D’Urso, and Massimo Menenti. Remote sensing for crop water management: From et modelling to services for the end users. *Sensors*, 17(5), 2017.
- [26] G.S. Campbell and S. Shiozawa. *Indirect methods for estimating the hydraulic properties of unsaturated soils*. University of California, California, 1992.
- [27] J.G. Caputo and Y. A. Stepanyants. Front solutions of richards equation. *Transp. Porous Media*, 74:1–20, 2008.
- [28] V. Casulli and P. Zanolli. A nested newton-type algorithm for finite volume methods solving richards equation in mixed form. *SIAM J. Sci. Comput.*, 34:2255–2273, 2010.
- [29] M. Celia, E. Bouloutas, and R. Zarba. A general mass conservative numerical solution of the unsaturated flow equation. *Water Resour. Res.*, 26:1483–1496, 1990.
- [30] F. Chen and L. Ren. Application of the finite difference heterogeneous multiscale method to the richards equation. *Water Resour. Research*, 44, 2008.
- [31] Angelo Chianese, Fiammetta Marulli, Francesco Piccialli, Paolo Benedusi, and Jai E Jung. An associative engines based approach supporting collaborative analytics in the internet of cultural things. *Future Generation Computer Systems*, 2016.

- [32] C. Paniconi C.M.F. D' Haese, M. Putti and N. E. C. Verhoest. Assessment of adaptive and heuristic time stepping for variably saturated flow. *Int. J. Numer. Methods Fluids*, 53:1173–1193, 2007.
- [33] A Comegna, A Coppola, V Comegna, G Severino, A Sommella, and CD Vitale. State-space approach to evaluate spatial variability of field measured soil water status along a line transect in a volcanic-vesuvian soil. *Hydrology and Earth System Sciences*, 14(12):2455–2463, 2010.
- [34] A Comegna, A Coppola, G Dragonetti, G Severino, A Sommella, and A Basile. Dielectric properties of a tilled sandy volcanic-vesuvian soil with moderate andic features. *Soil and Tillage Research*, 133:93–100, 2013.
- [35] A Comegna, G Severino, and A Sommella. Surface measurements of hydraulic properties in an irrigated soil using a disc permeameter. *WIT Trans. Ecol. Environ*, 96:341–353, 2006.
- [36] V Comegna and A Basile. Temporal stability of spatial patterns of soil water storage in a cultivated vesuvian soil. *Geoderma*, 62(1-3):299–310, 1994.
- [37] V Comegna, P Damiani, F D'Anna, and C Ruggiero. Comparison of different field methods for determining the hydraulic conductivity curve of a volcanic vesuvian soil. *Geoderma*, 73(3-4):231–244, 1996.
- [38] A. Coppola, A. Santini, P. Botti, S. Vacca, V. Comegna, and G. Severino. Methodological approach to evaluating the response of soil hydrological behaviour to irrigation with treated municipal wastewater. *J. Hydrol.*, 292:114–134, 2004.
- [39] A.T. Corey and A. Klute. Application of the potential concept to soil water equilibrium and transport. *Soil Science Soc. Am. Journal*, 49:3–11, 1985.
- [40] A. Couto, A. Ruiz Padín, and B. Reinoso. Comparative yield and water use efficiency of two maize hybrids differing in maturity under solid set sprinkler and two different lateral spacing drip irrigation systems in León, Spain. *Agr. Water Manage.*, 124:77–84, 2013.
- [41] C. Abhishek C.T. Miller and M. W. Farthing. A spatially and temporally adaptive solution of richards equation. *Adv. Water Resour.*, 29:525–545, 2006.
- [42] S Cuomo, G De Pietro, R Farina, A Galletti, and G Sannino. A revised scheme for real time ecg signal denoising based on recursive filtering. *Biomedical Signal Processing and Control*, 27:134–144, 2016.
- [43] Salvatore Cuomo, Pasquale De Michele, Ardelio Galletti, and Francesco Piccialli. A cultural heritage case study of visitor experiences shared on a social network. In *2015 10th International Conference on P2P, Parallel, Grid, Cloud and Internet Computing (3PGCIC)*, pages 539–544. IEEE, 2015.
- [44] P. Binning D. Kavetski and S.W. Sloan. Noniterative time stepping schemes with adaptive truncation error control for the solution of richards equation. *Water Resource Research*, 38, 2002.

- [45] G. Dagan. Models of groundwater flow in statistically homogeneous porous formations. *Water Resources Research*, 15:47–63, 1979.
- [46] G. Dagan. Stochastic modeling of groundwater flow by unconditional and conditional probabilities. *Water Resources Research*, 18:835–848, 1982.
- [47] G. Dagan. Solute transport in heterogeneous formations. *J. Fluid Mech.*, 145:151–177, 1984.
- [48] G. Dagan. Theory of solute transport by groundwater. 19:183–215, 1987.
- [49] G. Dagan. Time-dependent macrodispersion for solute transport in anisotropic heterogeneous aquifers. *Water Resources Research*, 24:1491–1500, 1988.
- [50] G. Dagan. *Flow and Transport in Porous Formation*. Springer-Verlag, New York, 1989.
- [51] G. Dagan. Transport in heterogeneous porous formations: spatial moments, ergodicity and effective dispersion. *Water Resources Research*, 26:1281–1290, 1990.
- [52] G. Dagan. Dispersion of a passive solute in non-ergodic transport by steady velocity fields in heterogeneous formations. *J. Fluid Mech.*, 233:197–210, 1991.
- [53] J.H. Dane and J.W. Hopmans. Hanging water column. *Soil Science Society of America*, pages 680–683, 2002.
- [54] S. De Pascale, L. Dalla Costa, S. Vallone, G. Barbieri, and A. Maggio. Increasing water use efficiency in vegetable crop production: From plant to irrigation systems efficiency. *Hort Technology*, 21(3):301–308, 2011.
- [55] J.P. Delhomme. Spatial variability and uncertainty in groundwater flow parameters: A geostatistical approach. *Water Resources Research*, 15:269–280, 1979.
- [56] G. D.Smith. *Numerical Solution of Partial Differential Equations: Finite Difference Methods*. Oxford University Press, New York, 1985.
- [57] L.C. Evans. *Partial differential equations*. American Mathematical Society, New York, 1998.
- [58] Tan F. Chen, Jiann-Mou, Yih-Chi, and Chu-Hui. Analytical solutions of one-dimensional infiltration before and after ponding. *Hydrol. Process*, 17:815–822, 2003.
- [59] Tan Yih-Ch and Chu-Hui F. Chen, Jiann-Mou and J.Y. Parlange. Analytical solutions for linearized richards equation with arbitrary time-dependent surface fluxes. *Water Resour. Research*, 37:1091–1093, 2001.
- [60] Carmine Fallico, Samuele De Bartolo, Massimo Veltri, and Gerardo Severino. On the dependence of the saturated hydraulic conductivity upon the effective porosity through a power law model at different scales. *Hydrological Processes*, 30(13):2366–2372, 2016.
- [61] Raffaele Farina, S Dobricic, A Storto, S Masina, and Salvatore Cuomo. A revised scheme to compute horizontal covariances in an oceanographic 3d-var assimilation system. *Journal of Computational Physics*, 284:631–647, 2015.
- [62] M.J Fayer and C.S Simmons. Modified soil water retention functions for all matric suctions. *Water Resources Research*, 31:1233–1238, 1995.

- [63] J. Feder. *Fractals*. Plenum, New York, 1988.
- [64] Marco Ferrante and T-C Jim Yeh. Head and flux variability in heterogeneous unsaturated soils under transient flow conditions. *Water Resources Research*, 35(5):1471–1479, 1999.
- [65] A. Fiori, P. Indelman, and G. Dagan. Correlation structure of flow variables for steady flow toward a well with application to highly anisotropic heterogeneous formations. *Water Resources Research*, 34(4):699–708, 1998.
- [66] Aldo Fiori, Francesca Boso, Felipe PJ de Barros, Samuele De Bartolo, Andrew Framp-ton, Gerardo Severino, Samir Suweis, and Gedeon Dagan. An indirect assessment on the impact of connectivity of conductivity classes upon longitudinal asymptotic macrodispersivity. *Water resources research*, 46(8), 2010.
- [67] R. A. Freeze and S. M. Gorelick. Convergence of stochastic optimization and decision analysis in the engineering design of aquifer remediation. *Ground Water*, 37(6):934–954, 1999.
- [68] R.A. Freeze. *Regionalization of hydrogeologic parameters for use in mathematical models of groundwater flow in Hydrogeology*. J.E. Gill, Gardenvale, Quebec, 1972.
- [69] R.A. Freeze. A stochastic-conceptual analysis of one-dimensional groundwater flow in nonuniform homogeneous media. *Water Resources Research*, 11:725–741, 1975.
- [70] E.O. Frind and S.F. Pinder. Galerkin solution to the inverse problem for aquifer transmissivity. *Water Resources Research*, 9:1397–1410, 1973.
- [71] H. Fujita. The exact pattern of concentration-dependent diffusion on a semi-infinite medium ii. *Text. Res. J.*, 22:823–827, 1952.
- [72] A. Nicola G. Juncu and C. Popa. Nonlinear multigrid methods for numerical solution of the variably saturated flow equation in two space dimensions. *Transp. Porous Media*, 91:35–47, 2012.
- [73] W. R. Gardner. Some steady state solutions of unsaturated moisture flow equations with application to evaporation from a water table. *Soil Science*, 85:228–232, 1958.
- [74] L. W. Gelhar. *Stochastic Subsurface Hydrology*. Prentice Hall, New Jersey, 1993.
- [75] M.T. Van Genuchten. A comparison of numerical solution of the one-dimensional unsaturated-saturated flow and mass transport equations. *Adv. Water Resour.*, 5:47–55, 1982.
- [76] R.W. Gillham. The capillary fringe and its effect on water-table response. *Journal of Hydrology*, 67(1):307 – 324, 1984.
- [77] E. P. Glenn, T. Anday, R. Chaturvedi, R. Martinez-Garcia, S. Pearlstein, D. Soliz, S. G. Nelson, and R. S. Felger. Three halophytes for saline-water agriculture: An oilseed, a forage and a grain crop. *Environ. Exp. Bot.*, 92:110–121, 2013.
- [78] S Gómez, G Severino, L Randazzo, G Toraldo, and JM Otero. Identification of the hydraulic conductivity using a global optimization method. *agricultural water management*, 96(3):504–510, 2009.

- [79] J.J. Gomez-Hernandez and S.M. Gorelick. Effective groundwater model parameter values: Influence of spatial variability of hydraulic conductivity, leakance and recharge. *Water Resources Research*, 25:405–419, 1989.
- [80] P. Goovaerts. *Geostatistics for Natural Resources Evaluation*. Oxford Press, Uk, 1997.
- [81] W.H. Green and G.A. Ampt. Studies on soil physics: I. flow of air and water through soils. *J. Agric. Sci.*, 4:1–24, 1911.
- [82] C. N. Dawson H. Li, M. W. Farthing and C. T. Miller. Local discontinuous galerkin approximations to richards equation. *Adv. Water Resour.*, 30:555–575, 2007.
- [83] W.B. Haines. Studies in the physical properties of soils. *Journal Agric. Science*, 20:97–116, 1930.
- [84] M. A. Hanjra, J. Blackwell, G. Carr, F. Zhang, and T. M. Jackson. Wastewater irrigation and environmental health: Implications for water governance and public policy. *Int. J. Hyg. Envir. Heal.*, 215(3):255–269, 2012.
- [85] M. Hayek. Water pulse migration through semi-infinite vertical unsaturated porous column with special relative-permeability functions: Exact solutions. *Water Resource Research*, 517:668–676, 2014.
- [86] M. Hayek. An exact explicit solution for one-dimensional, transient, nonlinear richards equation for modeling infiltration with special hydraulic functions. 535:662–670, 2015.
- [87] M. Hayek. Analytical solution to transient richards equation with realistic water profiles for vertical infiltration and parameter estimation. 52:4438–4457, 2016.
- [88] D. Hillel. *Applications of soil physics*. Academic Press, New York, 1980.
- [89] D. Hillel. *Environmental soil physics*. Academic Press, New York, 1998.
- [90] D. Hillel. *Environmental Soil Physics Academic*. San Diego, CA, 1998.
- [91] A. Hirich, Jelloul, R. Choukr-Allah, and S.-E. Jacobsen. Saline water irrigation of quinoa and chickpea: Seedling rate, stomatal conductance and yield responses. *J. Agron. Crop Sci.*, 2014.
- [92] J. D. Hoffman. *Numerical Methods for Engineers and Scientists*. Marcel Dekker, Inc, New York, 2001.
- [93] R. J. Hutton and B. R. Loveys. A partial root zone drying irrigation strategy for citrus—Effects on water use efficiency and fruit characteristics. *Agr. Water Manage.*, 98(10):1485–1496, 2011.
- [94] J.F. Artiola I. Yolcubal, M.L. Brusseau, P. Wierenga, and L.G. Wilson. Environmental physical properties and processes. *Environmental Monitoring and Characterization*, pages 207–239, 2004.
- [95] W. A. Illman. Type curve analyses of pneumatic single-hole tests in unsaturated fractured tuff: direct evidence for a porosity scale effect. *Water Resources Research*, 41(4):1–14, 2005.
- [96] P. Indelman, D. Or, and Y. Rubin. Stochastic analysis of unsaturated steady state flow through bounded heterogeneous formations. *Water Resources Research*, 29(4):1141–1148, 1993.

- [97] Peter Indelman and GEDEON Dagan. Solute transport in divergent radial flow through heterogeneous porous media. *Journal of Fluid Mechanics*, 384:159–182, 1999.
- [98] G. Infanger, editor. *Stochastic Programming: The State of the Art*. Springer, New York, 2010.
- [99] J. N. M. Stricker J. C. van Dam and P. Droogers. Inverse method to determine soil hydraulic functions from multistep outflow experiments. *Soil Science Society of America Journal*, 58:647–652, 1992.
- [100] I. Jankovic, A. Fiori, and G. Dagan. Flow and transport in highly heterogeneous formations: 3. numerical simulations and comparison with theoretical results. *Water Resources Research*, 39(SBH 16-1), 2003.
- [101] J.C. Parker J.B. Kool and M.T. van Genuchten. Determining soil hydraulic properties from onestep outflow experiments by parameter estimation:i. *Soil. Sci. Soc. Am. J.*, 49:1348–1354, 1985.
- [102] J.B. Koolr J.C. Parke and M.T. van Genuchten. Determining soil hydraulic properties from onestep outflow experiments by parameter estimation:ii. *Soil. Sci. Soc. Am. J.*, 49:1354–1359, 1985.
- [103] M. P. Jones and W. F. Hunt. Performance of rainwater harvesting systems in the southeastern United States. *Resour. Conserv. Recy.*, 54(10):623–629, 2010.
- [104] A. Journel. The lognormal approach to predicting local distributions of selective mining unit grades. *Math Geology*, 12:285–303, 1980.
- [105] T. Kanety, A. Naor, A. Gips, U. Dicken, J. H. Lemcoff, and S. Cohen. Irrigation influences on growth, yield, and water use of persimmon trees. *Irrig. Sci.*, 32(1):1–13, 2014.
- [106] P. K. Kitanidis. *Introduction to Geostatistics - With Applications in Hydrogeology*. Cambridge University Press, Uk, 1996.
- [107] P.K. Kitanidis. A geostatistical approach to the inverse problem in groundwater modeling (steady state) and one-dimensional simulations. *Water Resources Research*, 19:677–690, 1983.
- [108] A. Klute. Water retention: laboratory methods. *Agronomy series*, 9:635–662, 1986.
- [109] K. Kosugi. Three-parameter lognormal distribution model for soil water retention. *Water Resources Research*, 30:891–901, 1996.
- [110] R. Zhang K.R. Huang and M.T. Van Genuchten. An eulerian-lagrangian approach with an adaptively corrected method of characteristics to simulate variably saturated water flow. *Water Resource Research*, 30:499–507, 1994.
- [111] A.W. Warrick L. Pan and P.J. Wierenga. Finite elements methods for modeling water flow in variably saturated porous media: Numerical oscillation and mass distributed schemes. *Water Resource Research*, 32:1883–1889, 1996.
- [112] D. W. Lawlor. Genetic engineering to improve plant performance under drought: physiological evaluation of achievements, limitations, and possibilities. *J. Exp. Bot.*, 64(1):83–108, 2013.

- [113] M. Lees. A linear three level difference scheme for quasi-linear parabolic equations. *Math. Comp.*, 20:516–522, 1966.
- [114] S.C. Lessoff and P. Indelman. Analytical model of solute transport by unsteady unsaturated gravitational infiltration. 72:85–107, 2004.
- [115] B. Li and T.-C.J. Yeh. Sensitivity and moment analyses of head in variably saturated regimes. *Advances in Water Resources*, 21(6):477 – 485, 1998.
- [116] J. David Logan. *Transport Modeling in Hydrogeochemical Systems*. Springer, New York, 2001.
- [117] A. Younes M. Fahs and F. Lehmann. An easy and efficient combination of the mixed finite element method and the method of lines for the resolution of richards equation. *Environ. Modell. Software*, 24:1122–1126, 2009.
- [118] S. Pugnaghi M. Menziani and S. Vincenzi. Analytical solutions of the linearized richards equation for discrete arbitrary initial and boundary conditions. *J. Hydrol.*, 332:214–225, 2007.
- [119] M. D. Pirouz M. Nasser, Y. Daneshbod, Gh. R. Rakhshandehroo, and A. Shirzad. New analytical solution to water content simulation in porous media. *J. Irrig. Drain. Eng.*, 138:328–335, 2012.
- [120] N. Shokri M. Sadeghi and S.B. Jones. A novel analytical solution to steady-state evaporation from porous media. *Water Resource Research*, 48, 2002.
- [121] D. Or M. Tuller and L.M. Dudley. Adsorption and capillary condensation in porous media: liquid retention and interfacial configurations in angular pores. *Water Resources Research*, 35:1949–1964, 1999.
- [122] M. Mahbod and S. Zand-Parsa. Prediction of soil hydraulic parameters by inverse method using genetic algorithm optimization under field conditions. *Journal Archives of Agronomy and Soil Science*, 56:13–28, 2010.
- [123] A. Maimon, A. Tal, E. Friedler, and A. Gross. Safe on-site reuse of greywater for irrigation - A critical review of current guidelines. *Environ. Sci. Technol.*, 44(9):3213–3220, 2010.
- [124] G. De Marsily. *Quantitative hydrogeology*. Academic Press, 1986.
- [125] D.A. McQuarrie. *Statistical Mechanics*. University Science Books, 2000.
- [126] G.A. Gander M.L. Sharma and C.G. Hunt. Spatial variability of infiltration in a watershed. *J. of Hydrology*, 45:101–122, 1980.
- [127] Y. Mualem. A new model for predicting the hydraulic conductivity of unsaturated porous media. *Water Resources Research*, 12(3):513–522, 1976.
- [128] C.E. Kees M.W. Farthing and C.T. Miller. Mixed finite element methods and higher order temporal approximations for variably saturated groundwater flow. *Adv. Water Resour.*, 26:373–394, 2003.
- [129] Y. A. Mylopoulos, N. Theodosiou, and N. A. Mylopoulos. A stochastic optimization approach in the design of an aquifer remediation under hydrogeologic uncertainty. *Water Resour. Manage.*, 13:335–351, 1999.

- [130] J. Vanderborght H. Hardelauf N. Suciú, C. Vamos and H. Vareecken. Numerical investigations on ergodicity of solute transport in heterogeneous aquifers. *Water Resources Research*, 42, 2006.
- [131] P.J. Ross N. Varado, I. Braud and R. Haverkamp. Assessment of an efficient numerical solution of the 1d richards equation on bare soil. *Journal of Hydrology*, 323:244–257, 2005.
- [132] S.P. Neuman and Y.K. Zhang. A quasi-linear theory of non-fickian and fickian subsurface dispersion. *Water Resources Research*, 26:887–902, 1990.
- [133] D. Or and M. Tuller. Liquid retention and interfacial area in variably saturated porous media: upscaling from single-pore to sample-scale model. *Water Resources Research*, 35:3591–3605, 1999.
- [134] D. Or and M. Tuller. Flow in unsaturated fractured porous media: Hydraulic conductivity of rough surfaces. *Water Resources Research*, 36:1165–1177, 2000.
- [135] Th. Oweis and A. Hachum. Water harvesting and supplemental irrigation for improved water productivity of dry farming systems in West Asia and North Africa. *Agr. Water Manage.*, 80(1-3):57–73, 2006.
- [136] F. Pedrero, A. Allende, M. I. Gil, and J. J. Alarcón. Soil chemical properties, leaf mineral status and crop production in a lemon tree orchard irrigated with two types of wastewater. *Agr. Water Manage.*, 109:54–60, 2012.
- [137] J.R. Philip. Numerical solution of equations of diffusion type with diffusivity concentration-dependent. *Aust. J. Phys.*, 10:29–42, 1957.
- [138] J.R. Philip. Theory of infiltration. *Adv. Hydrosci.*, 5:215–305, 1969.
- [139] U. Pinto, B.L. Maheshwari, and H. S. Grewal. Effects of greywater irrigation on plant growth, water use and soil properties. *Resour. Conserv. Recy.*, 54(7):429–435, 2010.
- [140] M. Pivato. *Linear Partial Differential Equations and Fourier Theory*. Cambridge, United Kingdom, 2010.
- [141] D.W. Pollock. Semianalytical computation of path lines for finite difference models. *Ground Water*, 26, 1988.
- [142] A. Quarteroni, R. Sacco, and F. Saleri. *Numerical Mathematics*. Springer, New York, 2000.
- [143] L. Smith R.A. Freeze, J. Massmann, T. Sperling, and B. James. Hydrogeological decision analysis. *Ground Water*, 28:738–766, 1990.
- [144] R. Ragab and J. D. Cooper. Variability of the unsaturated zone water transport parameters: Implications for hydrological modelling, 2. predicted vs in-situ measurements and evaluation methods. *Journal of Hydrology*, 148:133–147, 1993.
- [145] R Ragab and JD Cooper. Variability of unsaturated zone water transport parameters: implications for hydrological modelling. 1. in situ measurements. *Journal of hydrology*, 148(1-4):109–131, 1993.
- [146] L.R. Ahuja R.E. Green and S.K. Chong. Hydraulic conductivity, diffusivity, and sorptivity of unsaturated soils. *American Society of Agronomy*, 9:771–798, 1986.

- [147] L.A. Richards. Capillary conduction of liquids through porous medium. *Physics*, 1:318–333, 1931.
- [148] L.A. Richards and M. Fireman. Pressure plate apparatus for measuring moisture sorption and transmission by soils. *Soil Science*, 56:395–404, 1943.
- [149] R.D. Richtmyer and K.W. Morton. *Difference methods for initial-value problems*. Interscience Publishers, New York, 1967.
- [150] J. Touma R.M. Haverkamp, M. Vauclin, P. J. Wierenga, and G. Vachaudc. A comparison of numerical simulation models for one dimensional infiltration. *Soil Sci. Soc. Am. J.*, 41:285–294, 1977.
- [151] D.F. Rogers. *Laminar flow analysis*. Cambridge University Press, UK, 1992.
- [152] N Romano, P Nasta, G Severino, and JW Hopmans. Using bimodal lognormal functions to describe soil hydraulic properties. *Soil Science Society of America Journal*, 75(2):468–480, 2011.
- [153] D.U. Von Rosenberg. *Methods forthe numerical solution of partial differential equation*. Elsevier, New York, 1969.
- [154] P.J. Ross. Efficient numerical methods for infiltration using richards equation. *Water Resour. Research*, 26:279–290, 1990.
- [155] P.J. Ross and J.Y. Parlange. Comparing exact and numerical solutions of richards equation for one-dimensional infiltration and drainage. *Soil science*, 157:341–344, 1994.
- [156] C. Rossi and J.R. Nimmo. Modeling of soil water retention from saturation to oven dryness. *Water Resources Research*, 30:701–708, 1994.
- [157] K. Roth. *Lecture Notes in Soil Physics*. Institute of Soil Science University of Hohenheim, Germany, 1996.
- [158] Y. Rubin. *Applied Stochastic Hydrogeology*. Oxford University Press, Oxford, 2003.
- [159] D. Russo. Determining soil hydraulic properties by parameter estimation: On the selection of a model for the hydraulic properties. *Water Resources Research*, 24:453–459, 1988.
- [160] D. Russo. Determining soil hydraulic properties by parameter estimation: On the selection of a model for the hydraulic properties. *Water Resource Research*, 24:453–459, 1988.
- [161] D. Russo. Stochastic modeling of macrodispersion for solute transport in a heterogeneous unsaturated porous formation. *Water Resources Research*, 29(2):383–397, 1993.
- [162] D. Russo and A. Fiori. Equivalent vadose zone steady-state flow. an assessment of its applicability to predict transport in a realistic combined vadose zone-groundwater flow system. *Water Resources Research*, 44(W09436), 2008.
- [163] D. Russo, A. Laufer, A. Silber, and S. Assouline. Water uptake, active root volume and solute leaching under drip irrigation: A numerical study. *Water Resources Research*, 45(W12413), 2009.

- [164] David Russo. Upscaled conductivity in gravity-dominated flow through variably saturated heterogeneous formations. *Water Resources Research*, 39(9), 2003.
- [165] David Russo and Moshe Bouton. Statistical analysis of spatial variability in unsaturated flow parameters. *Water Resources Research*, 28(7):1911–1925, 1992.
- [166] David Russo and Eshel Bresler. Soil hydraulic properties as stochastic processes: I. an analysis of field spatial variability. *Soil Science Society of America Journal*, 45(4):682–687, 1981.
- [167] David Russo and Aldo Fiori. Stochastic analysis of transport in a combined heterogeneous vadose zone–groundwater flow system. *Water Resources Research*, 45(3), 2009.
- [168] David Russo, Itay Russo, and Asher Laufer. On the spatial variability of parameters of the unsaturated hydraulic conductivity. *Water Resources Research*, 33(5):947–956, 1997.
- [169] S. Salsa. *Equazioni a derivate parziali*. Springer, Italia, 2010.
- [170] G.D. Salvucci. An approximate solution for steady vertical flux of moisture through an unsaturated homogeneous soil. *Water Resource Research*, 29, 1993.
- [171] J.O. Selroos. *Contaminant transport by groundwater: stochastic travel time analysis and probabilistic safety assessment*. Doctoral thesis, Royal Institute of Technology of Stockholm, 1996.
- [172] S.E. Serrano. Analytical decomposition of the nonlinear unsaturated flow equation. *Water Resource Research*, 34:397–407, 1998.
- [173] S.E. Serrano. Modeling infiltration with approximate solutions to richards equation. *Journal of Hydrology Eng.*, 9:421–432, 2004.
- [174] G. Severino, A. Comegna, A. Coppola, A. Sommella, and A. Santini. Stochastic analysis of a field-scale unsaturated transport experiment. *Advances in Water Resources*, 33(10):1188–1198, 2010.
- [175] G Severino and S De Bartolo. Stochastic analysis of steady seepage underneath a water-retaining wall through highly anisotropic porous media. *Journal of Fluid Mechanics*, 778:253–272, 2015.
- [176] G. Severino and P. Indelman. Analytical solutions for reactive solute transport under an infiltration-redistribution cycle. *J. Contam. Hydrol.*, 70:89–115, 2004.
- [177] G Severino, VM Monetti, A Santini, and G Toraldo. Unsaturated transport with linear kinetic sorption under unsteady vertical flow. *Transport in porous media*, 63(1):147–174, 2006.
- [178] G. Severino and A. Santini. On the effective hydraulic conductivity in mean vertical unsaturated steady flows. *Advances in Water Resources*, 28:964–974, 2005.
- [179] G Severino, DM Tartakovsky, G Srinivasan, and H Viswanathan. Lagrangian models of reactive transport in heterogeneous porous media with uncertain properties. *Proceedings of the Royal Society A*, 468(2140):1154–1174, 2012.

- [180] Gerardo Severino. Macrodispersion by point-like source flows in randomly heterogeneous porous media. *Transport in porous media*, 89(1):121–134, 2011.
- [181] Gerardo Severino. Stochastic analysis of well-type flows in randomly heterogeneous porous formations. *Water Resources Research*, 47(3), 2011. W03520.
- [182] Gerardo Severino. Stochastic analysis of well-type flows in randomly heterogeneous porous formations. *Water Resources Research*, 47(3), 2011.
- [183] Gerardo Severino, Rosanna Campagna, and Daniel M. Tartakovsky. An analytical model for carrier-facilitated solute transport in weakly heterogeneous porous media. *Applied Mathematical Modelling*, 44:261 – 273, 2017.
- [184] Gerardo Severino and Antonio Coppola. A note on the apparent conductivity of stratified porous media in unsaturated steady flow above a water table. *Transport in porous media*, 91(2):733–740, 2012.
- [185] Gerardo Severino, Vladimir Cvetkovic, and Antonio Coppola. Spatial moments for colloid-enhanced radionuclide transport in heterogeneous aquifers. *Advances in Water Resources*, 30(1):101–112, 2007.
- [186] Gerardo Severino, Samuele De Bartolo, Gerardo Toraldo, Gowri Srinivasan, and Hari Viswanathan. Travel time approach to kinetically sorbing solute by diverging radial flows through heterogeneous porous formations. *Water Resources Research*, 48(12), 2012.
- [187] Gerardo Severino, Guido D’Urso, Maddalena Scarfato, and Gerardo Toraldo. The iot as a tool to combine the scheduling of the irrigation with the geostatistics of the soils. *Future Generation Computer Systems*, pages –, 2018.
- [188] Gerardo Severino, Francesco Giannino, Fabrizio Cartení, Stefano Mazzoleni, and Daniel M. Tartakovsky. Effects of hydraulic soil properties on vegetation pattern formation in sloping landscapes. *Bulletin of Mathematical Biology*, 2017.
- [189] Gerardo Severino, Alessandro Santini, and Valeria Marina Monetti. Modelling water flow water flow and solute transport in heterogeneous unsaturated porous media. In *Advances in Modeling Agricultural Systems*, pages 361–383. Springer, 2009.
- [190] Gerardo Severino, Alessandro Santini, and Angelo Sommella. Determining the soil hydraulic conductivity by means of a field scale internal drainage. *Journal of Hydrology*, 273(1):234–248, 2003.
- [191] Gerardo Severino, Alessandro Santini, and Angelo Sommella. Steady flows driven by sources of random strength in heterogeneous aquifers with application to partially penetrating wells. *Stochastic Environmental Research and Risk Assessment*, 22(4):567–582, 2008.
- [192] Gerardo Severino, Alessandro Santini, and Angelo Sommella. Macrodispersion by diverging radial flows in randomly heterogeneous porous media. *Journal of contaminant hydrology*, 123(1):40–49, 2011.

- [193] Gerardo Severino, Maddalena Scarfato, and Alessandro Comegna. Stochastic analysis of unsaturated steady flows above the water table. *Water Resources Research*, (53):6687–6708, 2017.
- [194] Gerardo Severino and Daniel M Tartakovsky. A boundary-layer solution for flow at the soil-root interface. *Journal of mathematical biology*, 70(7):1645–1668, 2015.
- [195] Gerardo Severino, Gerardo Toraldo, and Daniel M Tartakovsky. The frequency domain approach to analyse field-scale miscible flow transport experiments in the soils. accepted for publication in *Biosystems Engineering*, 2016.
- [196] Scarfato Maddalena Severino, Gerardo and and Gerardo Toraldo. Mining geostatistics to quantify the spatial variability of certain soil flow properties. *Procedia Computer Science*, 98:419–424, 2016.
- [197] H. Singh Grewal and B. L. Maheshwari. Treated effluent and saline water irrigation influences soil properties, yield, water productivity and sodium content of snow peas and celery. *J. Plant Nutr.*, 36(7):1102–1119, 2013.
- [198] M. Sinsbeck and D. M. Tartakovsky. Impact of data assimilation on cost-accuracy tradeoff in multifidelity models. *SIAM/ASA J. Uncert. Quant.*, 3(1):954–968, 2015.
- [199] R.E. Smith. *Infiltration theory for hydrologic applications*. American Geophysical Union, Washington DC, 2002.
- [200] R.E. Smith and R.H.B. Hebbert. A monte-carlo analysis of the hydrologic effects of spatial variability of infiltration. *Water Resources Research*, 15:419–429, 1979.
- [201] C.L. Winter S.P. Neuman and C.M. Newman. Stochastic theory of field-scale fickian dispersion in anisotropic porous media. *Water Resources Research*, 23:453–466, 1987.
- [202] G. Sposito. The "physics" of soil water physics. *Water resources research*, 22:83–88, 1986.
- [203] G. Sposito. *The Chemistry of Soils*. Oxford University Pressl, New York, 1989.
- [204] D. L. Suarez. Use of marginal-quality waters for sustainable crop production. In S. A. Shahid, M. A. Abdelfattah, and F. K. Taha, editors, *Developments in Soil Salinity Assessment and Reclamation: Innovative Thinking and Use of Marginal Soil and Water Resources in Irrigated Agriculture*, chapter 25, pages 367–381. Springer, 2013.
- [205] N. Suci. Diffusion in random velocity fields with applications to contaminant transport in groundwater. *Advances in Water Resources*, 69:114–133, 2014.
- [206] A. M. Tartakovsky, L. Garcia-Naranjo, and D. M. Tartakovsky. Transient flow in a heterogeneous vadose zone with uncertain parameters. *Vadose Zone Journal*, 3(1):154–163, 2004.
- [207] D. M. Tartakovsky. Assessment and management of risk in subsurface hydrology: A review and perspective. *Adv. Water Resour.*, 51:247–260, 2013.
- [208] D. M. Tartakovsky, A. Guadagnini, and M. Riva. Stochastic averaging of nonlinear flows in heterogeneous porous media. *Journal of Fluid Mechanics*, 492:47–62, 2003.

- [209] Daniel M Tartakovsky, Shlomo P Neuman, and Zhiming Lu. Conditional stochastic averaging of steady state unsaturated flow by means of kirchhoff transformation. *Water Resources Research*, 35(3):731–745, 1999.
- [210] G. Tassinari. *Manuale dell' agronomo*. REDA, Roma, 1976.
- [211] F Terribile, A Basile, R De Mascellis, M Iamarino, P Magliulo, S Pepe, and S Vingiani. Landslide processes and andosols: the case study of the campania region, italy. In *Soils of volcanic regions in Europe*, pages 545–563. Springer, New York, 2007.
- [212] D. Triadis and P. Broadbridge. Analytical model of infiltration under constant-concentration boundary conditions. *Water Resources Research*, 46, 2010.
- [213] F. T-C. Tsai, N-Z. Sun, and W. W-G. Yeh. Global-local optimization for parameter structure identification in three-dimensional groundwater modeling. *Water Resour. Res.*, 39(2):WR001135, doi:10.1029/2001, 2003.
- [214] M. Tuller and D. Or. Hydraulic conductivity of variably saturated porous medi. film and corner flow in angular pore space. *Water Resources Research*, 37:1257–1276, 2001.
- [215] J. L. Nieber V.A. Zlotnik, T. Wang and J. Simunek. Verification of numerical solutions of the richards equation using a traveling wave solution. *Water Resources Research*, 30:1973–1980, 2007.
- [216] C.H.M. van Bavel and D. Kirkham. Field measurement of soil permeability using auger holes. *Soil. Sci. Soc. Am. J.*, 13:90–96, 1948.
- [217] M. T. Van Genuchten. Some steady state solutions of unsaturated moisture flow equations with application to evaporation from a water table. *Soil Science Society of America Journal*, 44:892–898, 1980.
- [218] M. Th. van Genuchten. A closed-form equation for predicting the hydraulic conductivity of unsaturated soils. *Soil Sci. Soc. Am. J.*, 44:892–898, 1980.
- [219] E. Vanmarcke. *Random fields: Analysis and Synthesis*. The MIT Press, Cambridge, Mass., 1983.
- [220] P. M. Verderame, J. A. Elia, J. Li, and C. A. Floudas. Planning and scheduling under uncertainty: A review across multiple sectors. *Ind. Eng. Chem. Res.*, 49(9):3993–4017, 2010.
- [221] Francesco Vuolo, Guido D’Urso, Carlo De Michele, Biagio Bianchi, and Michael Cutting. Satellite-based irrigation advisory services: A common tool for different experiences from europe to australia. *Agricultural Water Management*, 147:82 – 95, 2015.
- [222] W.R. Gardner W.A. Jury and W.H. Gardner. *Soil Physics*. Wiley, New York, 1991.
- [223] P. Wang, P. Quinlan, and D. M. Tartakovsky. Effects of spatio-temporal variability of precipitation on contaminant migration in vadose zone. *Geophysical Research Letter*, 36:L12404, 2009.
- [224] Q.J. Wang and J.C.I. Dooge. Limiting cases of water fluxes at the land surface. *J. Hydrol.*, 155:429–440, 1994.
- [225] J.E. Warren and H.S. Price. Flow in heterogeneous porous media. *Soc. Petrol. Eng. J.*, 1:153–169, 1961.

- [226] A.W. Warrick. Analytical solutions to the one-dimensional linearized moisture flow equation for arbitrary input. *Soil Sci.*, 120:79–84, 1975.
- [227] A.W. Warrick. Additional solutions for steady-state evaporation from a shallow water table. *Soil science*, 146:63–66, 1988.
- [228] A.W. Warrick. *Soil Water Dynamics*. Oxford University Press, New York, 2003.
- [229] X.H. Wen. *Geostatistical methods for prediction of mass transport in groundwater*. Doctoral thesis, Royal Institute of Technology of Stockholm, 1996.
- [230] Chester K. Wentworth. A scale of grade and class terms for clastic sediments. *The Journal of Geology*, 30(5):377–392, 1922.
- [231] I. White and P. Broadbridge. Constant rate rainfall infiltration: A versatile nonlinear model: 2. applications of solutions. *Water Resources Research*, 24:155–162, 1988.
- [232] I White and MJ Sully. On the variability and use of the hydraulic conductivity alpha parameter in stochastic treatments of unsaturated flow. *Water resources research*, 28(1):209–213, 1992.
- [233] PJ Wierenga, RG Hills, and DB Hudson. The las cruces trench site: Characterization, experimental results, and one-dimensional flow predictions. *Water Resources Research*, 27(10):2695–2705, 1991.
- [234] T.P. Witelski. Perturbation analysis for wetting fronts in richards equation. *Transp. Porous Media*, 27:121–134, 1997.
- [235] T.P. Witelski. Motion of wetting fronts moving into partially pre-wet soil. *Adv. Water Resour.*, 28:1133–1141, 2005.
- [236] J.H.M. Wosten and M.T: van Genuchten. Using texture and other soil properties to predict the unsaturated soil hydraulic functions. *Soil. Sci. Soc. Am. J.*, 52:1762–1770, 1988.
- [237] S. Yang, B. Vanderbeld J. Wan, and Y. Huang. Narrowing down the targets: Towards successful genetic engineering of drought-tolerant crops. *Mol. Plant*, 3(3):469–490, 2010.
- [238] T-C J. Yeh, Gelhar, W. L., and Gutjahr A. Stochastic analysis of unsaturated flow in heterogenous soils 1. statistically isotropic media. *Water Resources Research*, 21(4):447–456, 1985.
- [239] W. Yeh. Review of parameter identification procedures in groundwater hydrology: The inverse problem. *Water Resource Research*, 22:95–108, 1986.
- [240] W. W-G. Yeh. Systems analysis in ground-water planning and management. *ASCE J. Water Resour. Plan. Manag.*, 118(3):224–237, 1992.
- [241] D. Zhang. *Stochastic Methods for Flow in Porous Media*. Academic Press, USA, 2002.
- [242] Dongxiao Zhang and C Larrabee Winter. Nonstationary stochastic analysis of steady state flow through variably saturated, heterogeneous media. *Water Resources Research*, 34(5):1091–1100, 1998.
- [243] J. Zhu and B.P. Mohanty. Analytical solutions for steady state vertical infiltration. *Water Resource Research*, 38, 2002.

- [244] R.W. Zimmerman and G.S. Bodvarsson. An approximate solution for one-dimensional absorption in unsaturated porous media. *Water Resource Research*, 25:1422–1428, 1989.